To the Graduate Council:

I am submitting herewith a dissertation written by Waleed Mohammed Albukhari entitled “Enhancing Power System Strength and Inertia in the Saudi Electric Grid for Solar Power Integration.” I have examined the final paper copy of this dissertation for form and content and recommend that it be accepted in partial fulfillment of the requirements for the degree of Doctor of Philosophy, with a major in Electrical Engineering.

Dr. Yilu Liu, Major Professor

We have read this dissertation
and recommend its acceptance:

Dr. David Icove

Dr. Seddik Djouadi

Dr. Khaled Alshuaibi

Accepted for the Council:

Dixie L. Thompson

Vice Provost and Dean of the Graduate School

To the Graduate Council:

I am submitting herewith a dissertation written by Waleed Mohammed Albukhari entitled "Enhancing Power System Strength and Inertia in the Saudi Electric Grid for Solar Power Integration." I have examined the final electronic copy of this dissertation for form and content and recommend that it be accepted in partial fulfillment of the requirements for the degree of Doctor of Philosophy, with a major in Electrical Engineering.

Dr. Yilu Liu, Major Professor

We have read this dissertation
and recommend its acceptance:

Dr. David Icove

Dr. Seddik Djouadi

Dr. Khaled Alshuaibi

Accepted for the Council:

Dixie L. Thompson

Vice Provost and Dean of the Graduate School

(Original signatures are on file with official student records.)

Enhancing Power System Strength and Inertia in the Saudi Electric Grid for Solar Power Integration

A Dissertation Presented for the

Doctor of Philosophy

Degree

The University of Tennessee, Knoxville

Waleed Mohammed Albukhari

May 2025

This dissertation is dedicated to my parents, brother, sisters, wife, and children, with special devotion to my country

Acknowledgements

First and above everything else, all praise to Allah for giving me the determination, patience, and strength to complete this dissertation.

I would like to express my deepest gratitude to my advisor, Dr. Yilu Liu, for her support, guidance, and encouragement throughout my PhD journey. Her expertise, insightful feedback, and patience have been invaluable in shaping this research. Dr. Liu's dedication to excellence and her passion for advancing knowledge have inspired me to push the boundaries of my own work. I am truly grateful for the countless hours she has invested in mentoring me and for believing in my potential. Thank you, Dr. Liu, for being an exceptional mentor and for making this journey a rewarding experience.

I extend my sincere thanks to Dr. David Icove, Dr. Seddik Djouadi, and Dr. Khaled Alshuaibi for their willingness to serve on my Ph.D. committee. I am thankful for their commitment, effort, and the helpful suggestions they provided throughout my dissertation.

I am deeply grateful to my beloved parents, brother, and sisters for their sacrifices, support and love. Additionally, I deeply appreciate the patience and assistance of my wife, Ghadeer, and my children, Lara and Mohammed, throughout this long and difficult journey.

Finally, I would like to express my warm gratitude to the Saudi Technical and Vocational Training Corporation and the Government of the Kingdom of Saudi Arabia for providing me with the scholarship that has enabled me to reach this achievement.

Abstract

As electricity demand continues to increase and environmental challenges from conventional power generation persist, a worldwide shift toward renewable energy sources (RESs) has been initiated. Saudi Arabia, with its advantageous geographical location, presents exceptional potential for solar photovoltaic (PV) integration. This natural advantage positions the country as an ideal adopter of solar PV, facilitating its path toward reduced reliance on fossil fuels.

While the shift toward renewable energy offers significant benefits, it also introduces complexities to power grid stability due to the inherent limitations of RESs in providing sufficient strength and inertia support. Successful integration requires adapting existing grid infrastructure and developing innovative solutions.

This dissertation addresses the emerging challenges associated with reduced grid strength and inertia. It primarily focuses on the implications of full solar PV integration, where conventional generators are entirely replaced within the Saudi Electricity Company (SEC) grid. The research explores several solutions, including implementing synchronous condensers (SynCons) to enhance grid strength by improving short-circuit capacity and inertia, ensuring stable voltage and frequency regulation. Protection systems were adapted to address the reduced fault current associated with solar PV integration. Using the short-circuit ratio (SCR) as a strength index, findings indicate that an SCR increase of 3 with SynCons significantly improved system stability and post-disturbance recovery. These insights offer adaptable

strategies and practical approaches to enhance grid resilience, supporting power systems worldwide in their transition to RESs.

Table of Contents

List of Tables

List of Figures

Nomenclature

AVR	Automatic Voltage Regulator
BESS	Battery Energy storage system
COS	Central Operating Area
ESS	Energy storage system
FACTS	Flexible AC Transmission System
FIDVR	Fault-induced delayed voltage recovery
IBR	Inverter-Based Resource
IEC	International Electrotechnical Commission
NRPF	Newton-Raphson Power Flow
PCC	Point of Common Coupling
PF	Power Factor
POI	Point of Interconnection
PSS/E	Power System Simulator for Engineers
PV Curve	Active Power-Voltage Curve
PV	Photovoltaic

P	Real Power
QV Curve	Reactive Power-Voltage Curve
Q	Reactive Power
RES	Renewable Energy Resource
RMS	Root Mean Square
SCMVA	Short Circuit Capacity
SCRX	Silicon-controlled rectifier excitation
SCR	Short Circuit Ratio
SEC	Saudi Electricity Company
SG	Synchronous Generator
SM	Synchronous Machine
SOA	Southern Operating Area
STATCOM	Static Synchronous Compensator
SynCon	Synchronous Condenser
WOS	Western Operating Area
WSCR	Weighted Short Circuit Ratio

Chapter 1

Introduction

1.1 Background

With the growth in electricity demand and the environmental challenges caused by traditional generation, the transition toward renewable energy sources (RESs) is being observed worldwide [1, 2]. This shift aims to decrease reliance on traditional energy sources that depend on fossil fuels for electricity generation and utilizes the significant advantages of RESs. As part of this global development, the energy sector of Saudi Arabia experiences significant changes by shifting from its historical reliance on conventional power generation methods towards sustainable and green alternatives [3, 4]. The country's Vision 2030 concentrates on diversifying energy sources by achieving 58 GW of renewable energy capacity. This movement aims to reduce its heavy reliance on fossil fuels for electricity generation [5].

Saudi Arabia has an advantageous geographical location, exceptionally well suited for solar power integration. It receives more than 2100 kWh/m^2 of solar radiation annually [6]. This natural potential makes the country a highly suitable adopter of solar power in its transition towards RESs. Several solar energy projects have already been initiated, with more under development [7, 8]. This change in the energy sector is expected to have major positive economic and environmental implications, forming the foundation for a more sustainable and diversified future.

While the transition of power grids to RESs offers valuable benefits, it also introduces new complexities in maintaining stability and reliability [9, 10, 11]. This integration requires the adaptation of existing grid infrastructure, as well as the development of innovative technologies and strategies [9, 11]. Addressing these challenges is crucial for ensuring a successful and sustainable shift to a renewable based energy system.

1.2 Motivation

The integration of inverter-based resources (IBRs) such as solar photovoltaic (PV) systems presents unique challenges [12, 13, 14, 15]. Unlike traditional synchronous generators (SGs), solar PV systems have intermittent power output and distinct fault current characteristics due to their reliance on power electronic devices [9, 10, 11]. Inverters typically produce much less fault current compared to traditional generators, making fault detection in IBR-dominated grids challenging, as fault current levels often do not differ significantly from normal operating conditions [12, 14]. Moreover, power flow analyses indicate that increasing PV generation along with the retirement of SGs directly weakens voltage stability [16, 17, 18]. Furthermore, the reduced available inertia in power grids, which are increasingly powered by IBRs lacking the rotational components found in SGs, raises significant concerns about overall system robustness [11, 12, 19]. This issue is further compounded by the inherent limitations of IBRs in providing essential reactive power compensation, which is crucial for maintaining grid stability during contingencies [10, 11].

Several studies have investigated various aspects of the impact on power system strength following the integration of RESs [20, 21, 22]. The reduction in system strength primarily depends on the levels of fault current within the power network. Replacing SGs with IBRs leads to decreased fault current levels due to the limited short-circuit current characteristics of IBRs, introducing a significant concern for the effectiveness of existing protection systems [13, 14, 15, 20]. Extensive studies [23, 24, 25, 26] have assessed system strength in the context of IBRs. Several studies [27, 28, 29, 30] have investigated the impact of energy storage on enhancing electric grid stability. Similarly, the use of Flexible AC Transmission Systems (FACTS) [31, 32, 33, 34] has been explored for their potential to improve these aspects of power systems. Additionally, synchronous condensers (SynCons) [19, 35, 36, 37, 38, 39] have been used to increase short-circuit capacity levels and inertia, further contributing to system robustness. Also, advanced inverter control strategies [40, 41] have been recognized for significantly enhancing both the dynamic performance and overall reliability of power systems by improving power quality and providing essential grid support services during disturbances, highlighting their importance in modern power system operations. With the ongoing research focused on advanced grid modeling and real-time monitoring, there is a growing potential to develop more advanced and integrated approaches. These solutions aim not only to address the immediate challenges of grid stability and security, but also to ease the way for a more resilient and sustainable energy future.

This dissertation addresses the emerging challenges that reduce power system strength and proposes solutions, with a focus on the transition of the Saudi Electricity Company (SEC) system to a fully integrated solar PV grid. It provides insights and methodologies that can be adapted to other power systems globally, enhancing the global energy sector by improving grid stability and security. The successful adoption of RESs is key to achieving the ambitious goals of countries worldwide, particularly for nations like Saudi Arabia, which aim for a sustainable future less dependent on fossil fuels.

1.3 Research contributions

The specific objectives of this dissertation are outlined below:

- Developing five case studies based on the original Saudi model by progressively replacing SGs with solar PV at increments of 20%, 40%, 60%, 80%, and 100% using the Power System Simulator for Engineers (PSS/E).
- Investigating the impact on short circuit capacity (SCMVA) and system strength indicators with gradual solar PV integration.
- Analyzing and determining the hosting capacity of IBRs under different solar PV penetration levels.
- Assessing the impact of incremental solar PV integration on voltage and frequency responses during contingencies, and its influence on fault current magnitudes relevant to protection system performance.
- Conducting a weak grid analysis to identify potential bus locations that require support for the implementation of SynCons.
- Evaluating how SynCons improve SCMVA and fault current levels within the grid.
- Determining the optimal size and capacity of SynCons to strengthen system robustness at various locations.
- Investigating the role of SynCons in mitigating voltage stability issues to enhance grid resilience under various load conditions.
- Studying the impact of adding a transmission line on voltage stability under high solar PV penetration.
- Examining the impact of relocating solar PV near central loads on voltage stability under high solar PV penetration.
- Conducting a comparison study on the impact of Static Synchronous Compensator (STATCOM) and SynCons in mitigating fault-induced delayed voltage recovery (FIDVR) issues in the Saudi power grid.

- Exploring the effectiveness of SynCons in enhancing frequency stability, especially in scenarios under high renewable energy integration.
- Studying the impact of adding a transmission line on frequency stability under high solar PV penetration.
- Examining the impact of relocating solar PV near central loads on frequency stability under high solar PV penetration.
- Evaluating protection system enhancement by analyzing changes in fault current levels at the Point of Interconnection (POI) before and after the implementation of SynCons.

1.4 Dissertation Organization

This dissertation is organized as outlined below:

- **Chapter 2:** provides an overview of global solar PV generation and a background on the Saudi Arabian power grid. It introduces power system strength and explains how the integration of RESs impacts grid robustness, focusing on key indicators such as short circuit ratio (SCR) and weighted short circuit ratio (WSCR) to establish a foundation for evaluation. The chapter includes a comprehensive review that highlights the differences in short circuit behavior between synchronous machines (SMs) and IBRs, emphasizing their distinct characteristics and effects on the grid. Additionally, it introduces the International Electrotechnical Commission (IEC) 60909, a globally recognized standard for calculating short circuit capacity. Finally, the chapter discusses the challenges posed by weak system strength, focusing on the implications for voltage and frequency stability, along with the necessary adaptations in protection systems.

- **Chapter 3:** provides a comprehensive evaluation of the impact of increasing solar PV penetration on the strength of the Saudi power grid. It begins with an introduction that clarifies the significance of this analysis. The chapter then explores the effects of higher solar PV integration on system strength, focusing on changes in SCMVA levels. The analysis extends to how these penetration levels influence key system strength indicators such as SCR and WSCR. The chapter also examines the hosting capacity of IBRs, evaluating how the increase in solar PV capacity impacts the ability of the grid to manage additional power. Further, it explores the influence of solar PV integration on voltage and frequency stability at different penetration levels. The chapter concludes by examining the effect of this integration on the protection system and exploring potential improvements for more robust protection solutions.

- **Chapter 4:** focuses on the role of SynCons in enhancing power system strength. The chapter begins by setting the stage for a detailed exploration of this topic. It then explains the principles and applications of SynCons, providing a foundational understanding of their functions and significance in power systems. The chapter progresses to discuss SynCons modeling, exploring the technical aspects and methodologies involved in accurately representing these components in system analyses. Furthermore, it introduces an examination of how SynCons can enhance the strength of power grids, including both the methodology used for integrating SynCons and the subsequent results. Overall, this chapter provides a thorough overview of SynCons, from their basic principles to their practical implications in enhancing power system strength.

- **Chapter 5:** begins with an introduction, followed by a discussion on the basics of voltage stability. It outlines the methods used to analyze voltage stability, such as PV and QV curves, and explores load classifications, including static and dynamic loads. The methodology section is followed by results and discussions of several case studies, including testing the highest solar PV penetration before the voltage response becomes unstable, analyzing voltage instability using SynCons with static load and composite load, comparing the performance of SynCons and STATCOM in mitigating voltage instability during a FIDVR event, and evaluating the impact of adding more transmission lines and relocating solar PV on voltage stability under high solar PV penetration.

- **Chapter 6:** starts with an introduction and a discussion on the basics of frequency stability. It then examines frequency stability behavior, followed by the methodology, results, and discussions of several case studies. These include determining solar PV penetration limits on frequency response, testing frequency response as SynCons gradually increase the SCR, and evaluating the impact of adding a transmission line and relocating solar PV near central loads under high solar PV penetration.

- **Chapter 7:** examines the challenges and solutions associated with power system protection in the context of increasing solar PV integration. It highlights the fundamental role of protection systems, the impact of the shift from traditional SGs to IBRs, and the proposed solutions to ensure a reliable and secure system.

- **Chapter 8:** summarizes the key findings of the research, discusses their implications for the Saudi power grid and the broader field of power systems, and proposes directions for future research to further advance the integration of renewable energy sources.

Chapter 2

Literature Review

2.1 Global Overview of Solar Photovoltaic Power Generation

The high demand for oil initiated interest in solar technology as an alternative to fossil fuels. This marked a historical turning point, setting the stage for the rapid evolution of solar technology observed today [42]. RESs, including solar PV, are recognized in the modern energy sector for their collective role in decreasing reliance on fossil fuels and promoting sustainability. According to IRENA annual review report, the global installed capacity for electricity generation using solar PV has reached a remarkable 1,055.61 GW, with 189 GW of this capacity being added in 2022 alone [43].

However, despite its significant adoption, solar PV technology faces several challenges. Its reliance on sunlight leads to variability in power output, making it less predictable and consistent than fossil fuel-based power plants [44]. This intermittency, combined with the fact that solar PV systems are connected to the grid via power electronic devices, presents distinct challenges that will be discussed later in this chapter.

2.2 Saudi Arabia Power Grid

The Saudi electric grid is operated by SEC and divided into four main regions: central, western, eastern, and southern. This segmentation corresponds to regional operational divisions within the SEC, with each region serving independently [45]. There are 477 power generating units distributed across these areas, with the eastern and western regions together contributing 74% of the total national electricity production, as detailed in **Table 2.1** [46]. The transmission system consists of high-voltage lines ranging from 110 kV to 380 kV and covers approximately 93,400 circuit kilometers across the country [45]. Furthermore, the distribution network, operating at voltages below 110 kV, extends over 786,419 circuit kilometers, ensuring efficient power delivery to end-users [46].

Historically, the SEC has relied on oil and natural gas for power generation through thermal units. However, the Saudi government recognized the need for renewable energy projects as shown in **Table 2.2**, marking a significant shift towards green energy and reduced fossil fuel dependence [47]. This transition is further illustrated in **Figure 2.1** as a percentage of the total electricity generation sources [47].

In the summer of 2022, the Saudi power grid reached a new peak demand of 65,800 MW. This increase was driven by factors such as population growth, industrial expansion, and the gradual adoption of electric vehicles, which is expected to accelerate in the coming years. **Figure 2.2** presents a typical summer week load profile published by the Saudi Water and Electricity Regulatory Authority [46]. The integration of solar PV requires additional infrastructure, including energy storage systems, to meet power demand during periods without sunlight. The solar generation profile, the power required to charge energy storage, and the power needed for other mitigation solutions such as SynCons and STATCOMs are depicted in the load profile presented in **Figure 2.3**.

Table 2.1: GW Capacity at the Saudi power grid by Region for 2022

Region	Capacity (GW)
Central Region	17.1
Western Region	32.4
Eastern Region	34.3
Southern Region	6.7
Total	**90.0**

Table 2.2: Solar PV Projects in Saudi Arabia

Project	Capacity (MW)
Layla Solar PV Project	80
Wadi Al Dawaser Solar PV Project	120
Saad Solar PV Project	300
Ar Rass Solar PV Project	700
Sakaka Solar Power Plant in Al-Jouf	300
Total	**1500**

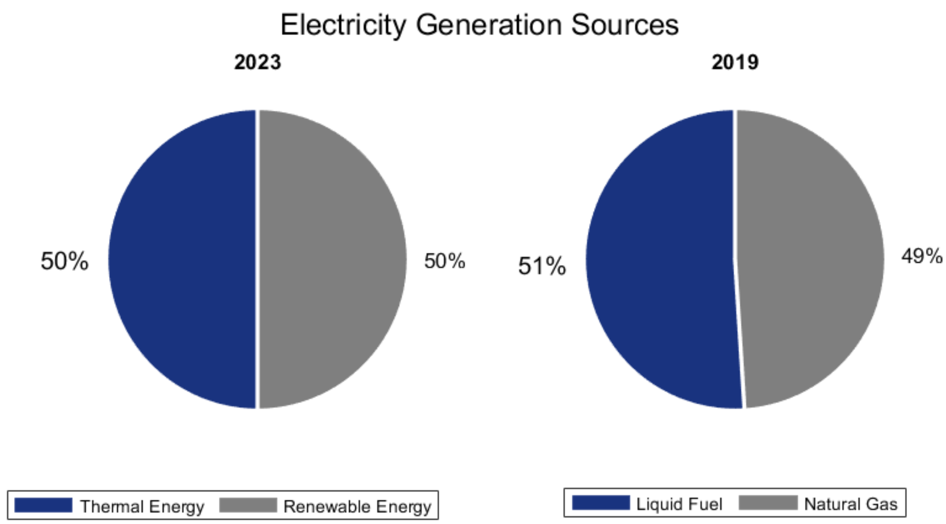

Figure 2.1: Electricity generation by source at the Saudi power grid.

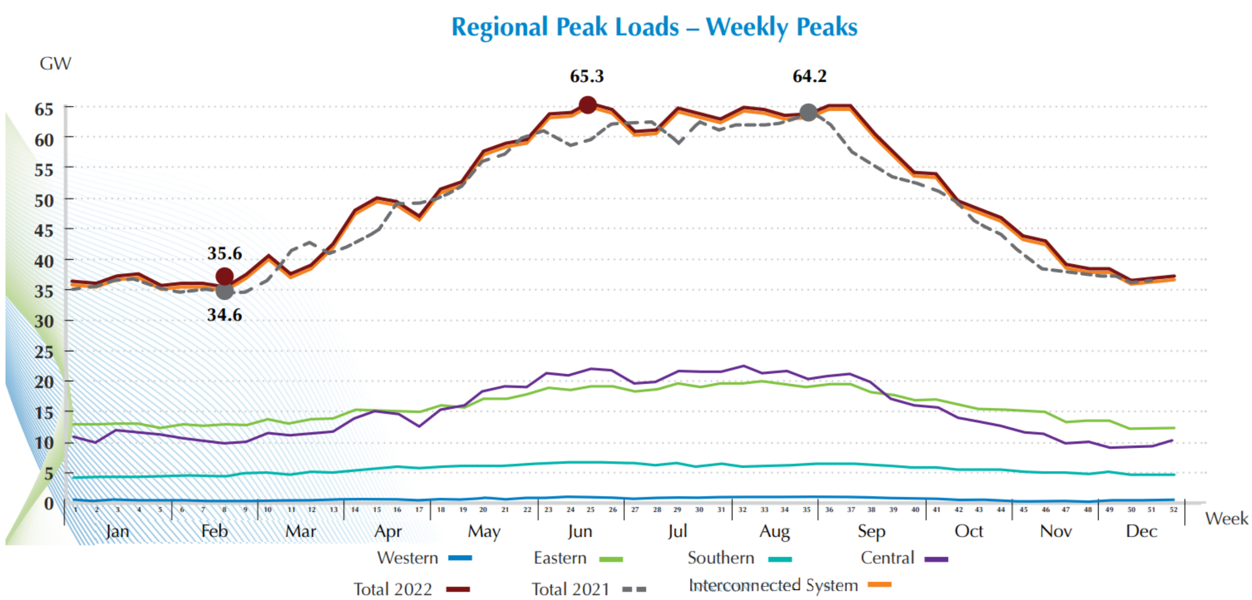

Figure 2.2: Typical weekly load profile at 2022.

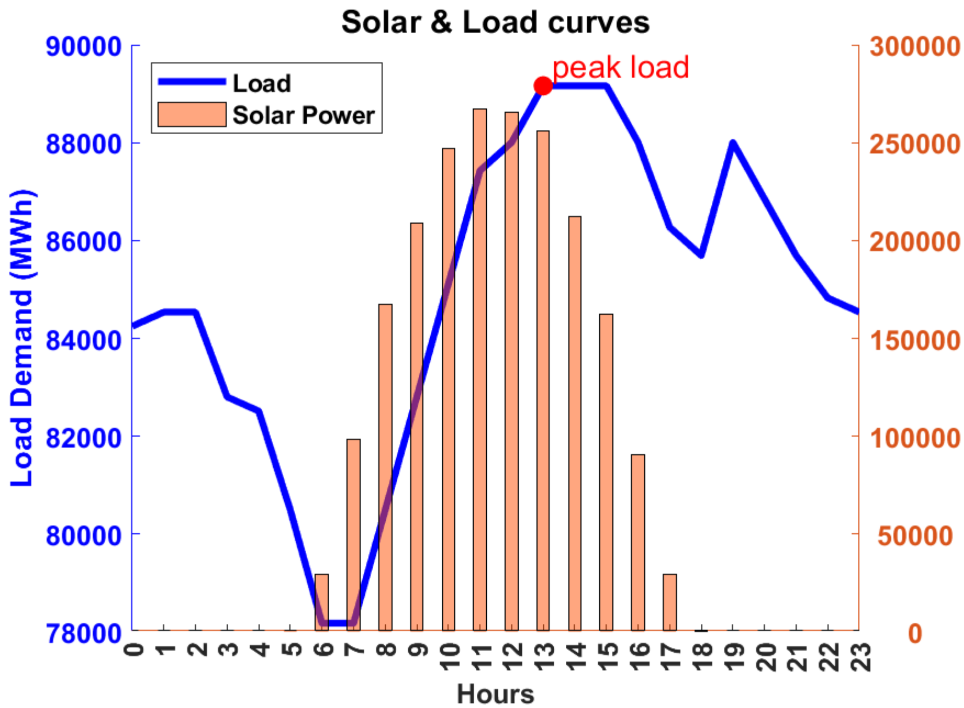

Figure 2.3: Solar and anticipated load profiles.

2.3 Evaluation of Power System Strength

Power system strength is a critical metric for assessing the impact of IBRs integration. It reflects the ability of electrical grids to maintain stable operation and recover effectively from significant disturbances [11]. The Australian Energy Market Commission offers an alternative perspective, identifying system strength in terms of voltage regulation, with fault level serving as a key indicator [16]. Higher fault levels are associated with smaller voltage variations across the network following a disturbance, indicating a more resilient and robust power system [16]. A grid with high system strength can more effectively integrate IBRs, ensuring better power quality and maintaining voltage within the desired limits [11, 16]. In contrast, low system strength can result in unstable power conditions, voltage fluctuations, reduced fault ride-through capabilities, and delayed restoration of voltage and frequency after disturbances [13, 14, 48, 49, 50].

In traditional power systems, SGs are known for their significant contribution to system strength, as they can produce currents much higher than their rated capacity during a fault [48]. This characteristic makes them a primary source of system strength in conventional power grids. However, as RESs are integrated into power grids, SGs are often replaced, leading to a reduction in fault current levels and the overall strength of the system [16, 49]. To assess the impact of IBRs on power system strength, various evaluation methods are employed. For example, the North American Electric Reliability Corporation (NERC) utilizes the SCR as a strength indicator, recommending that a POI maintain an SCR of 3 or higher to ensure adequate strength [49]. Assessing system strength using an index like SCR is essential for understanding the implications of retiring fossil fuel generators and for determining the necessary enhancements to maintain grid resilience and stability.

2.3.1 Power System Strength Indicators

This section introduces the methodologies used to assess the system strength of power grids, which are critical for ensuring stable and reliable operation. It highlights key indicators that measure the ability of a grid to withstand and respond to disturbances, particularly focusing on the SCR and WSCR. These metrics are crucial in evaluating how well a power system can handle faults and maintain operational stability, particularly as the integration of RESs continues to grow [50].

2.3.1.1 Short Circuit Ratio (SCR)

SCR is defined as the ratio between the SCMVA and the rated power of the electronic equipment at the POI [25]. This index measures system strength or fault levels at the POI. The SCR is mathematically expressed as follows:

$$SCR = \frac{S_{\text{scmva}}}{P_{\text{RMW}}} \tag{2.1}$$

Where S_{SCMVA} represents the MVA capacity of the grid before connecting the IBR, and P_{RMW} denotes the rated power in MW from the solar PV at the POIs. An SCR value below a certain threshold, typically considered low, might prompt the need for additional measures to strengthen the grid.

2.3.1.2 Weighted Short Circuit Ratio (WSCR)

To obtain more accurate results and account for the full interactions among IBRs at the POI, the Electric Reliability Council of Texas (ERCOT) has adopted the WSCR method to evaluate the strength of a power system [51]. WSCR is the ratio between short circuit capacity and rated P_{RMW} considering the integration of all IBRs connected to a single POI and defined as follows:

$$\text{WSCR} = \frac{\text{Weighted } S_{\text{SCMVA}}}{\left(\sum_{i=1}^{N} P_{\text{Rmw}i}\right)} = \frac{\sum_{i=1}^{N} S_{\text{SCMVA}i} \times P_{\text{Rmw}i}}{\left(\sum_{i=1}^{N} P_{\text{Rmw}i}\right)^2} \tag{2.2}$$

Where N is the number of solar PV plants and i is the plant index [49].

2.3.2 Analysis of Short Circuit Current Characteristics

This section provides a foundation for understanding the principles and differences in short circuit current characteristics across traditional generation systems and RESs. It shows the various responses and impacts these characteristics have on grid stability and protection systems. Detailed analyses of SMs and IBRs are provided in subsequent sections, highlighting their unique behaviors and contributions to short circuit dynamics.

2.3.2.1 Synchronous Machines

During a short circuit at the terminals of SMs, the initial current can surge to a value significantly higher than its rated current before gradually decreasing to a steady-state level [52]. A key feature of the construction of SM is its external DC source, which supplies the field winding with the necessary excitation current [52, 53]. The fault current, as shown in **Figure 2.4**, shows two unique characteristics: a rapidly decreasing initial frequency, followed by slower stabilization, and a direct current component that declines exponentially over several cycles [52, 53]. During a fault, the external DC source continuously supplies excitation current, maintaining field winding voltage. Meanwhile, the turbine (or prime mover) maintains its rotation, inducing voltage in the stator winding [52, 53]. As a result, a sustained fault current is generated until the fault condition is cleared. The significant short circuit current produced by SMs directly increases the initial short-circuit capacity, emphasizing their substantial role in supporting system strength and enhancing grid resilience.

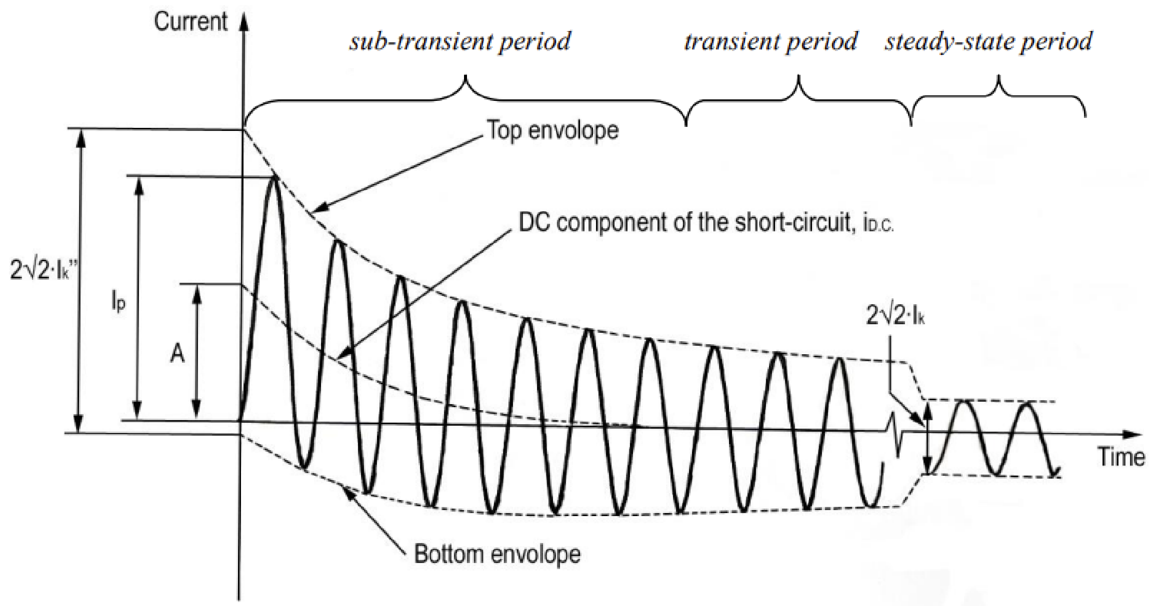

Figure 2.4: Synchronous machine short-circuit current [54].

2.3.2.2 Inverter Based Resources

IBRs, such as solar PV systems, have distinct response characteristics during short circuit events compared to SMs. This difference arises because IBRs connect to the electric network using solid-state power conversion devices, whereas SMs have inductive characteristics due to their rotating mechanisms and continuous field excitation [52]. As a result, during a short circuit, the fault currents in IBRs, primarily controlled by inverters, decrease more rapidly compared to those in SMs. This rapid decrease occurs because IBRs cannot maintain fault current through electromagnetic behavior as SMs do [52, 54]. During grid short circuit events, the response of PV systems is determined by the design of their inverters [52, 55]. In normal operation, PV systems deliver their maximum power from the PV panels. However, during a fault where the current exceeds the maximum capacity, a typical inverter protects its electronic components from thermal overload by shutting down, unless it is programmed to ride through faults [55].

2.3.3 Short Circuit Current Analysis Standard

Short circuit current analysis helps understand how electrical systems respond to stress conditions and in identifying potential weaknesses in power grid design. Several standards have been published that provide a foundation for evaluating and upgrading existing infrastructure for higher efficiency. Due to the impact of RESs on system strength and the need for mitigation methods to address this impact, understanding short circuit components is essential to ensure the grid can maintain operational reliability with high levels of RES penetration.

2.3.3.1 IEC 60909 Standard

IEC 60909 provides guidelines for calculating and measuring the generated short-circuit current waveform at specific locations in a power grid. Equations 1.1 and 1.2

introduced the SCR and WSCR, respectively. Using WSCR as an example, it can be calculated based on the IEC 60909 standard [56, 57, 58, 59].

$$WSCR = \frac{\sum_{i=1}^{N} S''_{ki} \times P_{\mathrm{Rmw}i}}{\left(\sum_{i=1}^{N} P_{\mathrm{Rmw}i}\right)^2} \tag{2.3}$$

Where S''_{ki} is the initial symmetrical short-circuit capacity of bus i at the POI in MVA. P_{Rmwi} denotes the maximum power output capacity of the IBR installed at bus i in MW. The initial symmetrical short circuit capacity S''_{ki} is calculated using the following equation [54, 56, 57, 58, 59]:

$$S''_{ki} = \sqrt{3} \times I''_{ki} \times V''_{busi} \tag{2.4}$$

Where I''_{ki} is the root mean square (RMS) value of the alternating current (AC) component at bus i at the POI in KA, and V''_{busi} is the rated voltage of bus i at the POI in KV. The initial AC component of the short-circuit current can found when applying a three-phase short circuit event as follows [54, 56, 57, 58, 59]:

$$I''_{ki} = \left(\frac{C_{\max} \cdot V''_{\mathrm{busi}}}{\sqrt{3} \cdot Z'_k}\right) = \frac{C_{\max} \cdot V''_{\mathrm{busi}}}{\sqrt{R_k^2 + X_k^2}} \tag{2.5}$$

Where:

$C_{\max}$: is the voltage factor, ranging between 0.9 and 1.1,

Z'_k : represents the impedance at the fault location during a short-circuit event,

R_k : represents the total resistance connected in series of a single phase,

X_k : represents the total reactance connected in series of a single phase.

2.4 Challenges of High Renewable Resources Penetration on System Strength and Protection

This section explores the critical distinctions between SMs and IBRs, and their implications for grid stability and protection systems. One key distinction is the contribution to grid inertia. The rotating mass found in SGs inherently provides physical inertia, which is important for stabilizing grid frequency during sudden changes in load or generation [10, 11]. This physical inertia acts as a buffer, maintaining frequency stability by storing and releasing kinetic energy [10]. In contrast, IBRs, being solid-state devices, do not possess this physical inertia [11, 16]. As a result, maintaining frequency stability in grids with a high concentration of IBRs becomes a significant challenge. Moreover, managing reactive power is essential for voltage regulation in power systems [53, 60]. SGs can effectively generate or absorb reactive power due to their electromechanical nature, aiding in voltage regulation [53]. However, inverters generally have limited capabilities in this regard, which can lead to difficulties in maintaining voltage stability [60]. Another critical difference lies in fault current capabilities. SGs are capable of supplying high fault currents, facilitating clear fault detection within the grid, while inverters typically generate limited fault currents, making fault detection more challenging in grids dominated by IBRs [52]. The response of systems with high IBR penetration to short circuit events can strain the capabilities of existing protection systems. This situation necessitates modifications and enhancements to ensure effective detection and isolation of faults.

2.4.1 Voltage Stability

Voltage stability is defined as the ability of the system to sustain consistent voltage levels at all bus locations following a disturbance [61]. The integration of IBRs requires a robust system that can handle sudden increases in power demand, enhance power quality, and maintain voltage within desirable limits [11, 60]. In fact, reactive power compensation and voltage control limits are significant influencers in the domain of voltage stability [53, 60, 62, 63]. The dynamic response of IBRs to voltage disturbances is determined by the employed control strategies, which, if not properly designed, can sometimes lead to instability events known as voltage collapse [62]. For instance, the inverter might reduce its output to protect itself during a fault, potentially worsening a low-voltage situation [55]. IBRs typically contribute less to system short-circuit capacity compared to traditional SGs, resulting in slower voltage recovery after faults and, consequently, reduced voltage stability. Chapter 5 in this dissertation provides a comprehensive investigation into mitigating voltage instability when high levels of solar PV are integrated into the Saudi electric grid.

2.4.2 Frequency Stability

Frequency stability is defined as the ability to maintain a consistent frequency during operation and return to a steady state after a major disruption that causes a mismatch between supply and demand [61]. Inertia, in power systems, represents the kinetic energy provided by rotational force within the grid [10, 64]. IBRs, such as solar PV, differ from traditional generators since they lack rotating components [10, 11]. A power system with high inertia is less likely to experience large frequency deviations after an unexpected loss of generation or load, while systems with low inertia are more sensitive to these changes, leading to a higher rate of change of frequency (RoCoF) [11]. Chapter 6 in this dissertation provides a comprehensive investigation into enhancing frequency stability when high levels of solar PV are integrated into the Saudi electric grid.

2.4.3 System Protection

Protection in power systems is primarily focused on the detection and isolation of faults to ensure the safety, reliability, and efficiency of the electrical network [65]. IBRs present new challenges in the field of system protection [13, 52, 66, 67, 68].

As previously mentioned, IBRs and SGs have significantly different fault current characteristics, which impact the performance of protection schemes [52, 54]. One critical aspect is the reduced fault current contribution from IBRs compared to conventional generators, which may affect the sensitivity and selectivity of overcurrent protection devices [14, 69]. This reduction in fault current can lead to delayed or even failed detection of faults, posing a risk to system stability and equipment safety [11]. Additionally, IBRs are configured to disconnect in the event of a short circuit to prevent thermal overload at their terminals [55, 66]. Chapter 7 of this dissertation explores system protection at SEC, focusing on the impact caused by IBRs and potential solutions to enhance fault detection and isolation in grids with high IBR penetration, ensuring both operational safety and system reliability.

2.5 Grid Strength Solutions

To enhance the ability of power grids to resist and recover from disturbances, several solutions can be implemented to increase the inherent strength of the system and improve its ability to respond to varying load and generation conditions. Considerations include enhancing physical infrastructure and improving operational strategies, as outlined below:

- Add synchronous condensers.
- Add transmission lines.
- Overdesign inverters with high short-circuit capability.
- Reduce IBR output or power curtailment.
- Improve IBR control.

Chapter 3

Analyzing the Impact of Solar PV Integration on the Power System Strength, Inertia, and Protection

3.1 Introduction

This chapter investigates the impact of gradually increasing solar PV penetration on system strength, with a specific focus on how replacing SGs with IBRs affects the SCMVA. As solar PV penetration increases, the dynamics of SCMVA levels change, reflecting the adaptive nature of the power grid. This shift influences system strength indicators such as the SCR and WSCR, essential metrics for assessing grid stability and resilience.

Additionally, a widely recognized method for determining the maximum power that IBRs can generate at a POI is referred to as 'Hosting Capacity'. This concept refers to the maximum capacity that a specific location on the power grid can accommodate without exceeding predefined system strength requirements. NERC employs the SCR as an indicator of grid strength. It suggests maintaining an SCR of at least 3 at any given location to ensure adequate system robustness. By assessing hosting capacity, planners can determine the acceptable amount of power that IBRs can produce at a POI while maintaining the desired SCR level, thereby ensuring that the preferred level of grid stability is maintained.

The analysis further extends to examine the effects of increasing solar PV penetration on voltage, frequency, and fault current responses. Understanding these factors is significant for recognizing the broader implications of solar PV integration, as power system stability and protection are fundamental to the overall health and efficiency of the electric grid.

3.2 Evaluating Power Grid Strength with Incremental Increases in Solar PV Penetration

The investigation begins by examining the baseline scenario with 0% solar PV penetration, gradually increasing to a full 100% penetration. This incremental analysis allows for a comprehensive understanding of how sequential changes in solar PV penetration affect the SCMVA and strength indicators.

3.2.1 Impact on Short Circuit MVA levels

As previously indicated in Chapter 2, SCMVA levels are affected by the reduction in fault current due to the distinct characteristics of IBRs compared to SGs. The highest SCMVA level occurs when the power system operates entirely with conventional generation, as illustrated in **Figure 3.1**. Conversely, as solar PV is incrementally integrated into the grid, the SCMVA begins to decrease as presented in **Figures 3.2** to **3.6**. For a better understanding of this effect, **Figures 3.7** to **3.11** present the ΔSCMVA%, which represents the percentage variation in SCMVA from the original

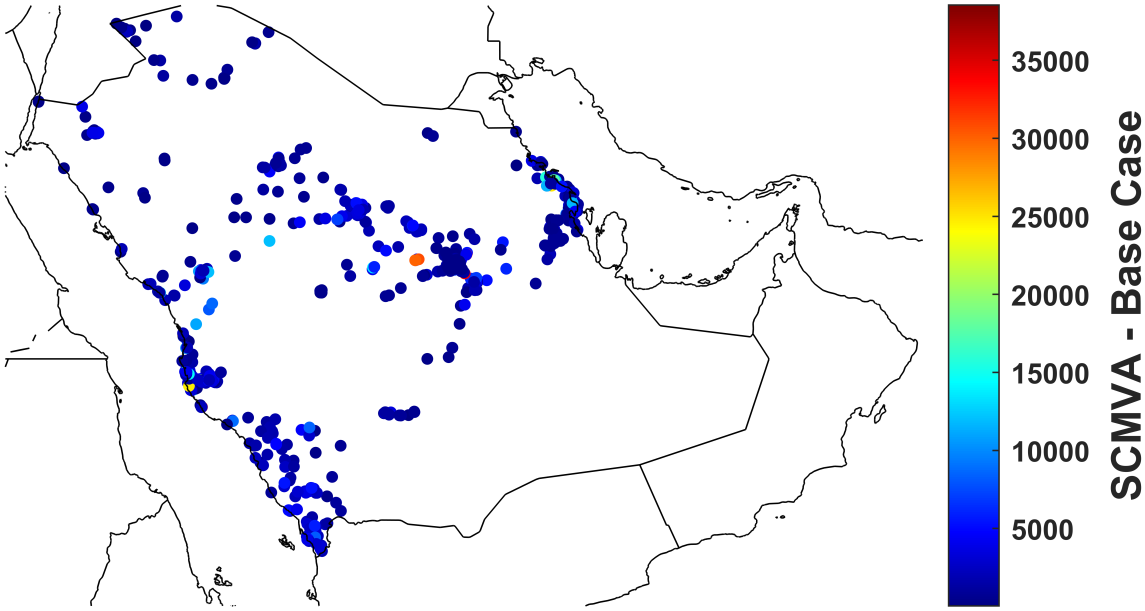

Figure 3.1: SCMVA at the base case with 0% solar PV penetration.

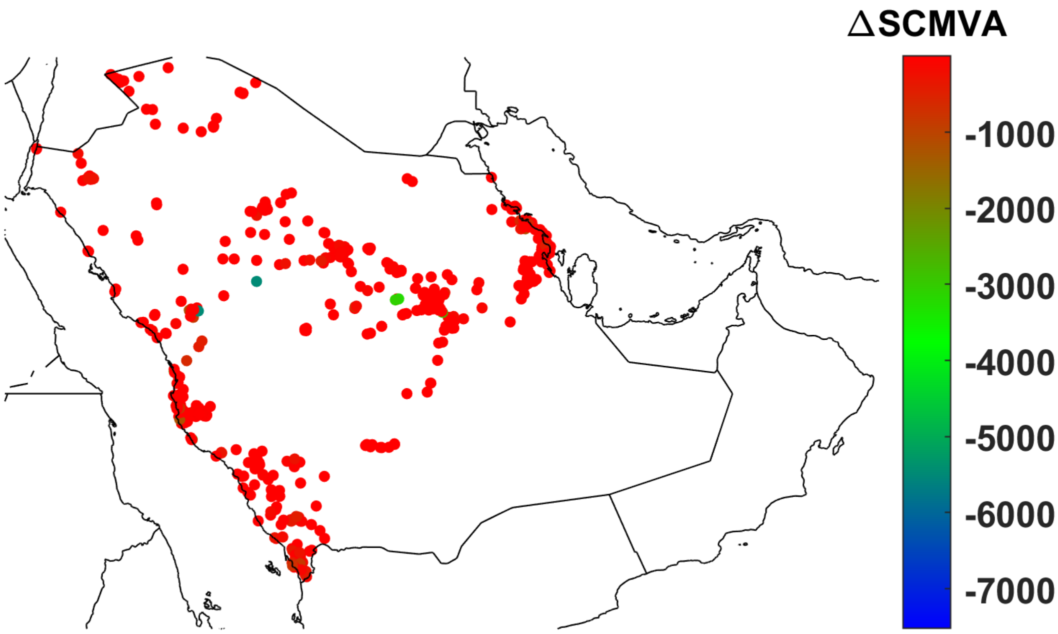

Figure 3.2: SCMVA reduction with 20% solar PV penetration.

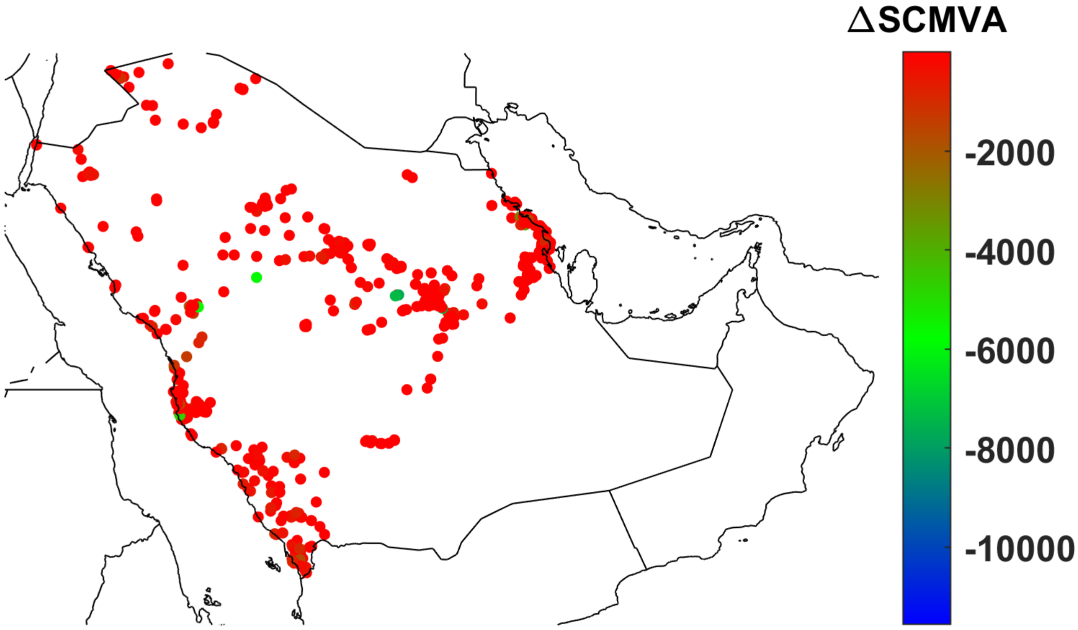

Figure 3.3: SCMVA reduction with 40% solar PV penetration.

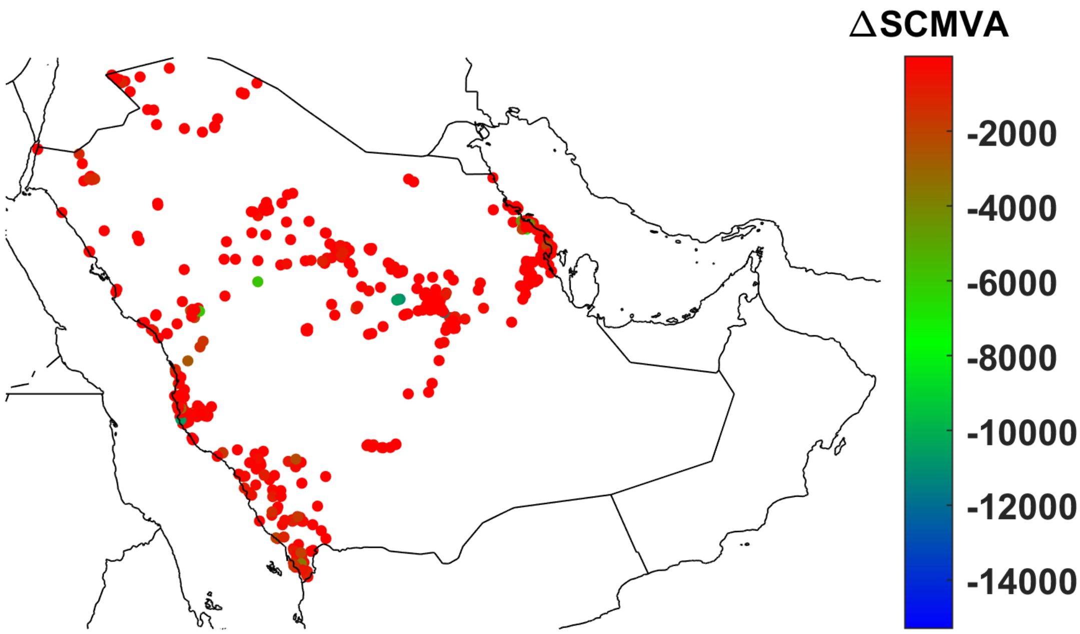

Figure 3.4: SCMVA reduction with 60% solar PV penetration.

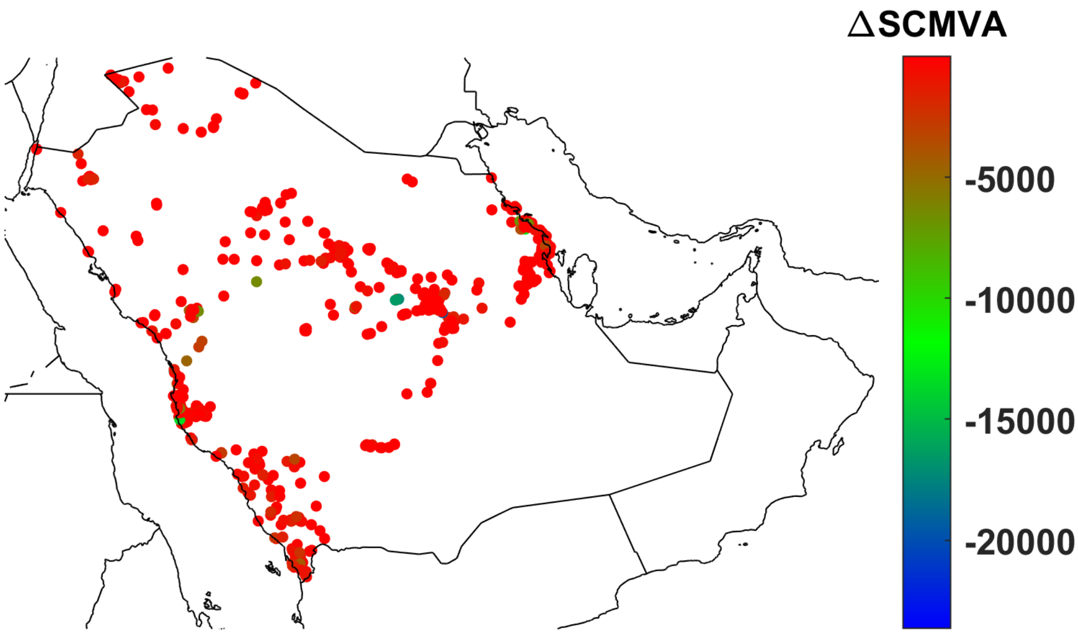

Figure 3.5: SCMVA reduction with 80% solar PV penetration.

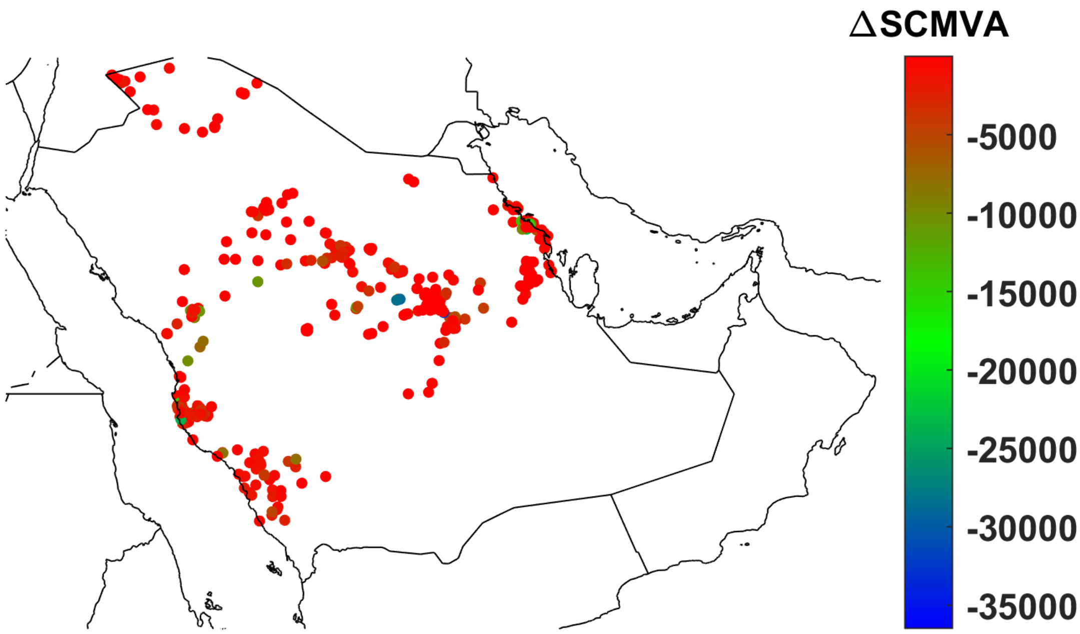

Figure 3.6: SCMVA reduction with 100% solar PV penetration.

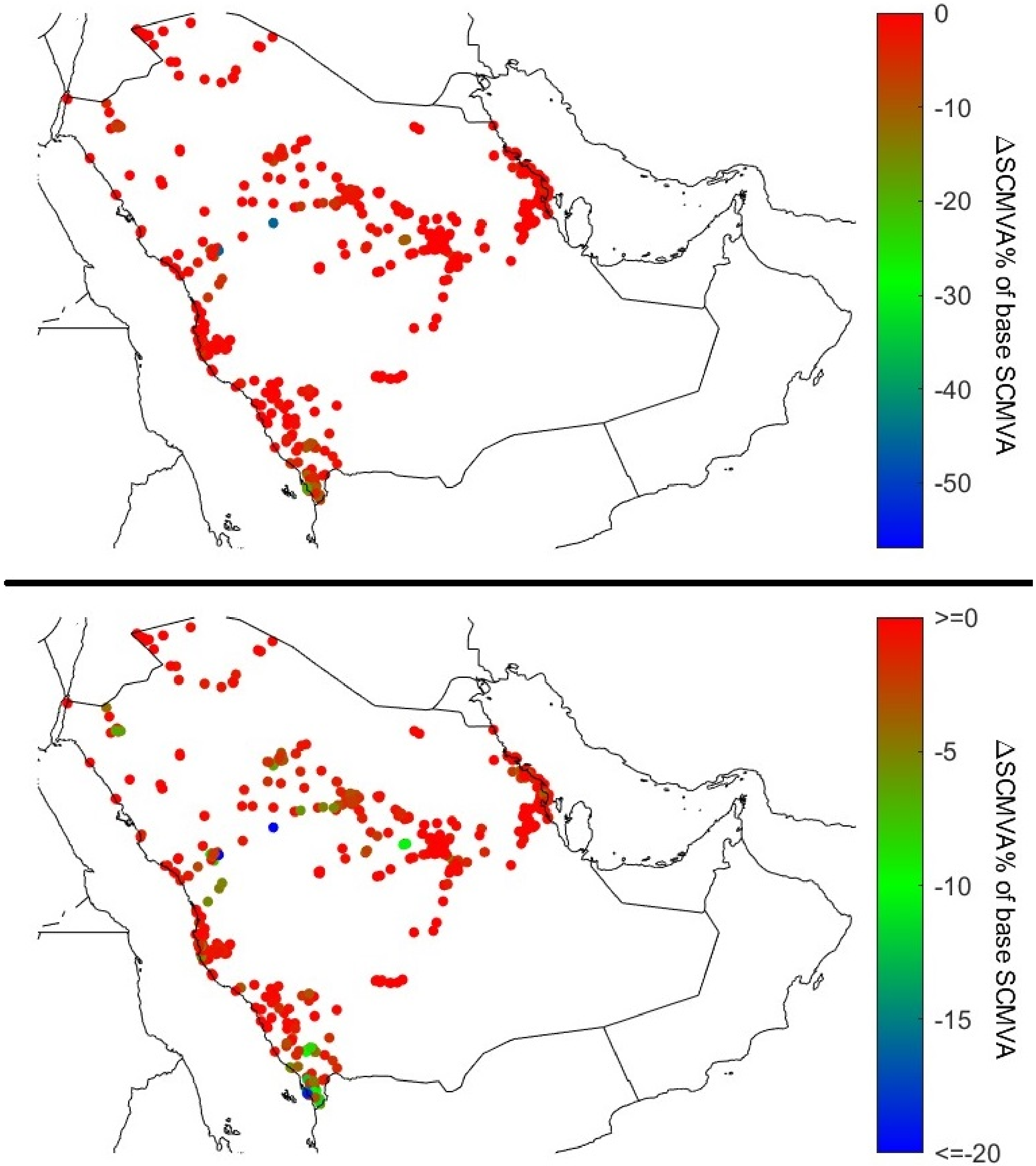

Figure 3.7: ΔSCMVA% with 20% solar PV penetration.

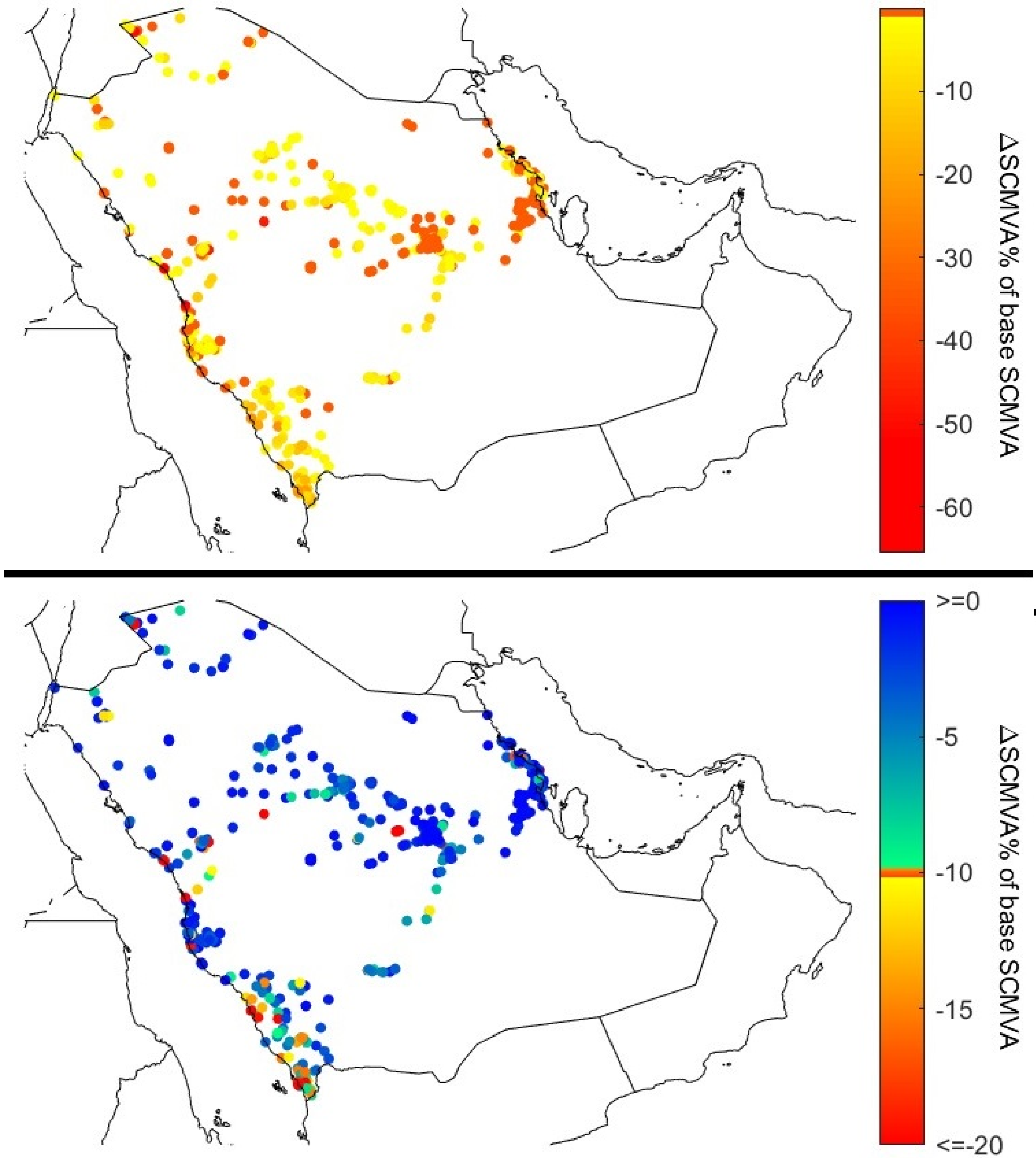

Figure 3.8: ΔSCMVA% with 40% solar PV penetration.

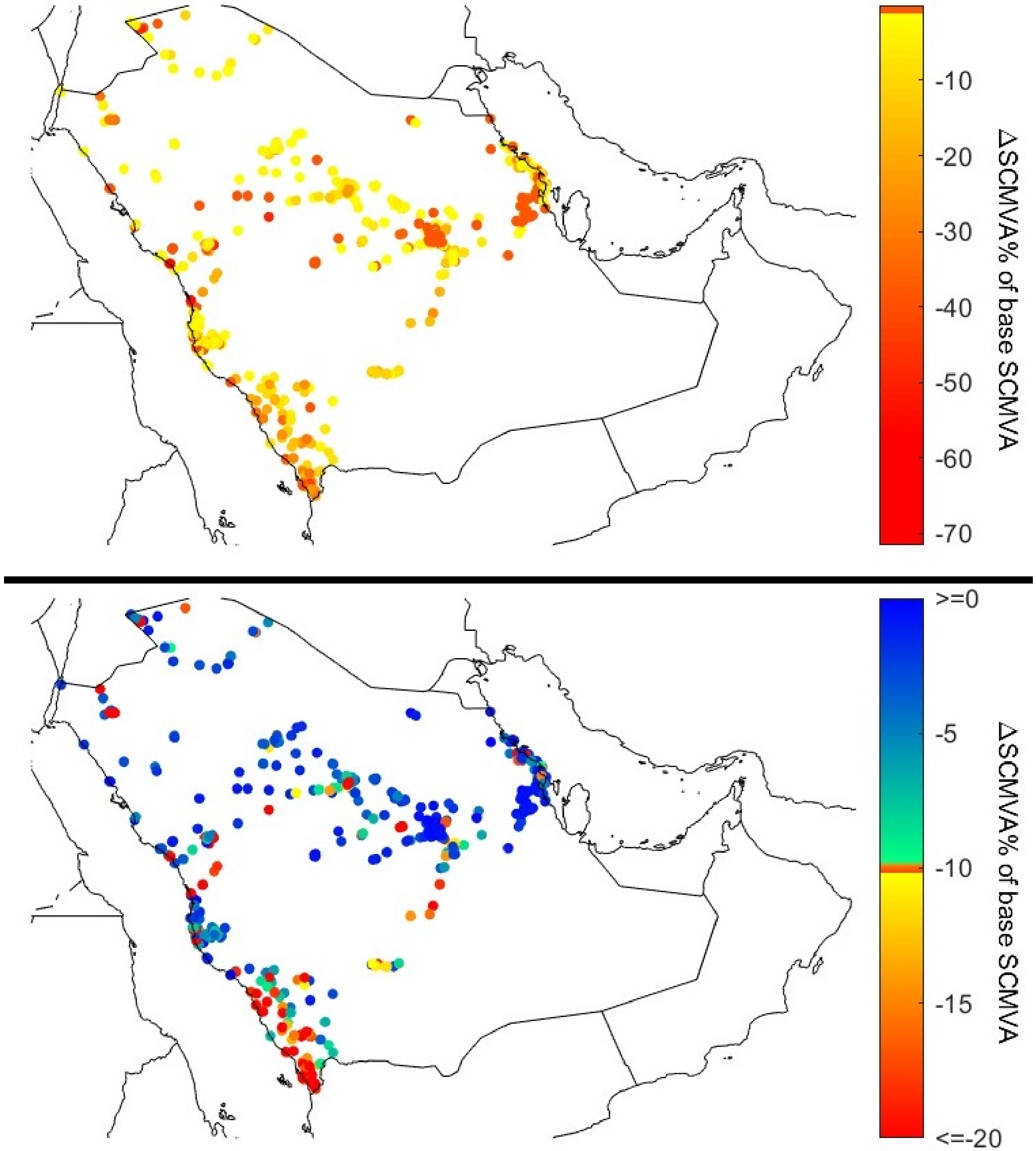

Figure 3.9: ΔSCMVA% with 60% solar PV penetration.

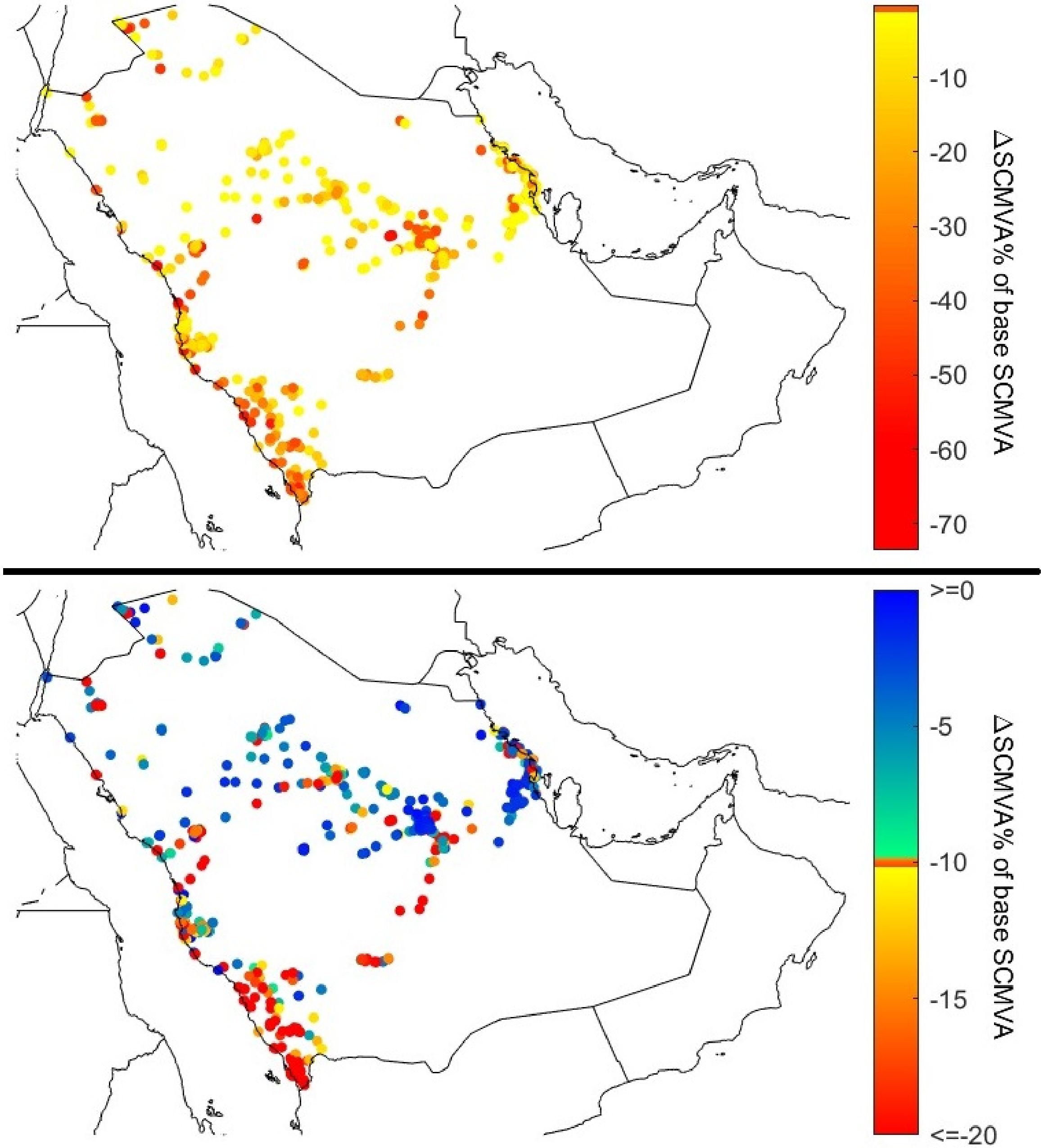

Figure 3.10: ΔSCMVA% with 80% solar PV penetration.

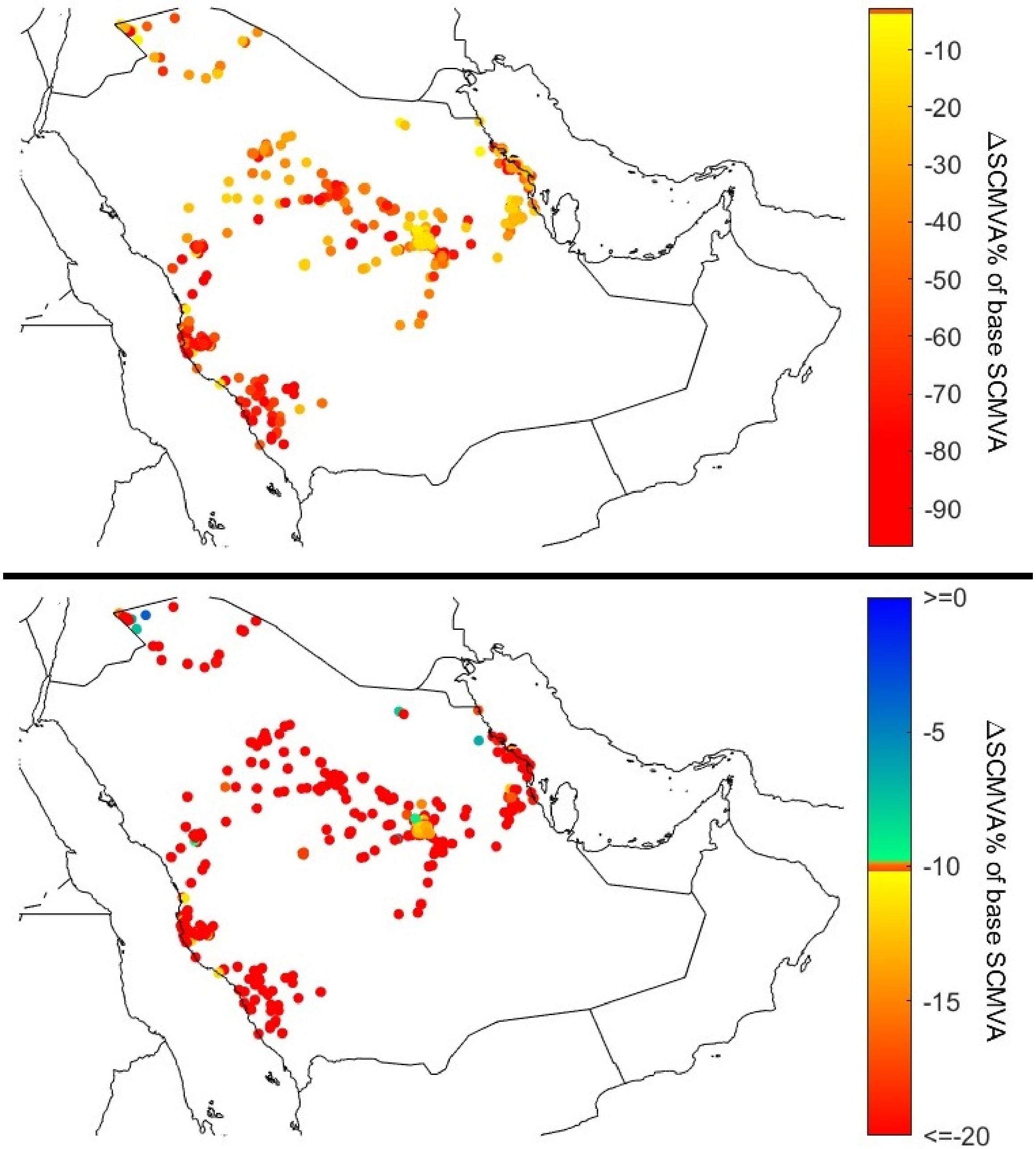

Figure 3.11: ΔSCMVA% with 100% solar PV penetration.

case (0%PV), given in Equation 3.1 as follows [70]:

$$\Delta\text{SCMVA}\% = \frac{SCMVA_{\text{integrated case}} - SCMVA_{\text{base case}}}{SCMVA_{\text{base case}}} \tag{3.1}$$

More detailed data for all buses within the Saudi power grid model can be seen in **Tables A.1** to **A.17** in Appendix A.

3.2.1.1 Influence on system strength indicators (SCR & WSCR)

In Chapter 2, the SCR and WSCR were introduced and defined in Equations 2.1 and 2.2 respectively. These indicators are directly tied to SCMVA capacity. A decrease in SCMVA has a direct and significant effect on these indicators, highlighting their importance in maintaining grid strength. To illustrate this, **Figures 3.12** to **3.17** show how solar PV integration influences the SCMVA, and as a result negatively impacts SCR across different bus locations in the Saudi power grid. Similarly, **Figures 3.18** and **3.19** depict the impact of solar PV integration on WSCR at different regions, offering a comparative view of its effects.

3.2.2 Inverter-Based Resources Hosting Capacity

Hosting capacity plays a crucial role in integrating IBRs into power grids. It determines the maximum new generation capacity that the current grid can support without requiring significant infrastructure upgrades or compromising reliability. This metric is a core factor for strategic planning, ensuring that any added IBRs are compatible with the existing capabilities of the power grid. Understanding hosting capacity is essential to avoid operational issues like frequency and voltage instability, thereby facilitating a smoother transition to renewable energy sources.

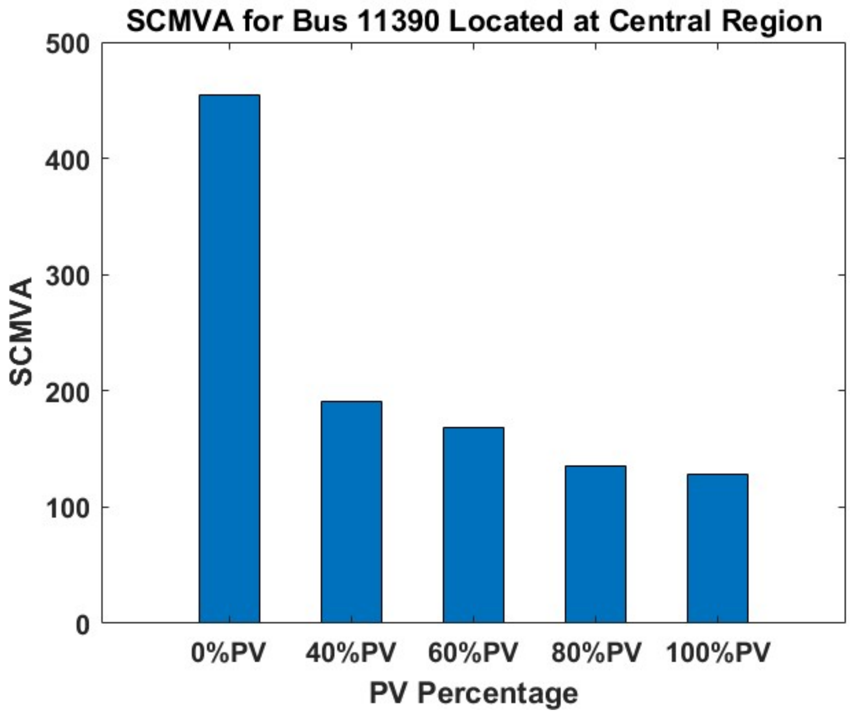

Figure 3.12: SCMVA reduction at bus 11390 (Central region).

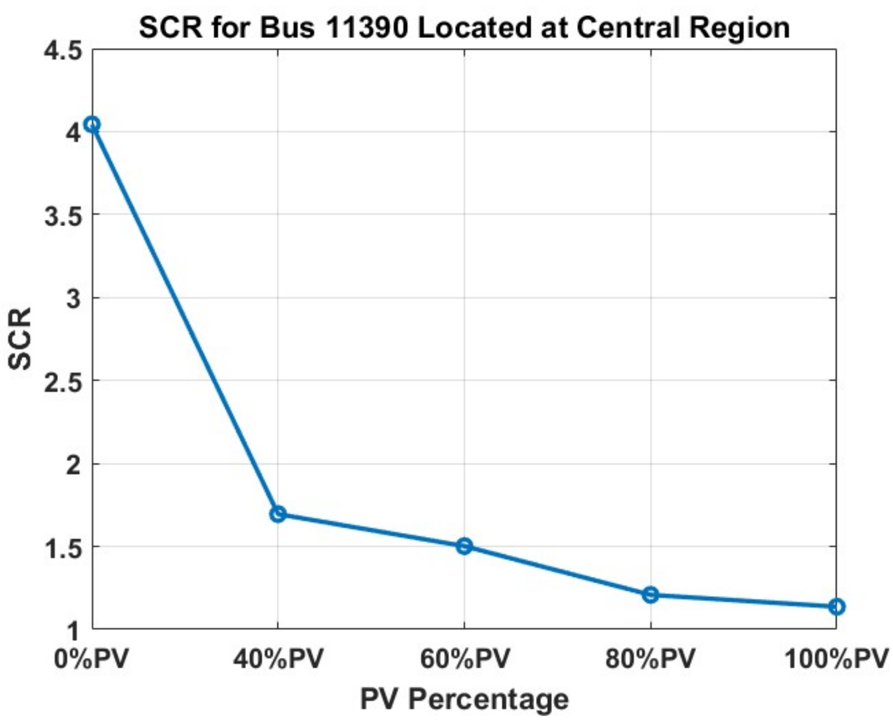

Figure 3.13: SCR decline vs. different solar PV penetration levels at bus 11390.

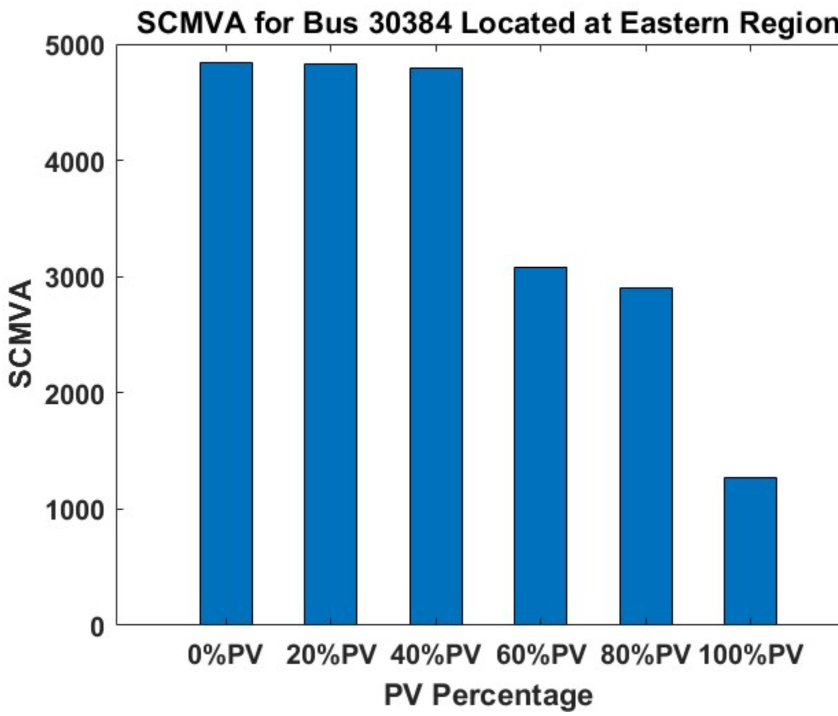

Figure 3.14: SCMVA reduction at bus 30384 (eastern region).

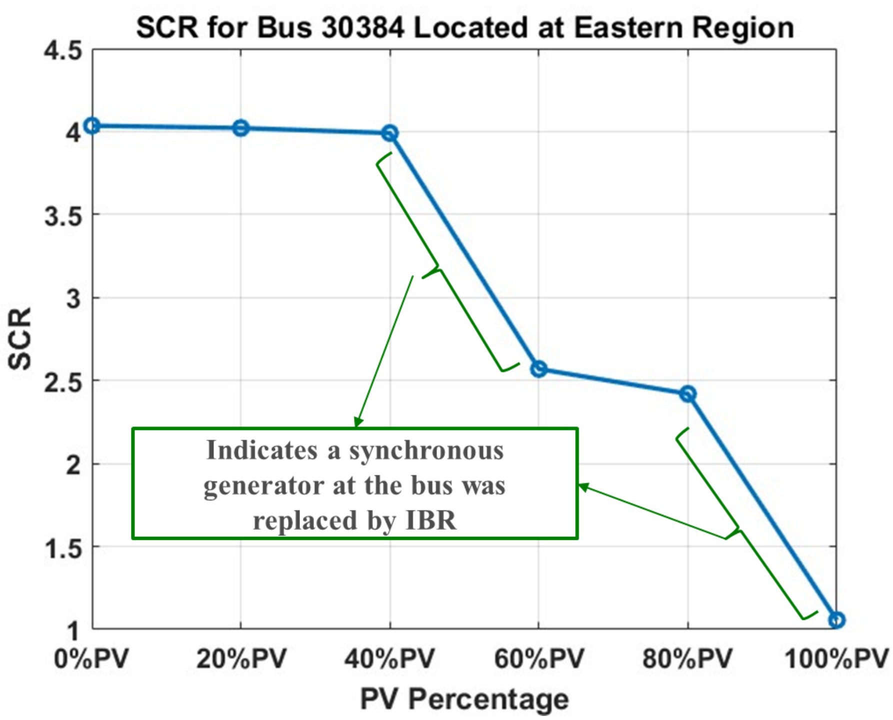

Figure 3.15: SCR decline vs. different solar PV penetration levels at bus 30384.

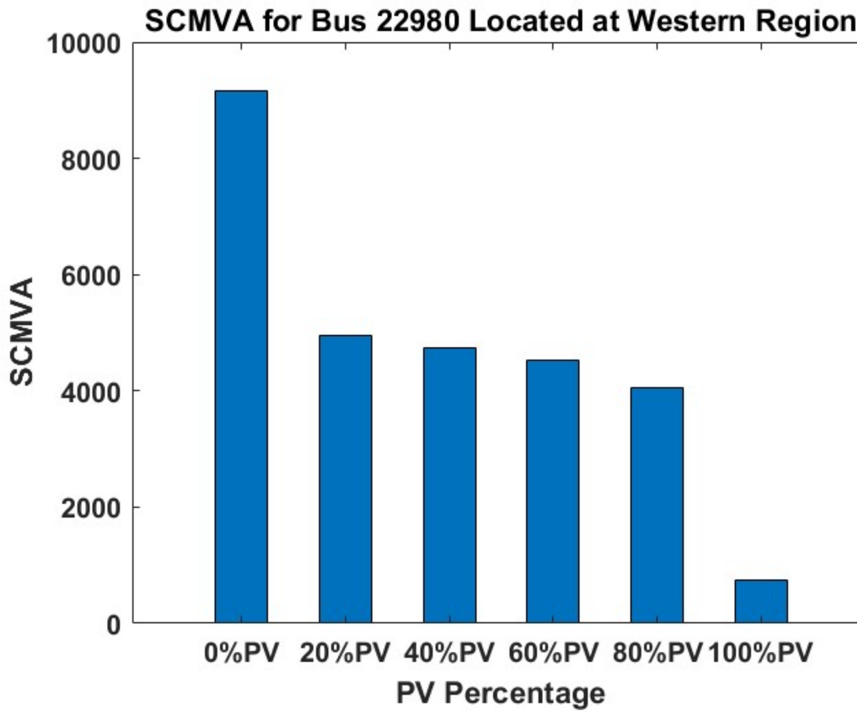

Figure 3.16: SCMVA reduction at bus 22980 (western region).

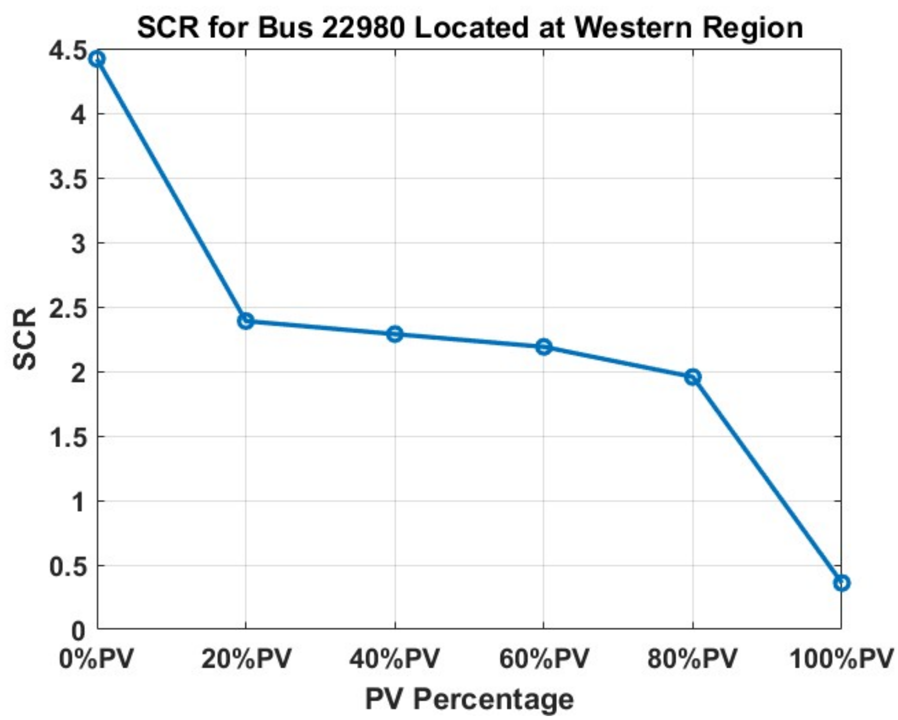

Figure 3.17: SCR decline vs. different solar PV penetration levels at bus 22980.

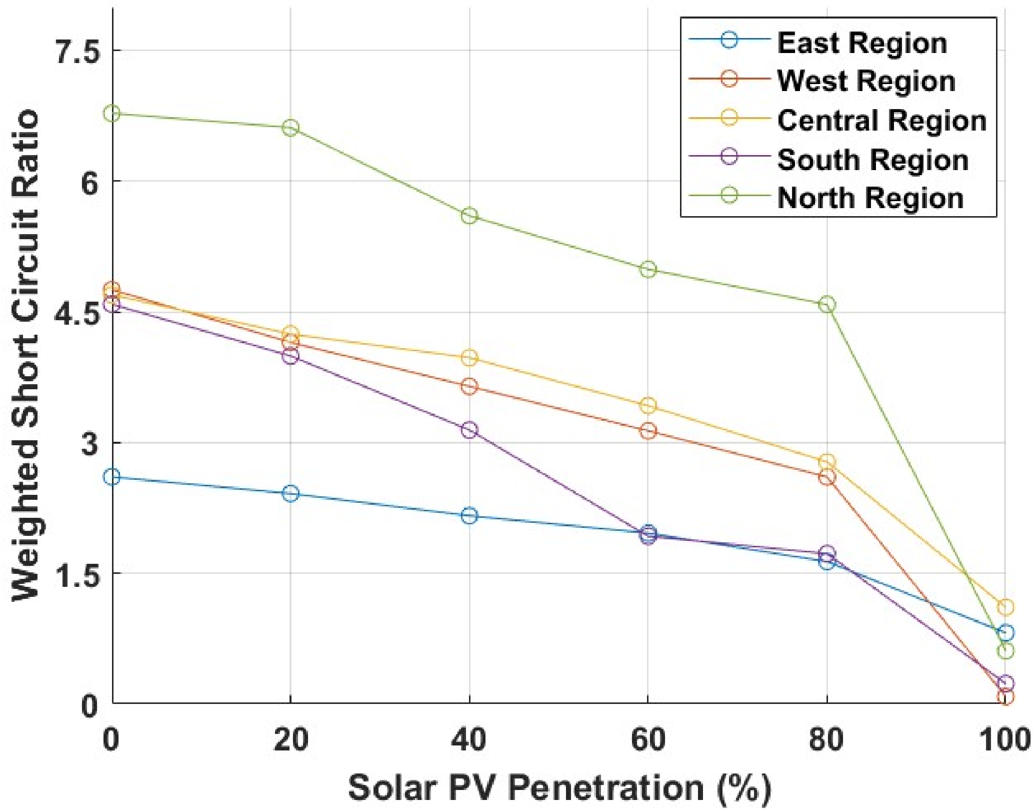

Figure 3.18: WSCR decline vs. different solar PV penetration levels.

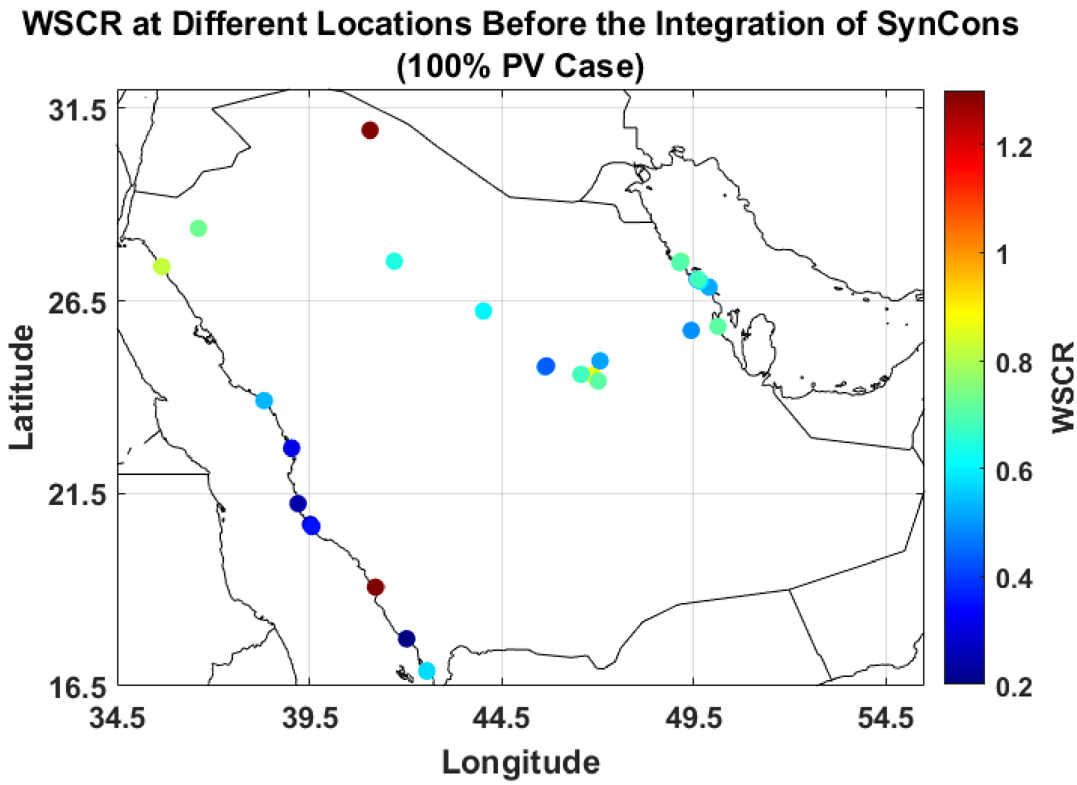

Figure 3.19: WSCR at 100% solar PV penetration.

To determine the hosting capacity, the desired SCR that a grid planner aims to maintain must first be established. **Figures 3.20** to **3.25** illustrate the maximum rated power that IBRs with various solar PV penetration can generate without causing the SCR to fall below 3. From these figures, it can be concluded that as solar PV penetration increases, the hosting capacity becomes lower. Furthermore, Equation 3.2 presents the formula for calculating hosting capacity as follows:

$$\text{Hosting Capacity}_i(\text{P}_{\text{RMW}}) = \frac{\text{Short Circuit MVA}_i}{\text{Desirable Short Circuit Ratio}} \tag{3.2}$$

where i is the bus number and hosting capacity is in MW.

3.2.3 Inverter-Based Resources Hosting Capacity

The concept of hosting capacity is important in the integration of IBRs into power grids. It determines the maximum new generation capacity, such as solar PV, that the current grid can support without requiring significant infrastructure upgrades or compromising reliability. This metric is a core factor for strategic planning, ensuring that any added IBRs are compatible with the existing capabilities of the power grid. Understanding hosting capacity is essential to avoid operational issues like frequency and voltage instability, thereby facilitating a smoother transition to renewable energy sources.

3.2.4 Voltage Response Impact with Incremental Increases in Solar PV Penetration

As previously discussed, the limited reactive power compensation capability of IBRs complicates their ability to enhance proper voltage recovery post-disturbance. Unlike traditional SGs, which inherently provide both active and reactive power support, IBRs often require additional control mechanisms or external devices to manage reactive power effectively. As a result, when disturbances occur, IBRs may struggle

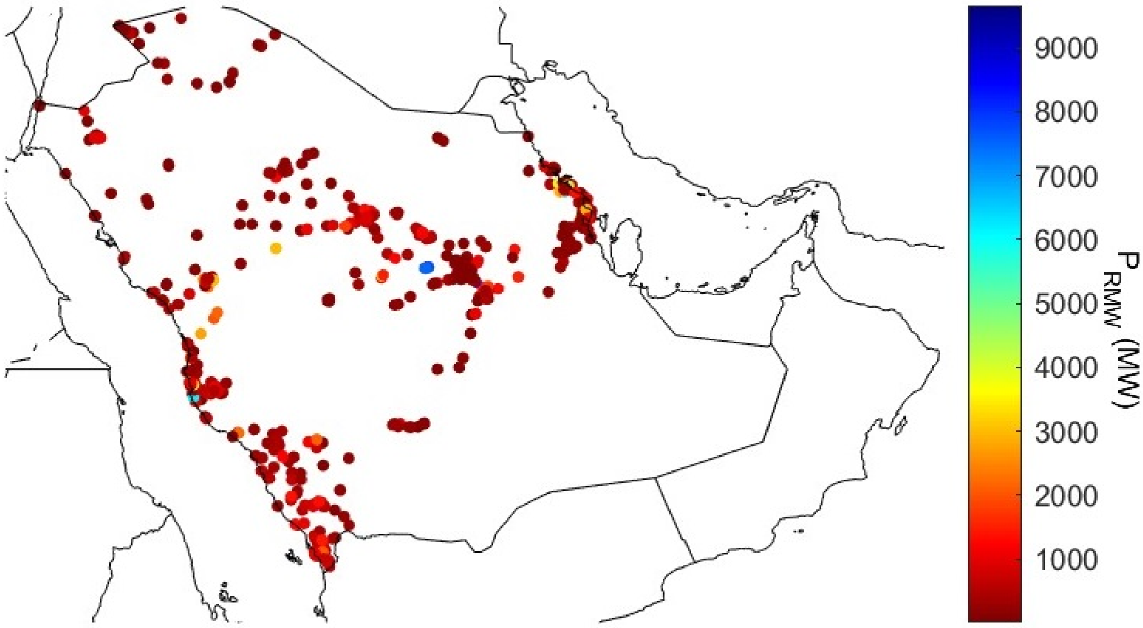

Figure 3.20: Hosting capacity in the Saudi grid with 0% solar PV penetration.

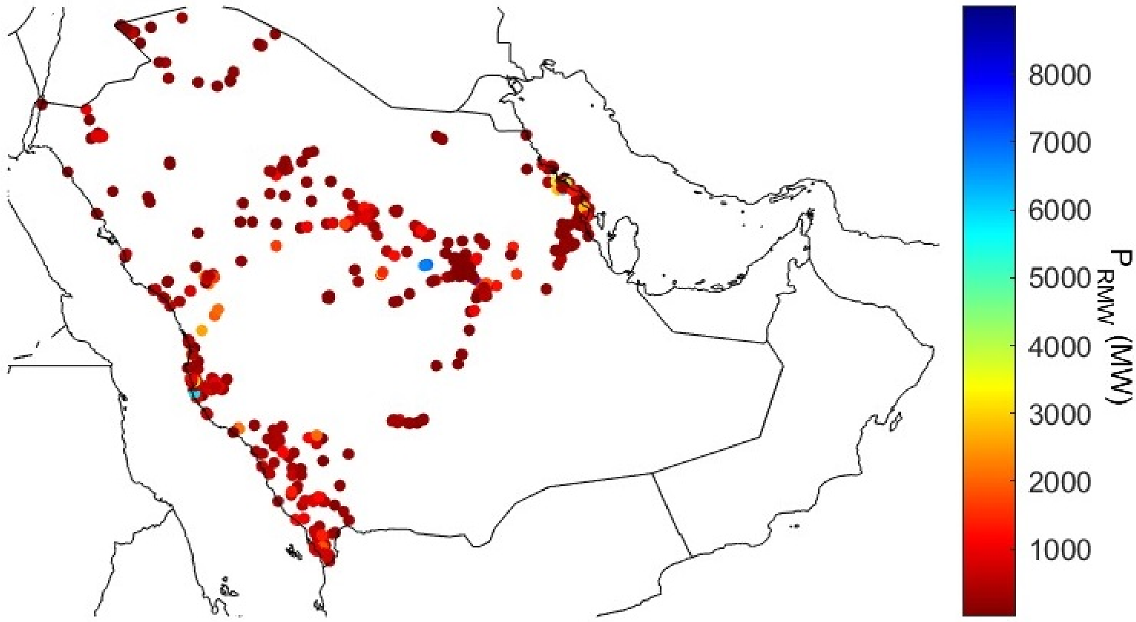

Figure 3.21: Hosting capacity in the Saudi grid with 20% solar PV penetration.

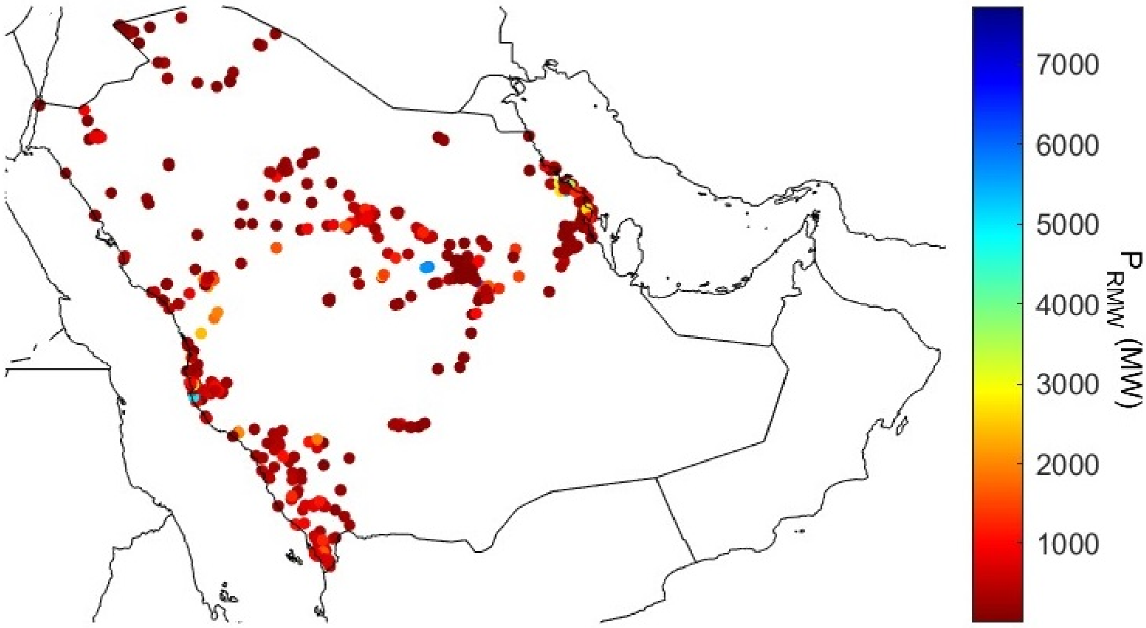

Figure 3.22: Hosting capacity in the Saudi grid with 40% solar PV penetration.

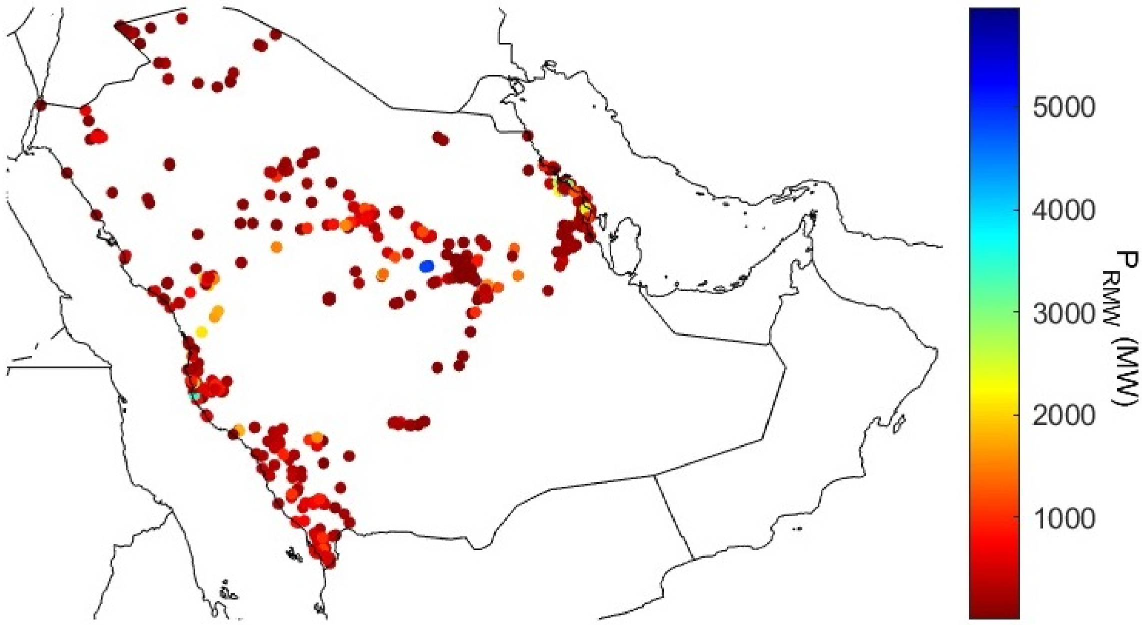

Figure 3.23: Hosting capacity in the Saudi grid with 60% solar PV penetration.

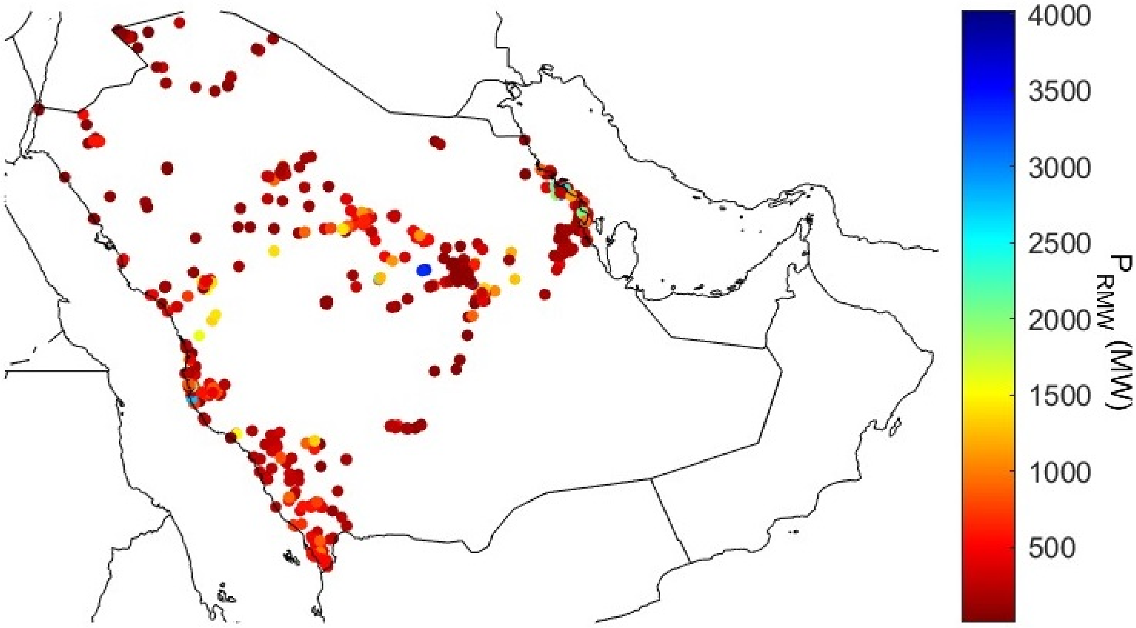

Figure 3.24: Hosting capacity in the Saudi grid with 80% solar PV penetration.

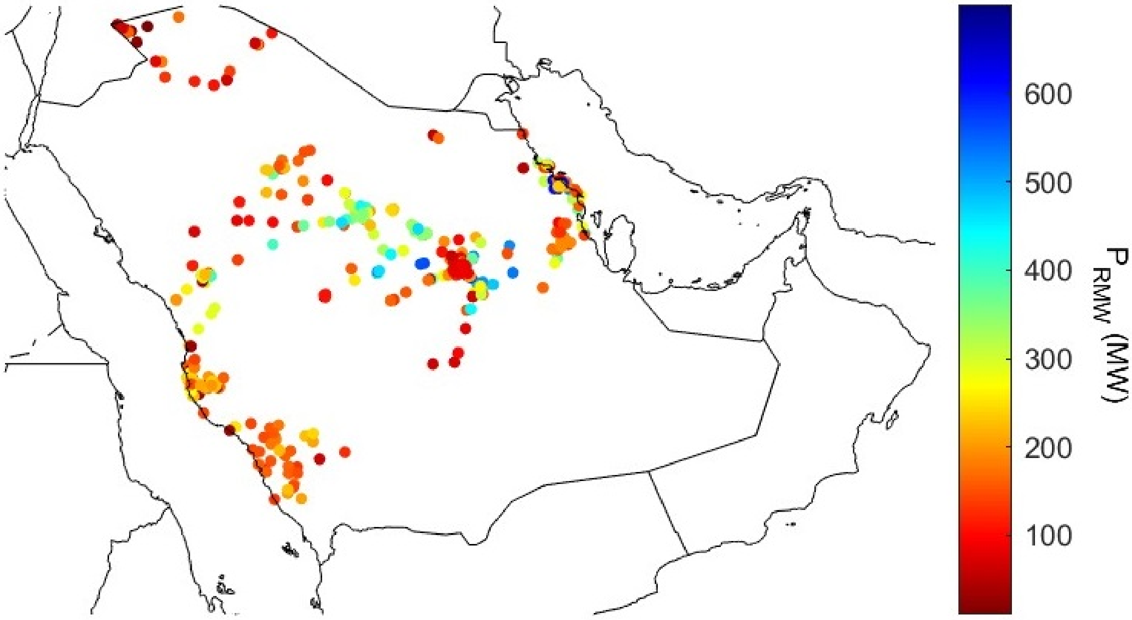

Figure 3.25: Hosting capacity in the Saudi grid with 100% solar PV penetration.

to provide the necessary reactive power to stabilize voltage levels. This limitation becomes clearer as these resources become more dominant, leading to a gradual decline in the ability of the grid to swiftly recover voltage to steady-state levels post-contingency. The increased reliance on IBRs without sufficient reactive power support can result in delayed voltage recovery or even voltage collapse under certain conditions, as illustrated in **Figure 3.26**. This emphasizes the importance of carefully managing the integration of solar PV and other IBRs to ensure grid stability [71].

3.2.5 Frequency Response Impact with Incremental Increases in Solar PV Penetration

The inertia provided by spinning SGs plays a critical role in compensating for power losses following a contingency, ensuring the stability and resilience of the power grid. As indicated in Chapter 2, the increased adoption of IBRs, which lack rotational components, notably reduces available inertia within the network. This reduction weakens the ability of the grid to resist changes in frequency, making it more subject to deviations during disturbances. As IBRs continue to integrate into power grids and reduce SCMVA levels, they also impact the frequency response. The reduction in inertia requires faster and more advanced compensation devices to prevent significant frequency dips and effectively restore stability. **Figure 3.27** illustrates the frequency response as the integration of solar PV increases [72].

3.2.6 Protection System Impact with Incremental Increases in Solar PV Penetration

As previously indicated, the reduction in fault current associated with IBRs integration creates significant challenges for protection system components. Lower current levels can make fault detection difficult, as they may be closer to normal

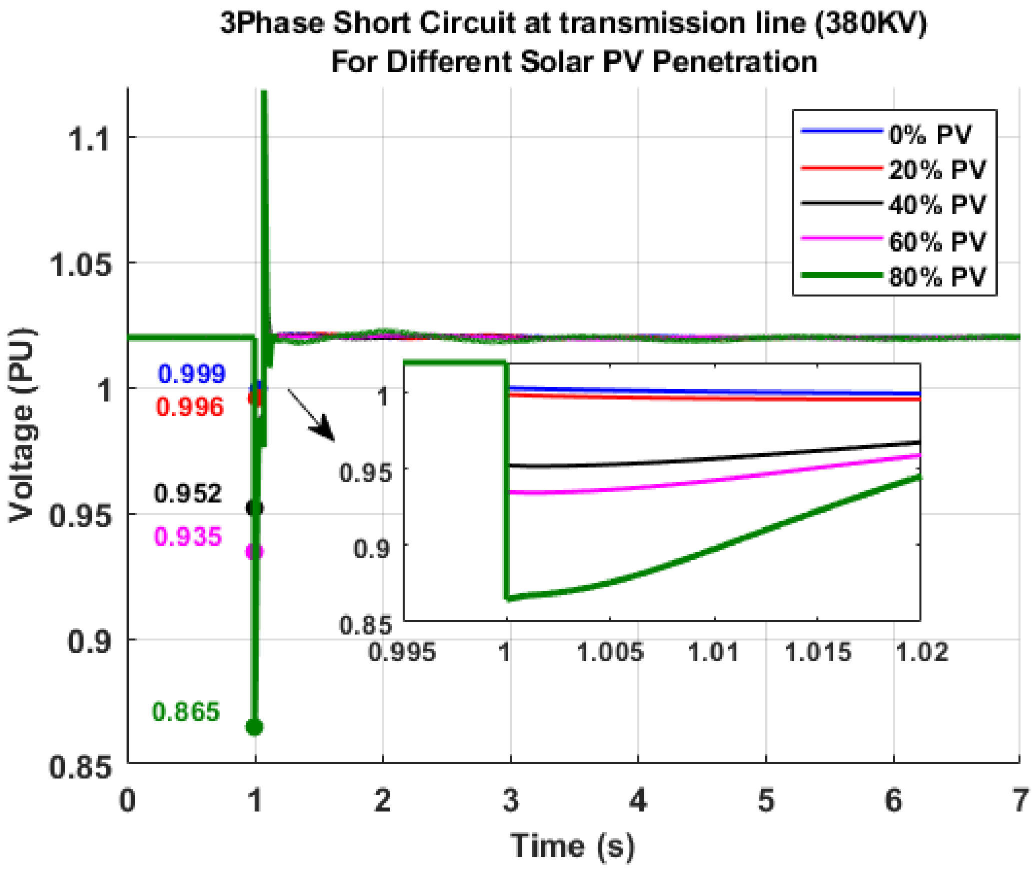

Figure 3.26: Voltage response to a contingency with different levels of solar PV penetration.

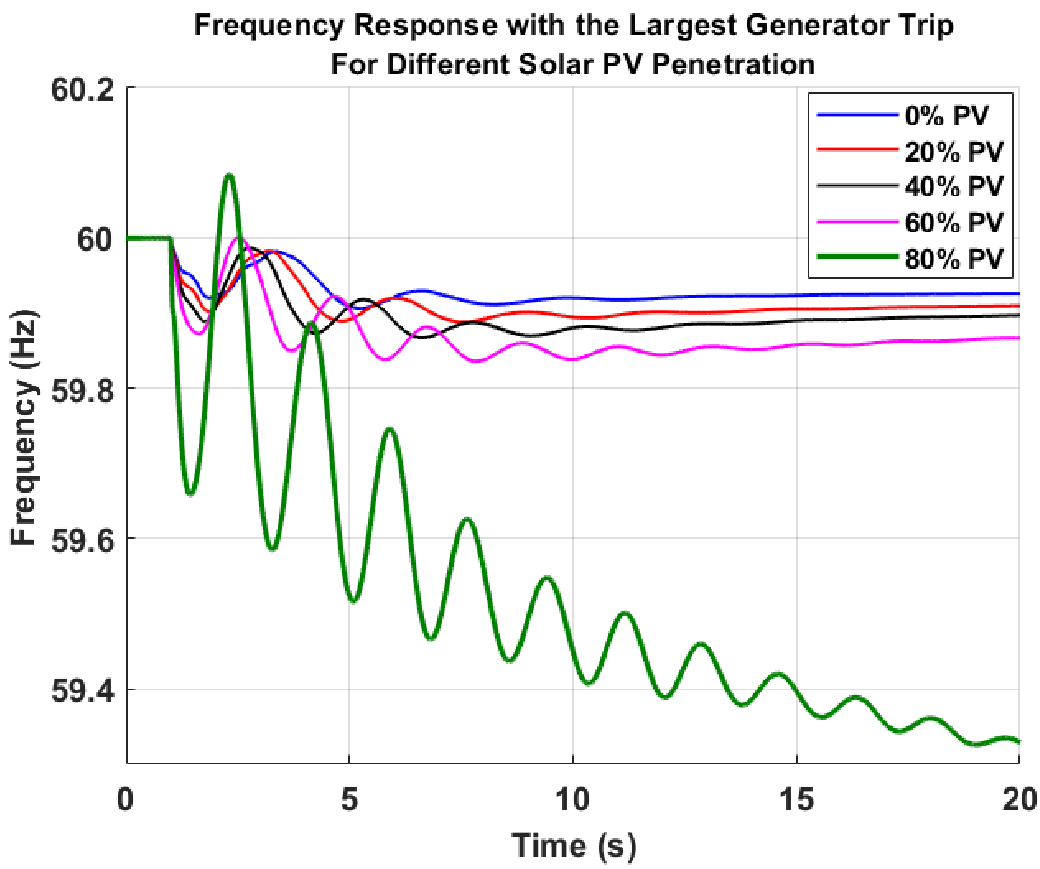

Figure 3.27: Frequency response to a contingency with different levels of solar PV penetration.

operating conditions, making it harder for protection relays to accurately distinguish between regular load behavior and fault situations where tripping is necessary. Inverters are equipped with terminal protection to prevent overheating, and will immediately disconnect during a short-circuit event unless they are properly programmed and controlled to ride through faults [55]. This immediate shutdown can negatively impact system stability if not managed correctly, particularly in scenarios with high IBR penetration. **Figure 3.28** illustrates the fault current during a 3-phase short-circuit event, comparing scenarios with SGs and IBRs. **Figures 3.29** and **3.30** indicate how fault current levels decrease as IBRs integration increases [55].

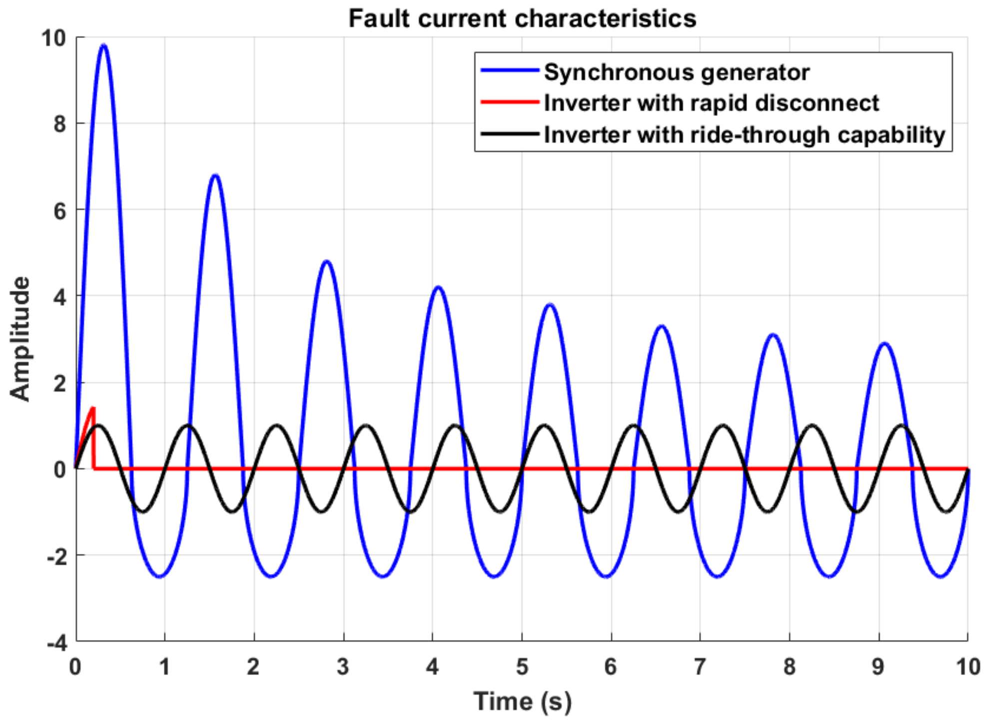

Figure 3.28: Fault current responses for different cases.

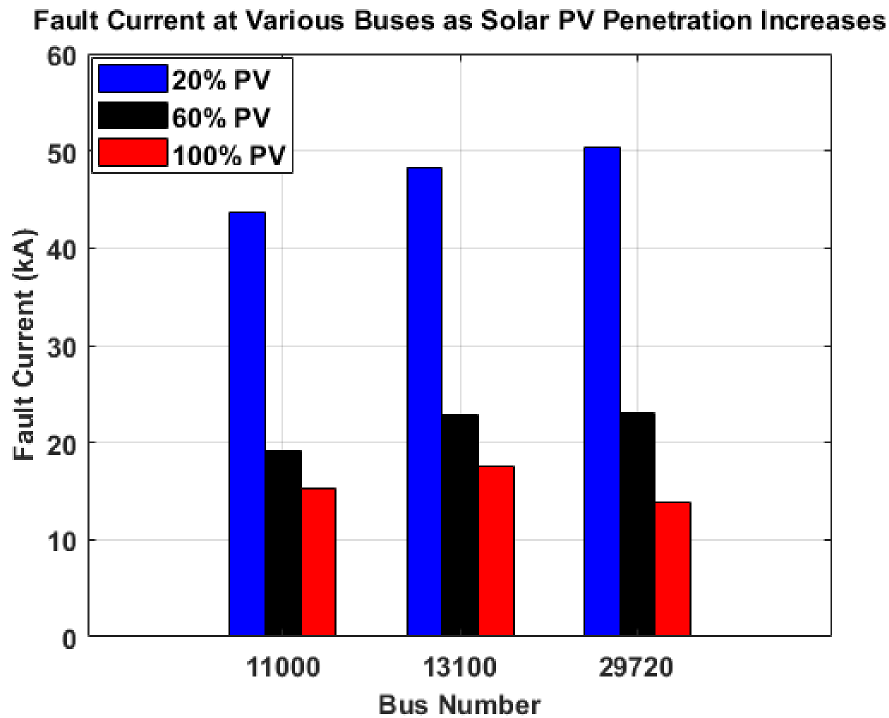

Figure 3.29: Fault current reduction as solar PV increase.

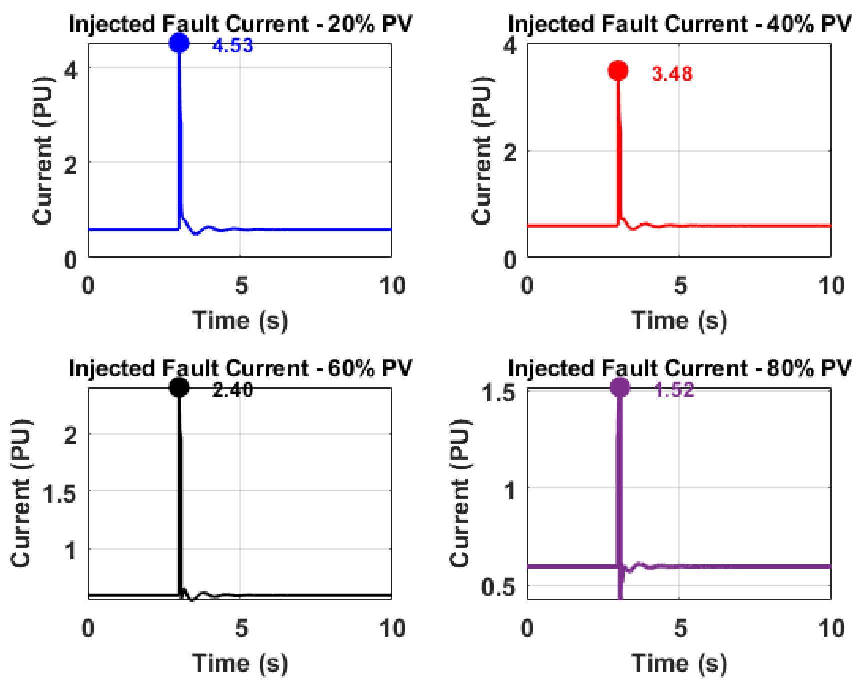

Figure 3.30: Fault current reduction among different solar PV penetration levels.

Chapter 4

The Role of Synchronous Condensers in Power System Improvement

4.1 Introduction

In recent years, the prominence of SynCons has grown significantly in the electricity generation sector [73, 74]. This shift is largely driven by the accelerated retirement of traditional SGs and the growing reliance on RESs, which have introduced new challenges in maintaining the robustness and stability of power systems [9, 12, 18, 20, 73]. Among the key challenges are reductions in short-circuit capacity, declines in system inertia, and a lack of reactive power compensation [10, 11, 12, 74]. In response, the deployment of SynCons has significantly expanded, as they offer a promising solution to these stability issues. SynCons can generate reactive power and provide both high short-circuit capacity and system inertia, making them significant components in modern power grids [75].

4.2 Operation Principle and Applications

SynCon, a form of synchronous motor, operates without a mechanical load such as a turbine [75, 76]. Their essential function is to regulate voltage levels and improve the power factor (PF) within the electrical grid [75, 77]. This is accomplished by dynamically producing or consuming reactive power in response to grid conditions [75, 77]. SynCons can operate in two modes, similar to synchronous motors, as depicted in **Figure 4.1** [78, 79, 80].

Typically, SynCons are operated in an over-excited mode, resulting in a leading PF [78]. In this mode, they supply reactive power to the grid, enhancing voltage support and stability. Conversely, when SynCons operate in an under-excited mode, they display a lagging power factor, thereby absorbing reactive power from the electrical system [81]. The mathematical characterization of SynCons is governed by the following differential equations, which describe their dynamic behavior [53, 78]:

$$\frac{d\delta}{dt} = (\omega - \omega_s) \tag{4.1}$$

$$\frac{d\omega}{dt} = \frac{1}{T_J}(-P_e - D\omega) \tag{4.2}$$

$$\frac{dE'_q}{dt} = \frac{1}{T'_{d0}}(-E'_q - (X_d - X'_d)i_d + E_{fq}) \tag{4.3}$$

where δ is the rotor angle relative to the stator, ω is the rotor angular velocity, ω_s is the synchronous speed, P_e represents the electrical power output, D_0 is the damping coefficient, T_J is the time constant of rotating inertia, E'_q is the transient electromotive force along the q-axis, X_d and X'_d are the synchronous reactance and transient reactance along the d-axis, i_d is the d-axis current component, and E_f is the field excitation voltage [53, 78].

In steady-state operation, the SynCons adhere to the following algebraic relationships [53, 78]:

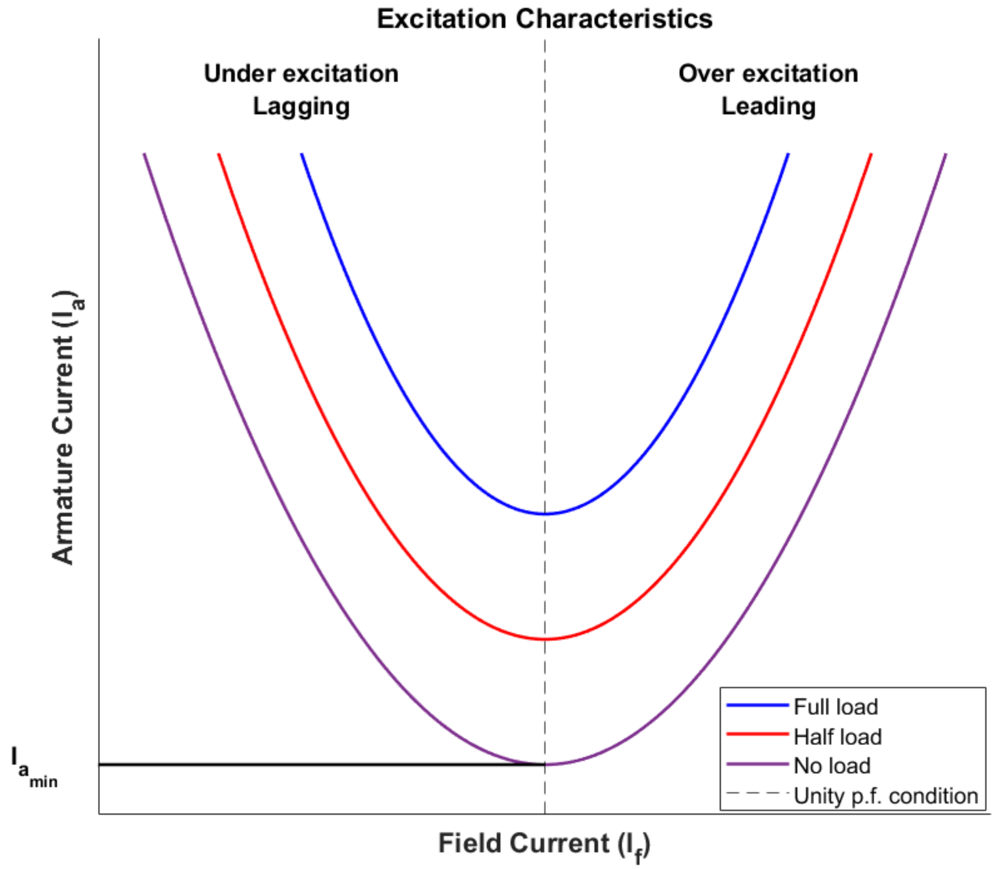

Figure 4.1: Operating characteristics of synchronous condenser modes.

$$E'_q = v_q + R_a i_q + X'_d i_d \quad (4.4)$$

$$0 = v_d + R_a i_d - X'_q i_q \quad (4.5)$$

Here, v_d and v_q are the d-axis and q-axis components of stator voltage, R_a is the stator resistance, and X'_q is the transient reactance along the q-axis [53, 78]. These equations are essential for the synchronization process and for ensuring that SynCons contribute effectively to voltage regulation and power factor correction within the power system. Several key features and applications of SynCons are summarized as follows:

- **Voltage control:** One of the key advantages of SynCons is their ability to maintain voltage stability in power systems through effective reactive power management. They control voltage levels by producing or absorbing reactive power based on the need of the grid [77, 79].

- **Inertia sustaining:** SynCons are equipped with a rotating mass and inherently possess rotational inertia, which is essential in stabilizing grid frequency. This inertia plays a critical role during fluctuations in power demand or supply, as it helps in smooth out the RoCoF [82, 83, 84].

- **Enhancement of short-circuit current and capacity:** SynCons significantly increase the short-circuit capability of power systems. They can provide robust support by delivering substantial short-circuit currents when a fault occurs. This capability is crucial for maintaining the stability of the power grid and ensuring the effective operation of protection mechanisms. The enhanced short-circuit current ensures that protection devices like circuit breakers and relays can efficiently identify and isolate faults, thus securing the electrical components [74, 82, 85, 86, 87].

- **Fault-ride through capability:** SynCons play a crucial role in enhancing the fault ride-through capability by assisting the power system in maintaining stable operation during and immediately after transient disturbances. This capability is critical for ensuring grid resilience and continuity, minimizing disruptions, and enhancing the overall reliability of the power system during sudden electrical faults [74, 82, 88, 89, 90].

4.3 Synchronous Condenser Modeling

SynCons are designed as SMs without a governor or prime mover. The automatic voltage regulator (AVR) is responsible for adjusting and managing the voltage levels of the SynCons [76]. Several excitation systems are available in PSS/E. The silicon-controlled rectifier excitation (SCRX) system was used to model the SynCons, as shown in the block diagram in **Figure 4.2** [91].

The exciter is a bus-fed type, featuring a lead/lag filter with time constants of 1 and 10 seconds, respectively, and an exciter time constant of 0.050 seconds. The parameters in the block diagram are explained in **Table 4.1**, which provides a description of variables in the SCRX excitation system [91]. Additionally, the appropriate ratings for the excitation system are illustrated in **Table 4.2**.

4.4 Enhancement of Power Grid Strength with Synchronous Condensers

This section presents three scenarios illustrating how SynCons contribute to increasing the robustness and resilience of the power grid by adding SCMVA at their installation points. As detailed in Chapter 2, increasing SCMVA can enhance grid strength indicators such as SCR and WSCR, as they are directly proportional to the available fault capacity.

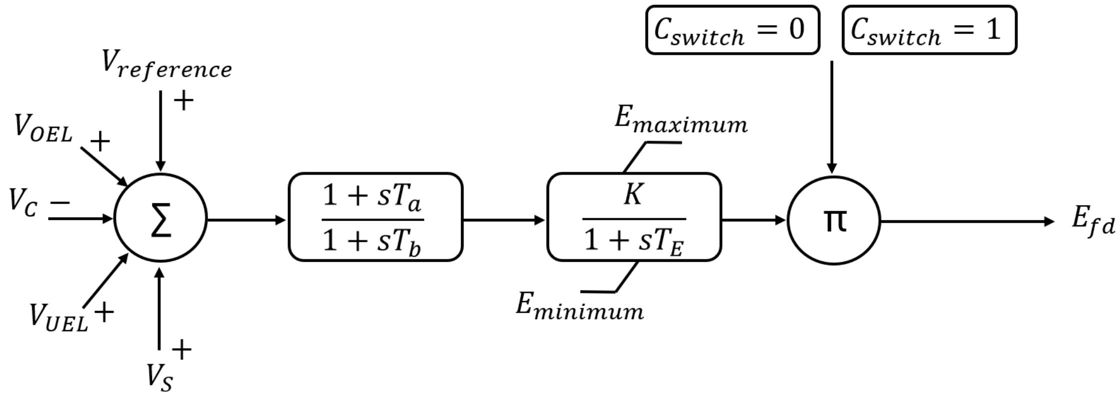

Figure 4.2: SCRX excitation system block diagram.

Table 4.1: Description of Variables in the SCRX Excitation System

Variable	**Description**
E_C	Compensated terminal voltage.
$V_{reference}$	Voltage regulator reference.
V_S	Output voltage of the Power System Stabilizer (PSS).
V_{OEL}	Output from the overexcitation limiter.
V_{UEL}	Output from the underexcitation limiter.
$\frac{T_a}{T_b}$	Gain reduction ratio.
T_b	Time constant.
K	Exciter gain.
T_E	Time constant.
$E_{maximum}$	Maximum field voltage output.
$E_{minimum}$	Minimum field voltage output.
C_{switch}	Voltage source switch
E_{fd}	Field voltage output.

Table 4.2: The ratings of the synchronous condenser

Parameter	Value
Rated Voltage	13.8 kV
Rated capacity	10-280 MVA
Inertia Constant (H)	1.9 s
Frequency	60 Hz
Max Rated Reactive Power	-10 MVar : 280 MVar

4.4.1 Methodology

This subsection introduces three scenarios to observe and analyze the gradual contribution of SynCons. Given that WSCR and SCR are indicators of power system strength, the integration of SynCons will be evaluated using SCR as the primary strength index for simplicity. As outlined in Equation 2.1, to increase the SCR by 1, the SCMVA contribution from the SynCon must be increased by an amount equivalent to the rated power P_{RMW} at the installed inverter in the POI.

Depending on the need and purpose, SynCons can be installed at the POIs, along transmission lines, or even near inductive loads. In this study, SynCons will be installed at the POIs where solar PV inverters are located, with the aim of increasing the SCMVA and overall power system strength. The rating of each condenser may vary from one location to another, depending on factors such as the specific impact occurring at that location following the integration of IBRs. The Newton-Raphson Power Flow (NRPF) method was applied to assess the system's response to various disturbances and identify bus locations with the highest priority for reactive power compensation and inertia support. The 'Active Power-Voltage' (PV) and 'Reactive Power-Voltage' (QV) curves are additional analytical tools used to identify weak grid locations [53].

Building upon this methodology, the study further investigates three specific case studies, each designed to incrementally increase the SCR and assess the corresponding impact on grid strength. The first case study focuses on enhancing the SCR by 1, requiring an increase in the SCMVA contribution from SynCons equivalent to the system's rated power at the POI. The second case study explores the effects of doubling the SCMVA relative to P_{RMW}, effectively raising the SCR by 2. The third and final case study examines the implications of a more substantial increase in the SCR by 3. Each of these studies offers insights into the adaptable benefits of SynCons in enhancing power system strength and stability under varying conditions of SCR enhancement.

4.4.2 Results and Discussion

This section presents and discusses the findings from the three case studies conducted to evaluate the impact of incremental increases in the SCR through the integration of SynCons.

- **Case Study A (Increasing the SCR by 1):** Increasing the SCR by 1, achieved by adding SCMVA equivalent to P_{RMW} at the POI, caused difficulties in solving the power flow following a contingency, as the network failed to converge in a grid powered entirely by solar PV. This indicates the need for a higher SCMVA after such disturbances. **Table 4.3** lists the SCMVA added for several buses across the Saudi model, while **Figure 4.3** shows ΔSCMVA% improvements as a percentage of the base case (0%PV).

- **Case Study B (Increasing the SCR by 2):** Doubling the SCR to 2 by enhancing the SCMVA to twice the amount of P_{RMW} at the POI resulted in notable improvements in the short circuit capacity. **Table 4.3** lists specific buses and the corresponding SCMVA increases across different regions, while **Figure 4.4** shows a map with ΔSCMVA% enhancements of the base case.

- **Case Study C (Increasing the SCR by 3):** Tripling the SCMVA relative to P_{RMW} at the POI to achieve an SCR increase of 3 resulted in notable improvements in short circuit capacity. Although the SCMVA enhancements did not restore the system to base case levels prior to solar PV integration, the improvements were still substantial, highlighting the effectiveness of SynCons in enhancing the grid's capabilities under high renewable integration conditions. **Table 4.3** provides a detailed breakdown of the SCMVA increases at various strategic buses within the Saudi model. Moreover, **Figure 4.5** illustrates ΔSCMVA% improvements, while **Figure 4.6** shows the WSCR improvement for Case C.

Table 4.3: SCMVA levels corresponding to increased SCR with 100% solar PV integration for buses located in different regions

Bus Number	SCMVA at base	SCMVA No SynCons contribution	SCMVA to Increase SCR by 1	SCMVA to Increase SCR by 2	SCMVA to Increase SCR by 3
11324	2025.02	669.69	869.68	1069.67	1269.66
11345	2609.21	878.35	1078.32	1278.29	1478.27
11364	2241.98	701.33	901.24	1101.18	1301.14
11374	1198.15	432.12	632.07	832.04	1032.02
13100	1248.66	464.24	664.12	864.06	1064.02
21272	1584.48	463.61	663.56	863.54	1063.52
29720	1284.23	365.21	565.17	765.15	965.14
29721	1692.88	463.12	663.08	863.05	1063.03
29723	1749.21	463.15	663.1	863.08	1063.06
29823	1151.15	332.42	532.39	732.38	932.38
31716	1884.45	527.21	727.18	927.16	1127.15
31721	2465.68	760.24	960.24	1160.24	1360.23
31725	1516.03	586.12	786.08	986.05	1186.04
31772	2823.15	836.59	1036.59	1236.59	1436.59
31780	1692.18	650.15	850.14	1050.13	1250.13

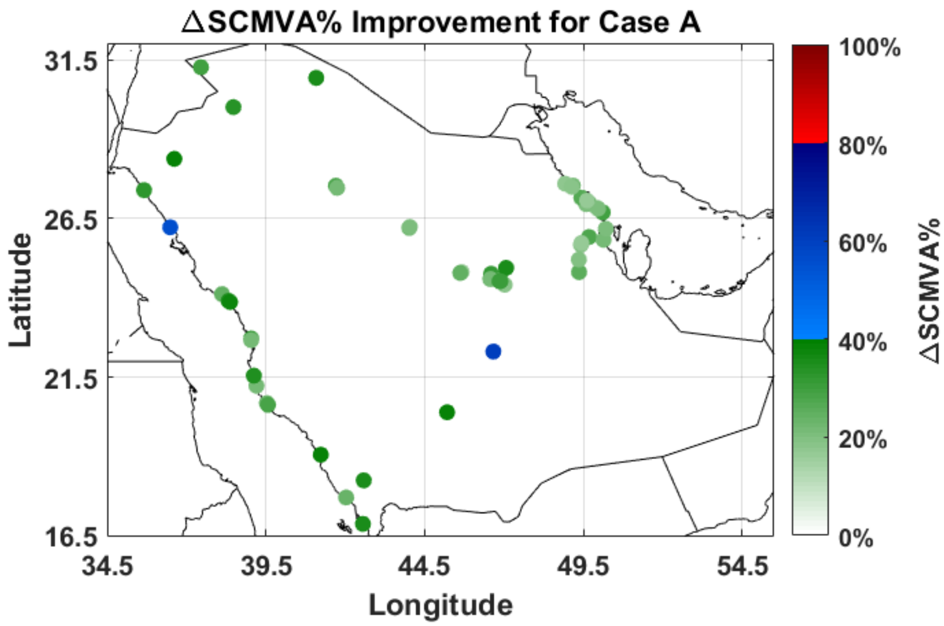

Figure 4.3: ΔSCMVA improvements as a percentage of the base case (case A).

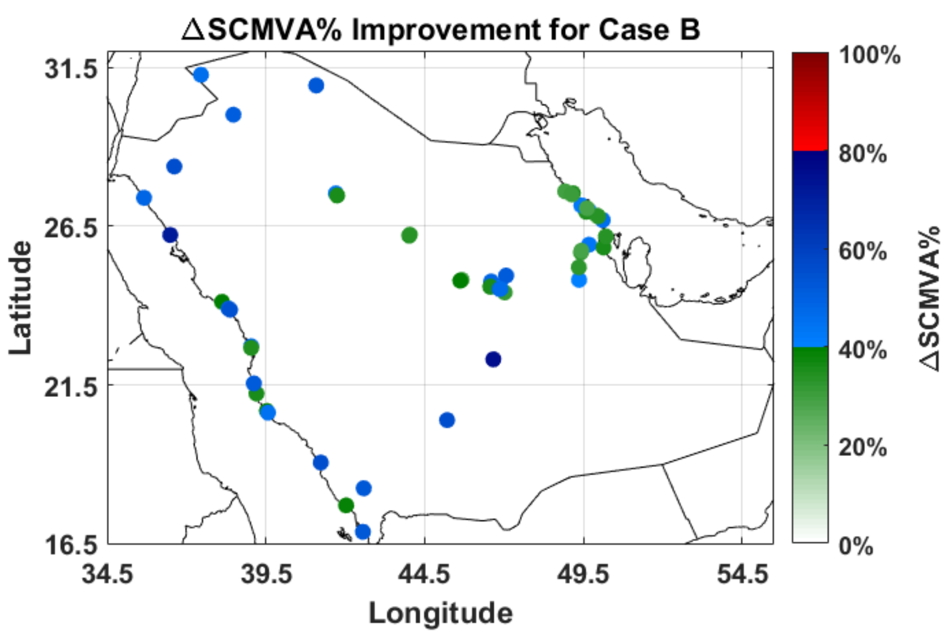

Figure 4.4: ΔSCMVA improvements as a percentage of the base case (case B).

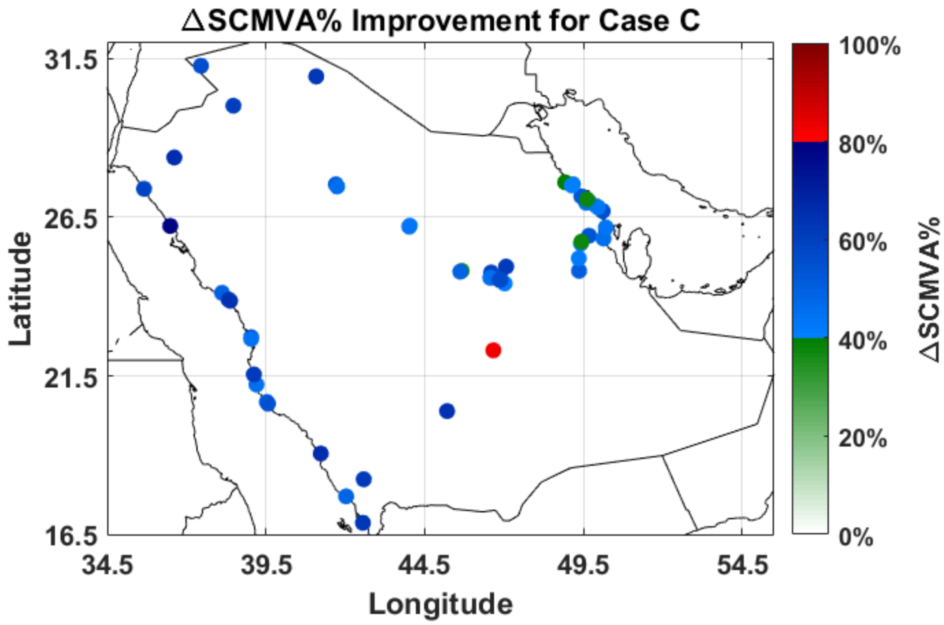

Figure 4.5: ∆SCMVA improvements as a percentage of the base case (case C).

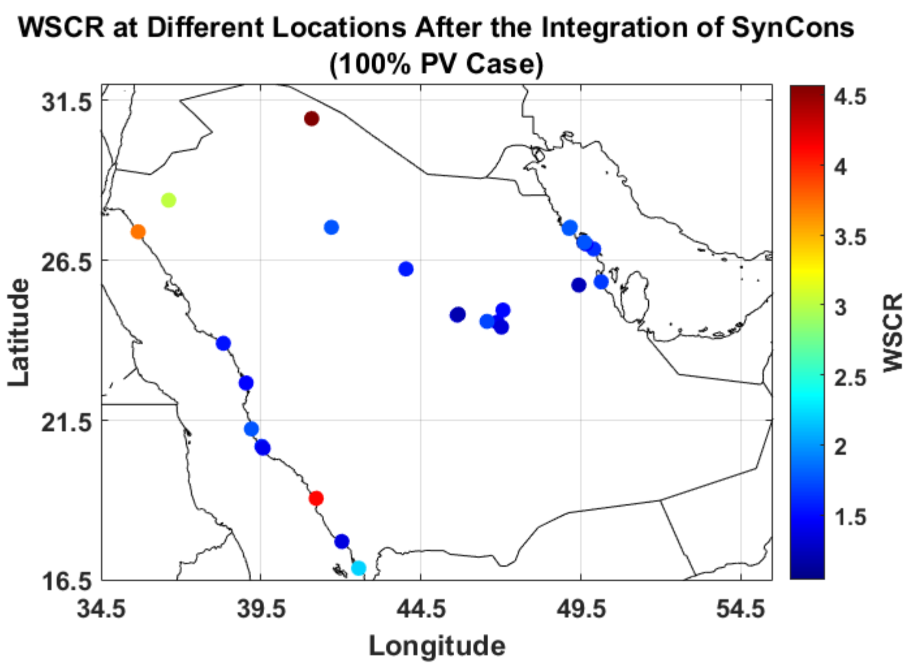

Figure 4.6: WSCR improvement for Case C.

Chapter 5

Mitigating Voltage Instability in the Saudi Electric Grid for Solar Power Integration

5.1 Introduction

With the continuous growth of RESs, voltage stability has become increasingly important in power system operation and planning. Essentially, it is defined as the ability of the grid to maintain acceptable voltage levels across all buses during normal operations and after disturbances [53, 61]. The significance of voltage stability becomes particularly clear when we consider the potential consequences of voltage collapse, such as blackouts and damage to electrical equipment [92, 93, 94]. These risks highlight the need for robust solutions to secure voltage levels under a variety of conditions.

Traditionally, SGs have played a key role in ensuring voltage stability by providing inherent voltage support and reactive power compensation. However, as the power grid transitions toward higher integration of IBRs, such as solar PV systems, new challenges arise. Moreover, the electric grid in Saudi Arabia has experienced significant growth in load demand and complexity over the last decade, increasing the risk of voltage stability issues. This chapter examines the challenges of high IBRs penetration and explores methods to enhance grid stability and system reliability through several case studies.

5.2 Problem Statement

The shift from synchronous-based generation to IBRs introduces significant challenges to voltage stability in modern power grids. Even during faults, SGs continuously supply excitation current from their external DC source, maintaining field winding voltage. Meanwhile, the turbine maintains its rotation, inducing voltage in the stator winding, resulting in a sustained fault current until the fault condition is cleared. This sustained fault current is critical for stabilizing voltage during disturbances.

In contrast, solar PV systems rely on power electronics that lack the inherent ability to contribute high fault currents during disturbances. The inverters used in solar PV reduce their output during faults to protect themselves, further reducing the grid's short-circuit capacity and weakening its ability to recover from voltage sags. This loss of fault current and reactive power support from SGs leads to voltage instability, where the grid struggles to maintain voltage levels during disturbances, resulting in a higher risk of voltage collapse.

5.3 Basic of Voltage Stability

The fundamental concept of voltage stability can be illustrated using a simple two-bus system, as shown in **Figure 5.1**. The real power (P) and reactive power (Q) transfer from the generator bus to the load are given by the following equations:

$$P = \frac{EV}{X} \sin(\delta) \tag{5.1}$$

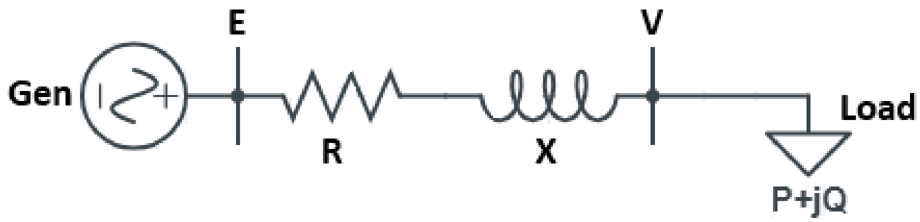

Figure 5.1: Simple two bus system.

$$Q = \frac{-V^2}{X} + \frac{EV}{X}\cos(\delta) \tag{5.2}$$

where:

- $E = E\angle\delta$ is the voltage at the generator side,
- $V = V\angle 0$ is the voltage at the load side,
- X is the neglected impedance of the line,
- δ is the voltage phase angle difference between the sending and receiving ends.

5.3.1 Voltage stability analysis methods

Various methods are employed to analyze voltage stability, particularly in the context of full solar PV integration, which significantly impacts grid operating conditions. Among the widely used techniques are the NRPF, 'Active Power-Voltage' (P-V) curve, and 'Reactive Power-Voltage' (Q-V) curve. These methods are instrumental in assessing voltage stability and providing valuable insights for identifying weak bus locations [53, 95, 96].

5.3.1.1 Newton-Raphson Power Flow (NRPF)

The NRPF method is one of the most widely used techniques for solving power flow problems in large-scale electrical power systems [96]. As the grid transitions from conventional generation to one powered by solar PV, NRPF becomes crucial for assessing voltage stability. By analyzing the voltage deviations obtained through NRPF, as illustrated in **Table 5.1**, it is possible to identify buses that may require additional support to maintain stability. This information is valuable when integrating large-scale solar PV, as it guides the strategic placement and sizing of compensation devices, ensuring the grid can resist the new operational conditions imposed by high levels of renewable energy penetration.

Table 5.1: Voltage responses for several buses obtained from NRPF analysis.

Bus Number	**Pre-Contingency Voltage Response (PU)**	**Post-Contingency Voltage Response (PU)**
13231	1.00	0.66
13246	1.00	0.68
11362	0.99	0.69
11377	1.01	0.72
29726	1.00	0.77
13288	1.00	0.78
13119	1.01	0.79
13115	1.01	0.81
11330	1.00	0.82
21535	0.98	0.84
29716	1.00	0.84
11401	1.02	0.85
22990	1.00	0.86
20976	0.98	0.87
21272	1.00	0.90
21274	1.00	0.90
21276	1.00	0.90
21278	1.00	0.90
30738	1.02	0.95
30411	1.02	0.95
20219	1.00	0.95
13297	1.00	0.96
20217	1.00	0.96
21297	1.00	0.97
21516	1.02	0.97
21584	1.02	0.97
21586	1.02	0.97
21588	1.02	0.97
21590	1.02	0.97
21562	1.03	0.98

5.3.1.2 PV Curve

The P-V curve is a critical tool in voltage stability analysis, illustrating the relationship between the active power transferred and the corresponding bus voltage. By plotting this curve, engineers can determine the maximum power transfer capability before voltage instability or collapse occurs. The curve typically presents a distinctive "nose" point, beyond which any further increase in power demand leads to a sharp voltage drop, indicating instability [53, 97]. The P-V curve is essential for determining stability margins under varying load conditions, identifying critical loading points, and assessing how different load types affect voltage stability as seen in **Figure 5.2** [95].

5.3.1.3 QV Curve

The Q-V curve is another essential tool in voltage stability analysis, depicting the relationship between reactive power and voltage at a specific bus, as shown in **Figure 5.3**. This curve provides insights into the reactive power support required to maintain voltage levels within acceptable limits [53]. By plotting the Q-V curve, it is possible to determine voltage sensitivity to changes in reactive power, thereby identifying weak buses subject to instability. The Q-V curve is particularly useful for assessing the reactive power compensation needed, especially in the presence of dynamic loads like induction motors [95, 98]. The Q-V curve also evaluates the effectiveness of compensation devices, such as STATCOMs and SynCons, in mitigating voltage drops and maintaining stability, which is especially important in systems with high variability, such as those with large-scale RESs.

5.3.2 Classification of Load

Voltage stability within a power grid is significantly influenced by both the demand and complexity of the loads it serves [95, 98]. As load demand increases, particularly during peak consumption periods, the strain on the power system get worse,

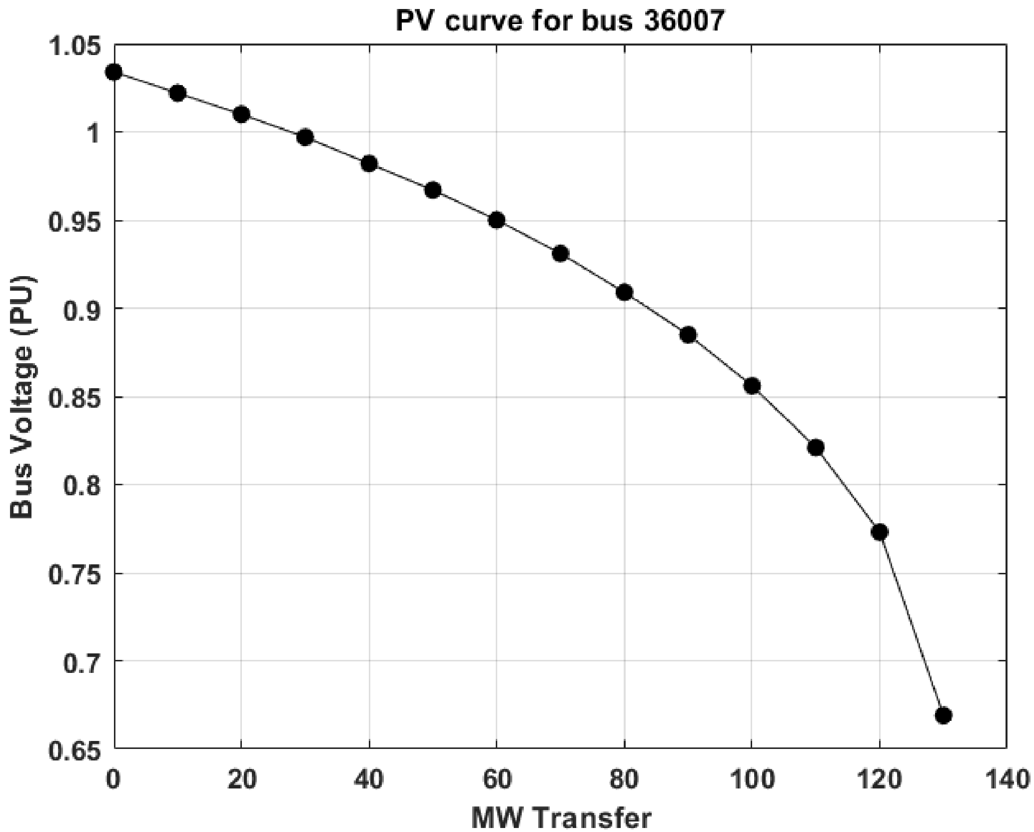

Figure 5.2: PV curve.

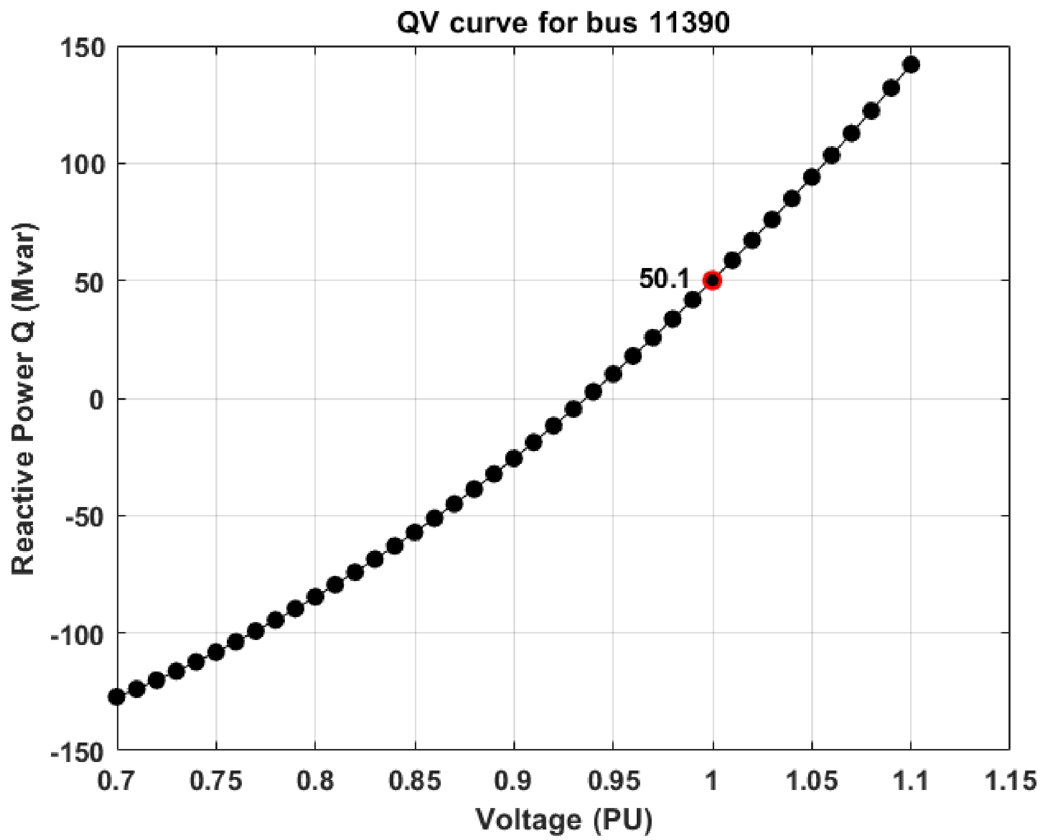

Figure 5.3: QV curve.

potentially leading to voltage drops and instability [98]. The complexity of loads including residential, commercial, and industrial consumers adds another layer of challenge, as each load type has unique characteristics that impact the overall voltage profile [99]. For instance, industrial loads often involve large motors and machinery that can cause sudden and substantial changes in power demand, whereas residential loads typically shows more gradual and predictable patterns. The integration of RESs, such as solar PV systems, further complicates the voltage stability context as previously explained. Understanding the relationship between load demand, load complexity, and voltage stability is essential for developing strategies to maintain stable and reliable power system operations.

5.3.2.1 Static loads

Static loads, which draw a constant amount of power regardless of voltage variations, typically include resistive elements such as incandescent lighting and simple heating devices that presents predictable and linear characteristics [100]. These loads are relatively simple to model and manage due to their steady power consumption patterns. **Figure 5.4** illustrates the relationship between voltage and power consumption for the three main types of static loads, which can be categorized as follows [101, 102]:

- **Constant Power (P):** These loads maintain constant power consumption regardless of voltage variations.

$$ \tag{5.3} $$

$$I = \frac{P}{V} \tag{5.4}$$

- **Constant Current (I):** These loads draw a constant current irrespective of voltage changes.

$$ \tag{5.5} $$

$$P = V \cdot I \tag{5.6}$$

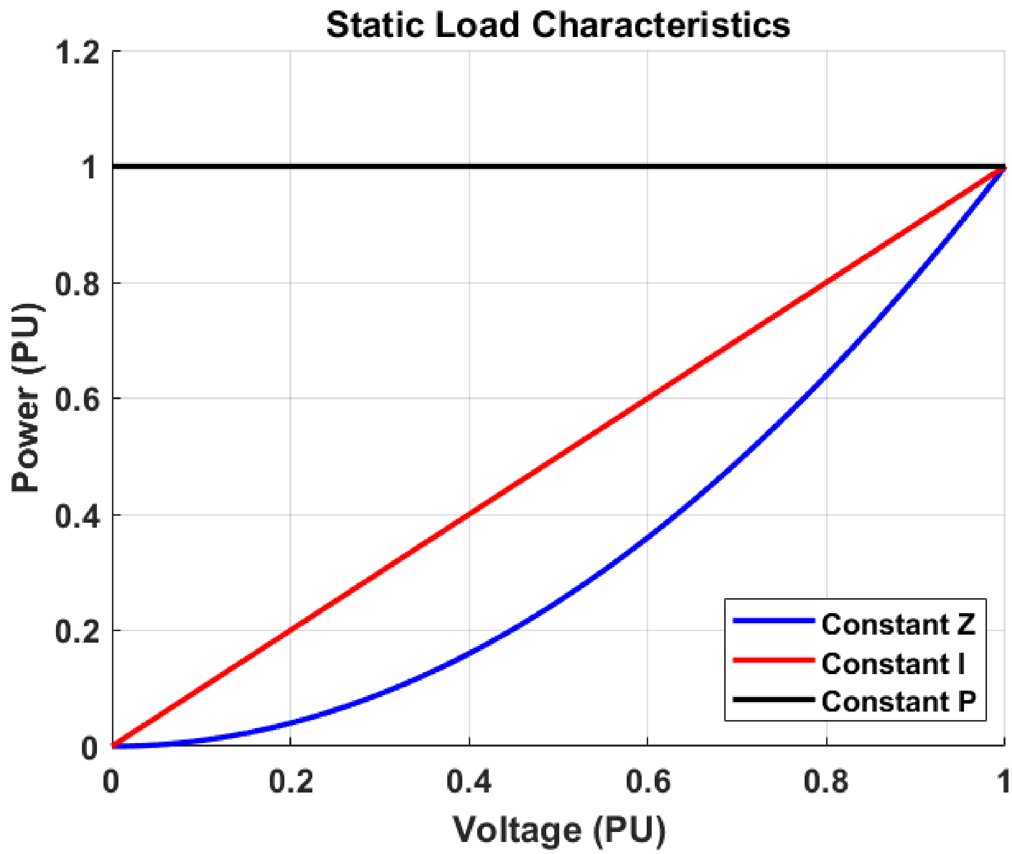

Figure 5.4: Static load characteristics.

- **Constant Impedance (Z):** These loads have a fixed impedance, meaning their power consumption varies with the square of the voltage.

$$P = \frac{V^2}{R} \tag{5.7}$$

The static load model equation is given by:

$$P = P_0 \left(C_1 \left(\frac{V}{V_0} \right)^2 + C_2 \left(\frac{V}{V_0} \right) + C_3 \left(\frac{V}{V_0} \right)^0 \right) \tag{5.8}$$

where:

P is the power consumption at voltage V,

P_0 is the nominal power consumption at the nominal voltage V_0,

C_1, C_2, C_3 are the coefficients for constant impedance, current, and power components, respectively.

The constraint is given by:

$$C_1 + C_2 + C_3 = 1 \tag{5.9}$$

5.3.2.2 Dynamic loads

Dynamic models of electrical components such as motors play a crucial role in accurately capturing the voltage response during system disturbances. Composite models are particularly effective as they integrate both static and dynamic loads, offering a more comprehensive representation of real-world systems. However, these models often introduce significant non-linearities, with phenomena like motor stalling and inrush currents posing challenges to voltage stability analysis [101, 102, 103, 104].

One of the most commonly used composite load models in the PSSE library is the CLOD model shown in **Figure 5.5** [91].

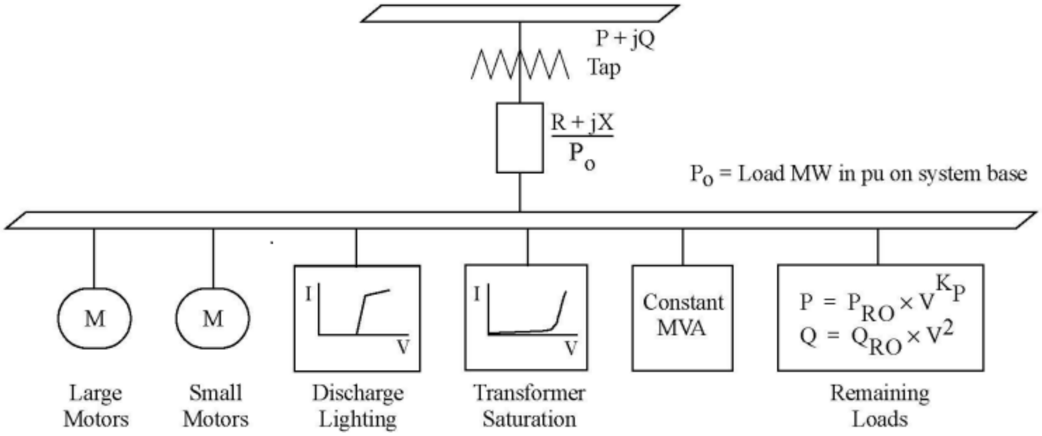

Figure 5.5: CLOD composition load [91].

This model represents a variety of loads including motors and transformers, as detailed in **Table 5.2**. The CLOD model is particularly useful in scenarios where detailed load information is unavailable, yet the dynamic behavior of components such as induction motors remains critical for accurate analysis. By simulating these dynamic behaviors, CLOD provides valuable insights into system performance under various operating conditions.

In addition to CLOD, the CIM5 dynamic load model is also used to represent induction motors. This model effectively simulates the stall of motors during system disturbances [101], enhancing the accuracy of system stability assessments. The main purpose is to have a robust framework for analyzing the complex interactions between different load types and system dynamics, enabling more reliable voltage stability studies.

5.4 Methodology

This section outlines the methodology used to mitigate voltage instability after transitioning the Saudi grid to fully solar PV. Dynamic simulations were performed using PSSE to analyze grid stability under several disturbances, including short circuits, generator trips, and transmission line outages. A weak grid analysis was conducted to identify locations or buses with significant reductions in SCMVA, based on results from NRPF, P-V, and Q-V curve analyses.

Short circuit calculations followed the IEC 60909 standard method, as introduced in Chapter 2, to evaluate the SCMVA. The voltage stability analysis included both static and dynamic load models to ensure a comprehensive assessment of system performance under various load conditions.

To mitigate voltage instability, SynCons were primarily employed, with a comparative case analysis involving STATCOMs to evaluate their relative effectiveness. The overall methodology and analysis steps are shown in the detailed flowchart in **Figure 5.6**.

Table 5.2: CLOD Load Model Elements [91].

Load Component	**Composition**
Large Motor (LM)	J
Small Motor (SM)	J+1
Discharge Lighting (DL)	J+2
Transformer Saturation (TS)	J+3
Constant Power (CP)	J+4
Kp	J+5
R	J+7
X	J+8

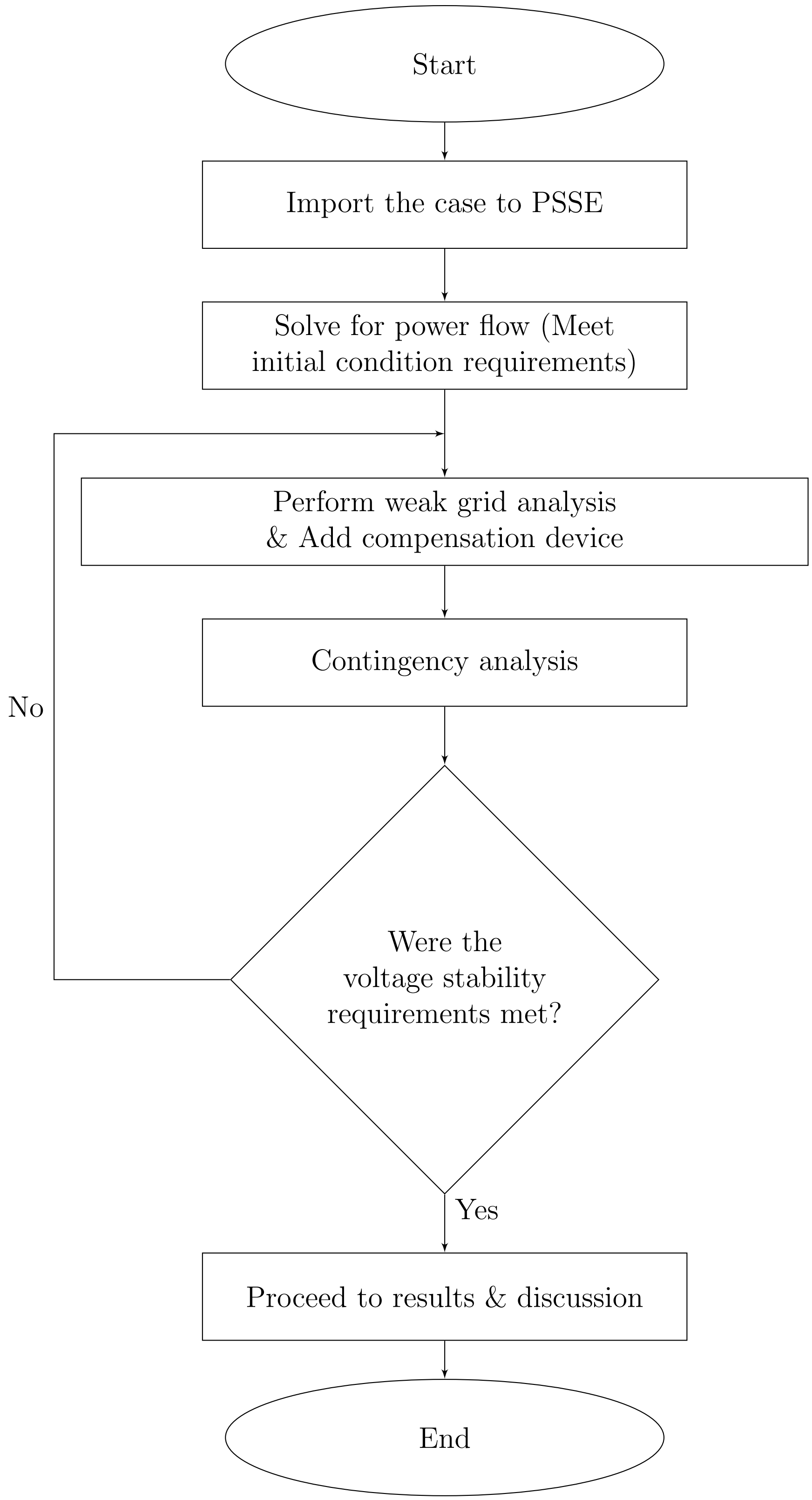

Figure 5.6: Voltage stability methodology.

The voltage stability testing, evaluation, and mitigation strategies were performed under different scenarios, categorized into several distinct cases as follows:

- **Case A: Determining the solar PV penetration limit for stable voltage response:**
  This case determines the penetration limit before voltage response becomes unstable (No mitigation applied).

- **Case B: Testing voltage stability with SynCons under three scenarios:**
  In each scenario, the SCR is increased by a specific value. Static loads are applied along with different types of contingencies [71].

- **Case C: Evaluating voltage stability using composition load models:**
  In this case, the CLOD composition load model is applied under various types of contingencies.

- **Case D: Comparing the performance of SynCons and STATCOMs during an FIDVR event:**
  This case compares the performance of SynCons and STATCOMs during short circuit events that cause voltage drops leading to an FIDVR event.

- **Case E: Investigating the impact of adding transmission lines on voltage stability with high solar PV penetration:**
  This case investigates how adding more transmission lines at weak locations can improve the voltage response.

- **Case F: Investigating the impact of relocating solar PV near central loads on voltage stability with high solar PV penetration:**
  This case evaluates how relocating solar PV near central loads mitigate voltage stability at weak locations.

These cases were proposed and analyzed to identify the most effective solutions for enhancing voltage stability in the Saudi electric grid post-transition to solar PV.

5.5 Results and Discussion

This section present the result and discussion for the cases proposed and indicated in the methodology section.

5.5.1 Case A: Determining the solar PV penetration limit for stable voltage response

This case examines the maximum level of solar PV penetration before voltage instability occurs, without applying any mitigation solutions. Two contingencies were introduced: a three-phase short circuit on a 380 kV transmission line and the tripping of the largest generator. With 60% solar PV penetration, the voltage response to both events remained stable, and the overall performance was evaluated as highly satisfactory. Detailed results for each contingency are presented in **Figures 5.7** and **5.8**.

At 80% solar PV penetration, the system was tested under a short circuit event. Stability became difficult to maintain, with challenges in returning to steady-state conditions, as shown in **Figure 5.9**.

Finally, a scenario with 100% solar PV penetration was tested under a short circuit event on a 13.8 kV distribution line, as shown in **Figure 5.10**. The system became unstable, with power flow unable to converge due to a significant power imbalance. This highlights the limitations of high PV penetration in the current grid infrastructure when no stability solutions are implemented.

5.5.2 Case B: Test voltage instability using SynCon with static load

This case study examines voltage instability using SynCons with static loads, distributed as follows: I constant at 34%, P constant at 33%, and Z constant at 33%. The use of SynCons is intended to increase the SCR in three scenarios, allowing

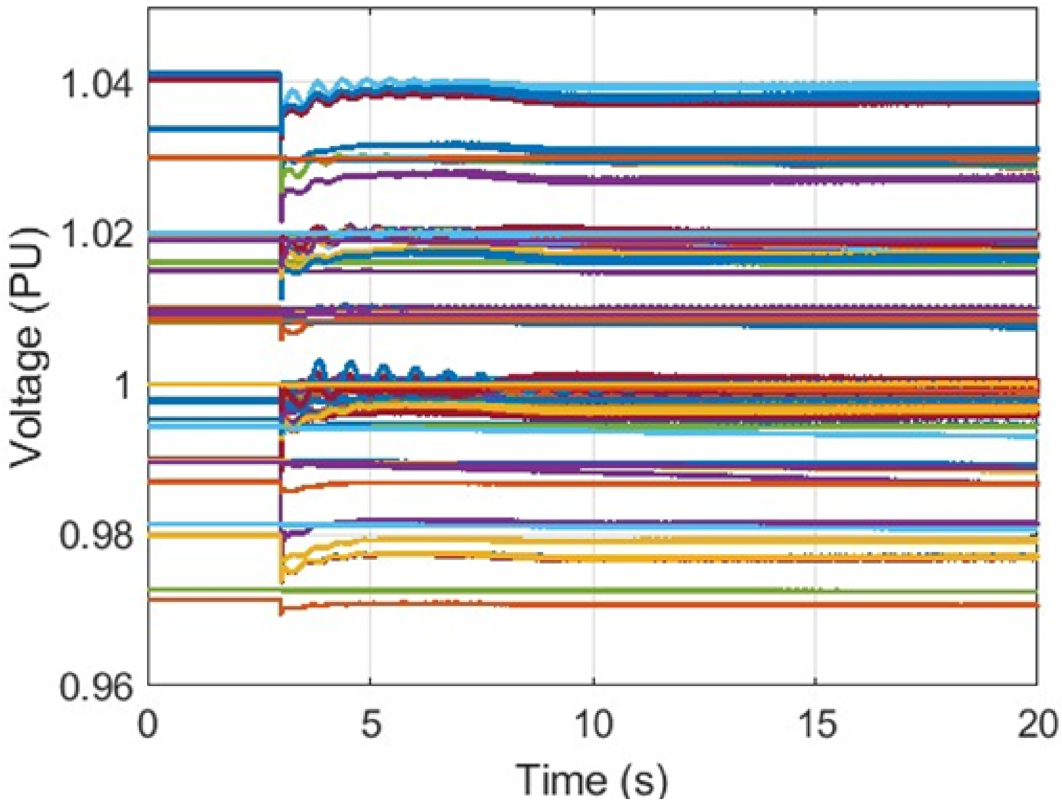

Figure 5.7: 60%PV – Largest unit trip.

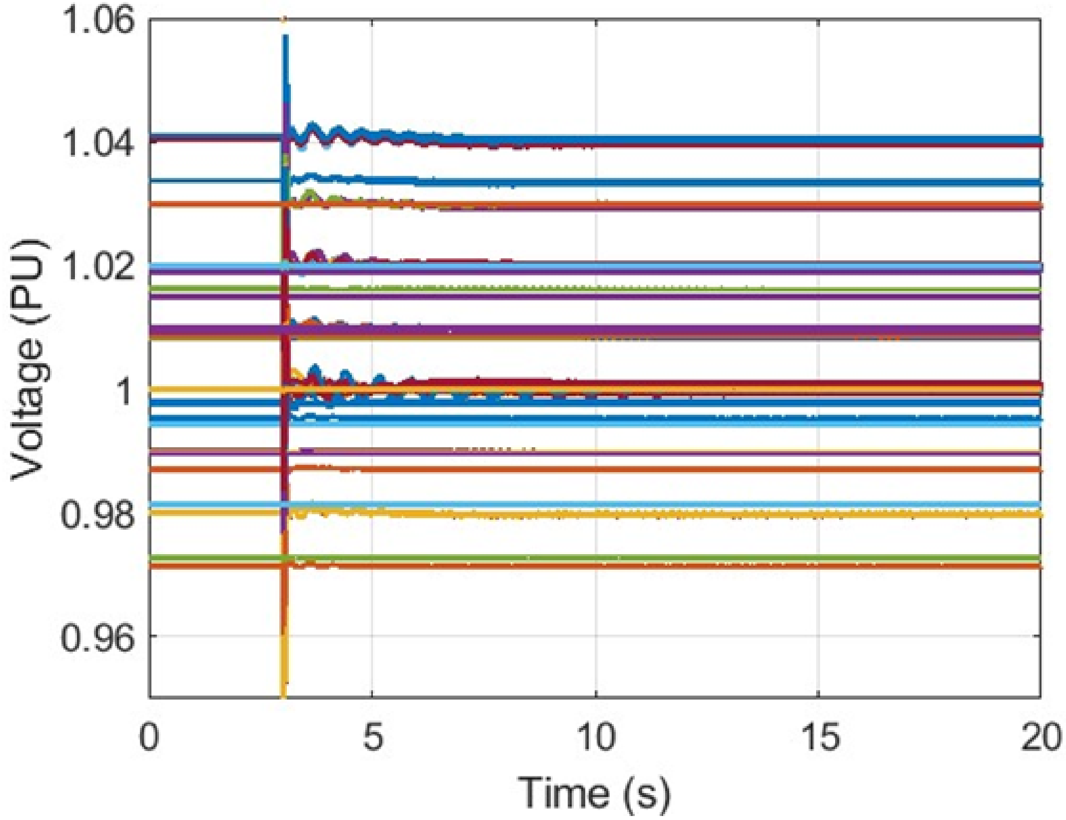

Figure 5.8: 60%PV – 3-phase short circuit at 380KV transmission line.

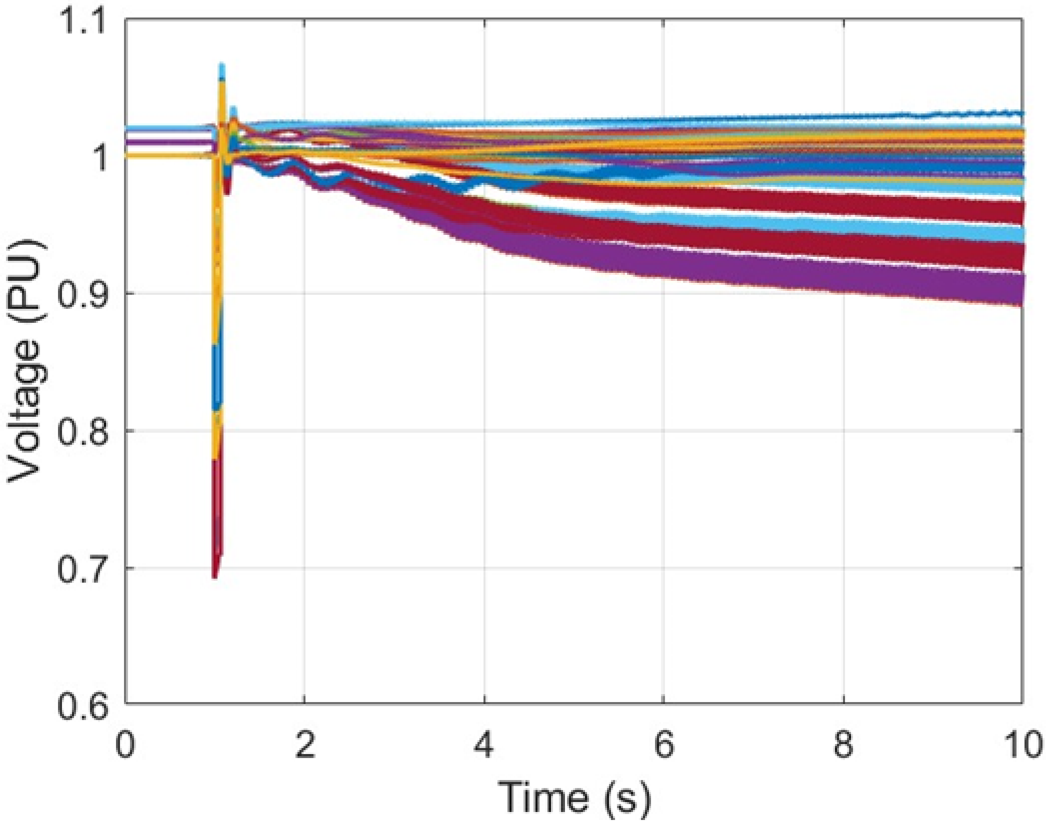

Figure 5.9: 80%PV – 3-phase short circuit at 380KV transmission line.

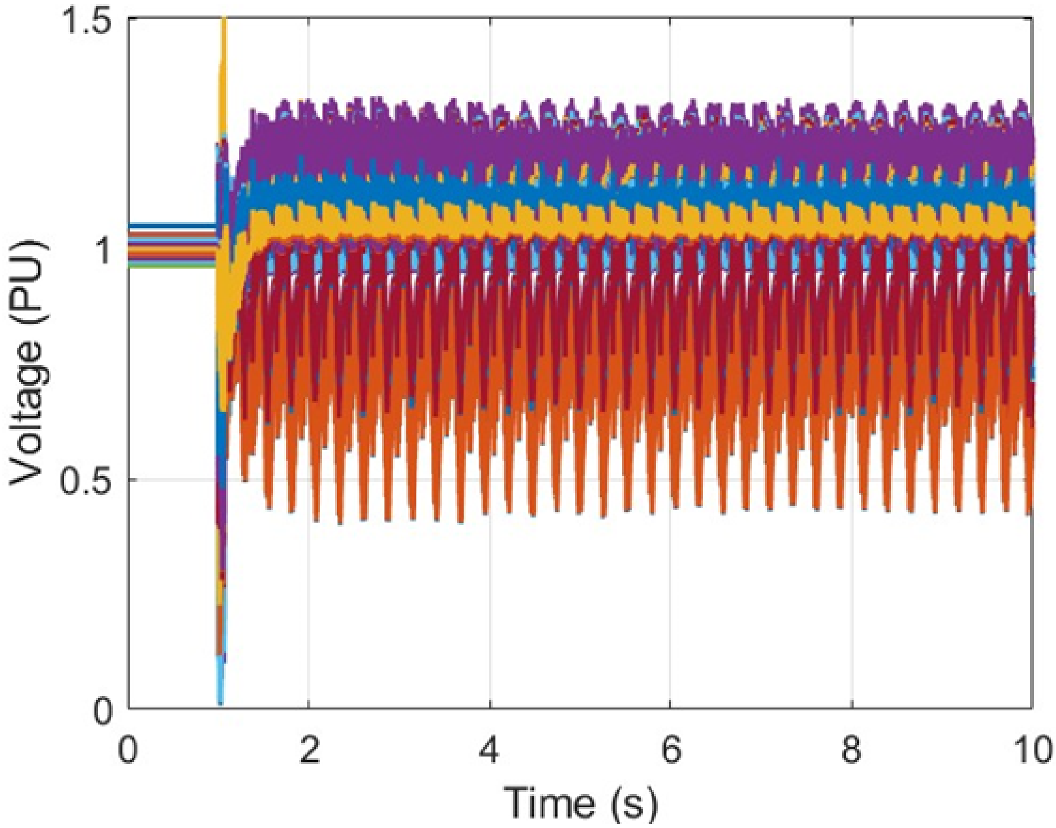

Figure 5.10: 100%PV – 3-phase short circuit at 13.8KV distribution line.

for better observation of improvements in voltage response. A short circuit event on 380 kV transmission line was applied in each scenario to analyze the voltage response.

- **Scenario 1:** in this case, SynCons increased the SCR by 1. However, the network failed to converge due to power imbalance. The PSS/E output report for this scenario is shown in **Figure 5.11**.

- **Scenario 2:** the SCR was increased by 2 through the resizing of SynCons. This scenario showed unstable voltage response with high voltage fluctuations and difficulties in returning to steady-state conditions post-contingency, as presented in **Figure 5.12**.

- **Scenario 3:** the SCR was further increased by 3 using larger SynCons. This adjustment resulted in an excellent voltage response, enabling the system to return to normal operational conditions after the contingency, as seen in **Figure 5.13**.

Each scenario reflects the impact of increasing the SCR through both resizing the capacity and strategic placement of SynCons, underlining their potential to enhance grid stability under different levels of loading stress [71].

5.5.3 Case C: Test voltage instability using SynCon with composition load

This case study examines testing voltage instability using SynCons with the composition load model previously introduced (CLOD). The study focuses on a single scenario where SynCons increase the SCR by 3. The percentage of each element in CLOD is distributed as follow: Large Motors (15%), Small Motors (45%), Discharge Lighting (0%), Transformer Saturation (20%), and Constant Power (6%), with impedance parameters set at $Kp = 1.25$, $R = 0$, and $X = 0.10$ [105]. Additionally, a map locating the buses where the CLOD composition load was applied is presented in **Figure 5.14**.

01_GeneratorTrip_V - Notepad

File Edit Format View Help

349	1.0694	1.0573	1.0530	1.0653	1.0529	1.0654
355	1.0530	1.0653	1.0529	1.0654	1.0530	1.0653
361	1.0529	1.0654	1.0596	1.0583	1.0529	1.0654
367	1.0567	1.0566	1.0566	1.0567	1.0573	1.0573
373	1.0574	1.0573	1.0566	1.0567	1.0566	1.0566
379	1.0567	1.0566	1.0566	1.0567	1.0566	1.0566
385	1.0383	1.0383	1.0383	1.0383	1.0383	1.0383
391	1.0385	1.0385	1.0385	1.0385	1.0384	1.0384
397	1.0569	1.0569	1.0569	1.0569	1.0234	1.0234
403	1.0049	1.0070	1.0266	1.0271	1.0266	1.0270
409	1.0270	1.0265	1.0268	1.0268	1.0271	1.0089
415	1.0089	1.0084	1.0084	1.0023	1.0033	1.0062
421	1.0062	1.0069	1.0069	1.0069	1.0071	1.0071
427	1.0038	1.0041	1.0047	1.0039	1.0027	1.0216
433	1.0128	1.0240	1.0244	1.0244	1.0244	1.0222
439	1.0311	1.0308	1.0109	1.0196	1.0196	1.0200
445	1.0200	1.0102	1.0102	1.0102	1.0102	1.0051
451	1.0198					

Network not converged at TIME = 0.4159

Network not converged at TIME = 0.416

Network not converged at TIME = 0.4161

Network not converged at TIME = 0.4162

Network not converged at TIME = 0.4163

Network not converged at TIME = 0.4164

Network not converged at TIME = 0.4165

Figure 5.11: SynCons increase SCR by 1 (PSS\e report).

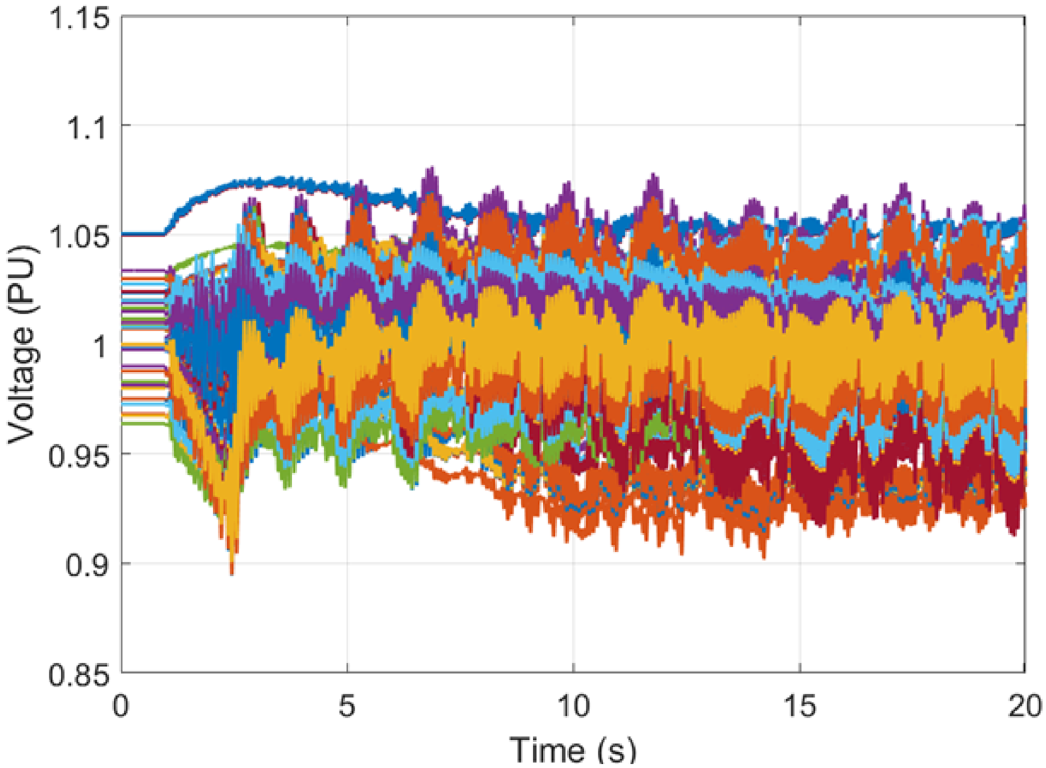

Figure 5.12: Voltage response when SynCons increase SCR by 2.

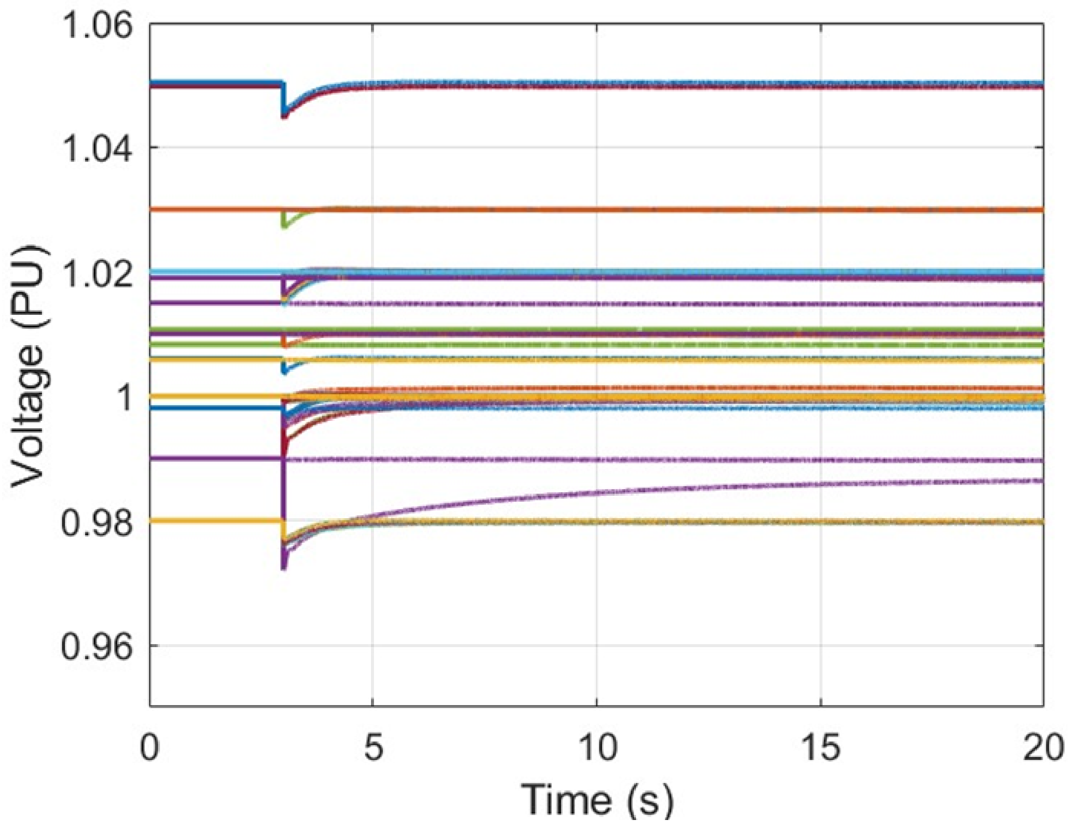

Figure 5.13: Voltage response when SynCons increase SCR by 3.

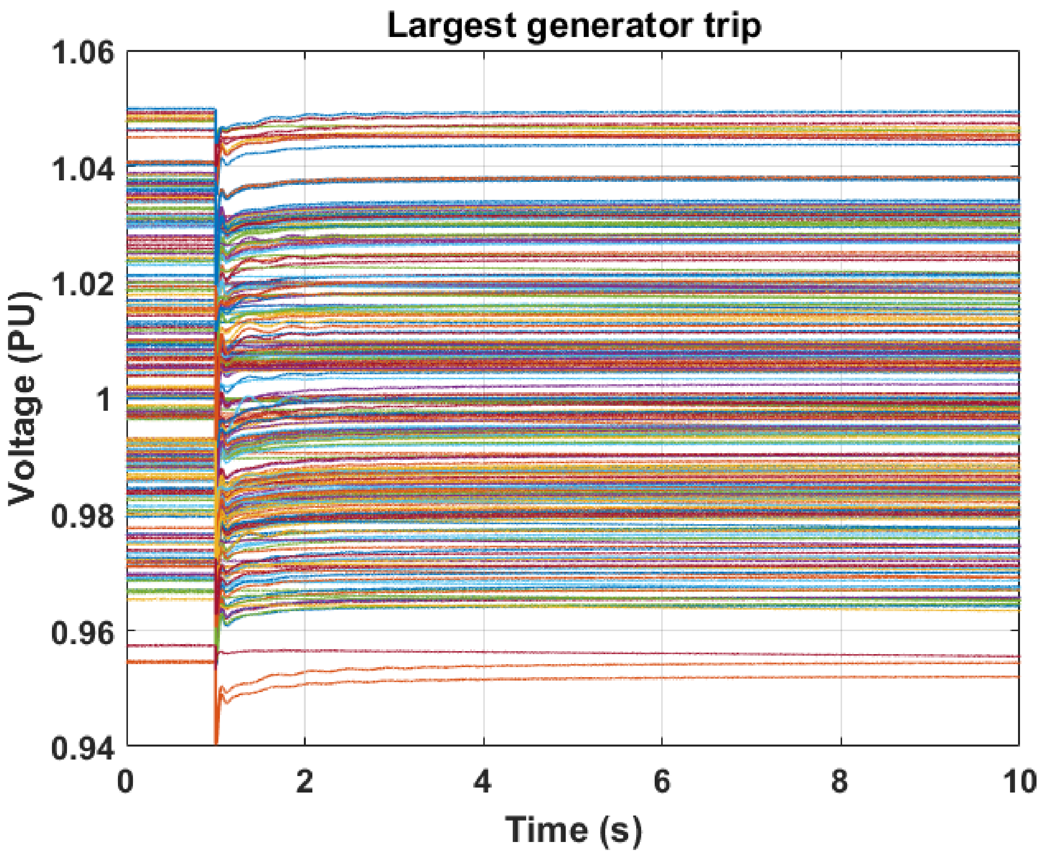

Figure 5.14: Voltage response with tripping the largest generator.

two different contingencies were examined to test the voltage response as follow:

- Tripping of the largest generator as presented in **Figure 5.15**.
- A 3-phase short circuit occurring in the eastern region at a 380 kV transmission line as shown in **Figure 5.16**.

The voltage response across both cases illustrated good overall stability when SynCons contributed to increasing the SCR by 3.

5.5.4 Case D: Compare the performance of SynCon and STATCOM during an FIDVR event

This analysis compares the performance of SynCon and STATCOM during an FIDVR event. This phenomenon involves sustained voltage dips following a contingency, which can lead to system instability [23]. This unstable condition largely results from the behavior of induction motors, which may draw excessive current to maintain power output under reduced voltage [106].

As discussed in Chapter 4, SynCon plays a key role in enhancing SCMVA and managing voltage stability. Similarly, STATCOM, a widely recognized FACTS device, provides reactive power compensation by generating or absorbing reactive power [107, 108]. It operates as a controlled voltage source, injecting reactive power by adjusting the internal voltage amplitude based on the voltage at the point of common coupling (PCC) [107, 108, 109]. It can supply its full rated current almost instantaneously after a voltage change [109]. The STATCOM model available in PSSE is shown in **Figure 5.17** [91].

5.5.4.1 Creating the FIDVR event

To accurately simulate the FIDVR phenomenon, this study employs a combination of CLOD and CIM5 load models, which are particularly effective in capturing the stalling behavior of motors after a contingency. The scenario involves a three-phase

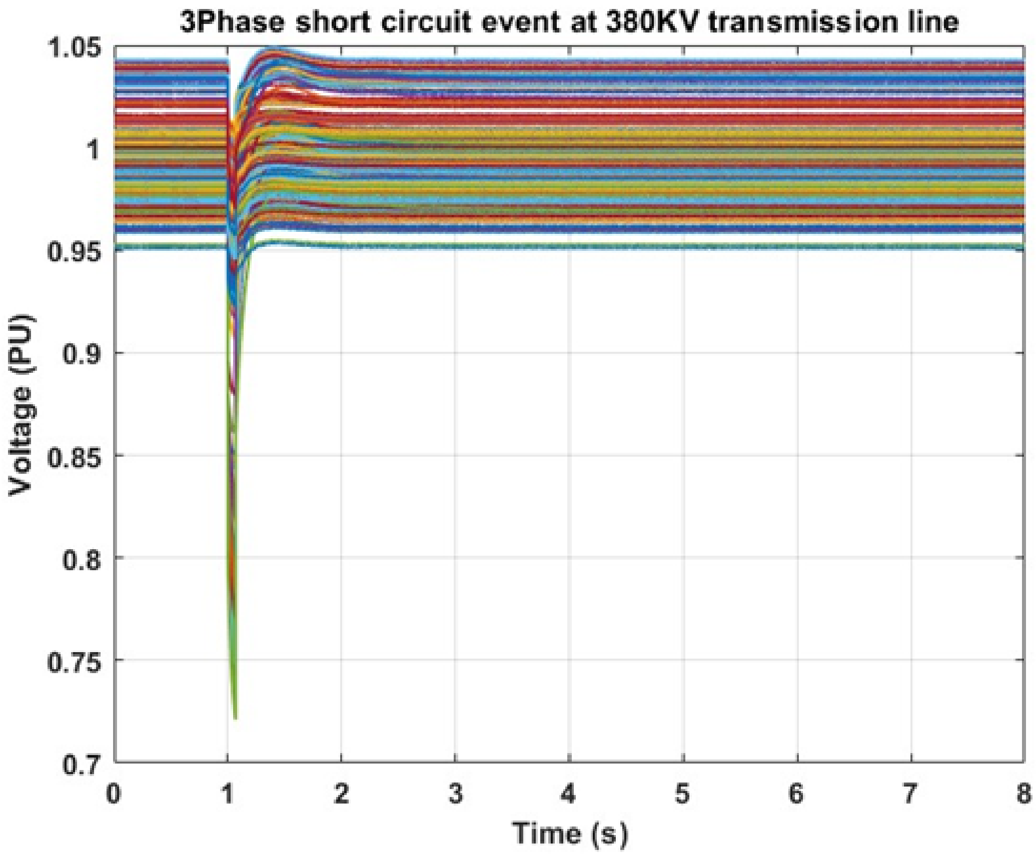

Figure 5.15: Voltage response with applying 3-phase short circuit event.

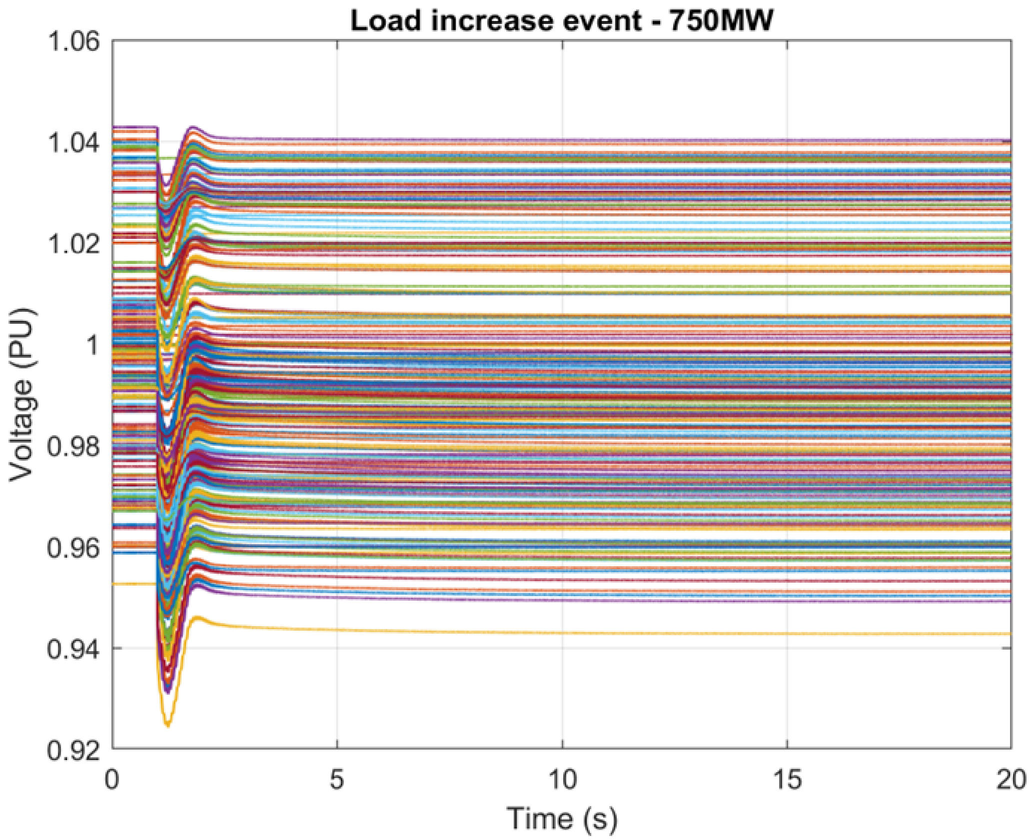

Figure 5.16: Voltage response with load increase event of 750MW.

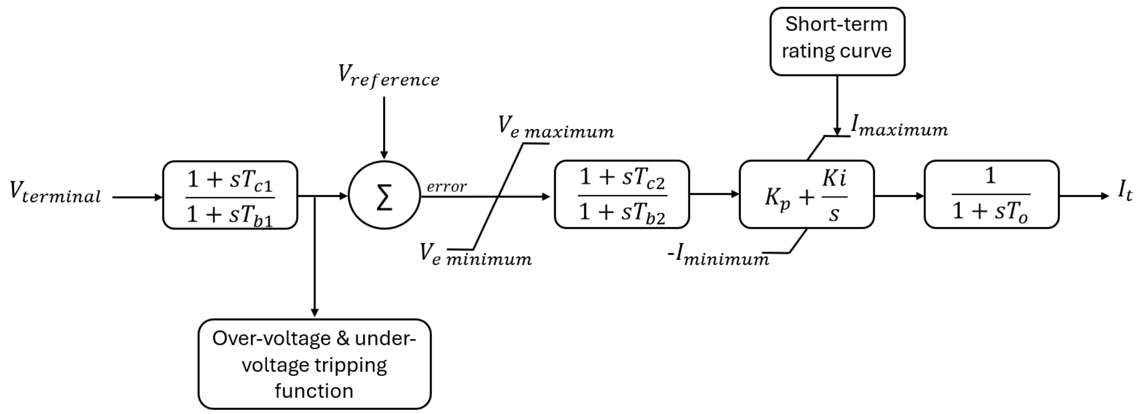

Figure 5.17: STATCOM model used in this chapter.

short circuit event occurs at various 380 kV transmission lines, with the fault being cleared after 5 cycles.

The CLOD model was configured as detailed in **Table 5.3**. CIM5 model settings were based on the PSSE Program Application Guide Volume 2, using motor ratings of 40 to 50 MVA to simulate large motor behavior [110]. This approach allows the simulation to capture how large motors respond under stress conditions.

Figure 5.18 illustrates the FIDVR event in the absence of any mitigation solutions, presenting a delayed voltage recovery lasting several seconds before stabilizing within 5% of the initial pre-contingency level. This scenario shows how heavy load modeling can create an FIDVR even, highlighting the significant challenges to voltage stability after a contingency when no mitigation methods are implemented.

5.5.4.2 Comparison between SynCon and STATCOM in Mitigating FIDVR

The purpose of this section is to compare the performance of SynCon and STATCOM in mitigating an FIDVR event. **Figure 5.19** illustrates a case comparison when the fault location is very close to the compensation devices. As shown in the figure, Scenario A presents the voltage response without any mitigation method, where the voltage dropped to almost 0 PU. In Scenario B, the SynCon showed an immediate fault current contribution, positively affecting the voltage response and illustrating its fault current contribution capability. Conversely, Scenarios C and D, representing STATCOMs rated at 200 MVA and 300 MVA respectively, showed no improvement, as the STATCOMs became blocked when the voltage dropped below the configured threshold value due to the close distance of the fault.

Figure 5.20 presents the voltage response when the fault location is slightly further from the compensation devices. In this scenario, the voltage drop reached approximately 0.34 PU without any mitigation method. Since the configured voltage threshold value of the STATCOM is below 0.34 PU, the device was able to contribute, enhancing the voltage response, as shown in Scenario C.

Table 5.3: CLOD Load distribution percentage.

Load Component	Composition presentage (%)
Large Motor (LM)	65
Small Motor (SM)	15
Discharge Lighting (DL)	0
Transformer Saturation (TS)	10
Constant Power (CP)	5
Kp	1.25
R	0
X	0.1

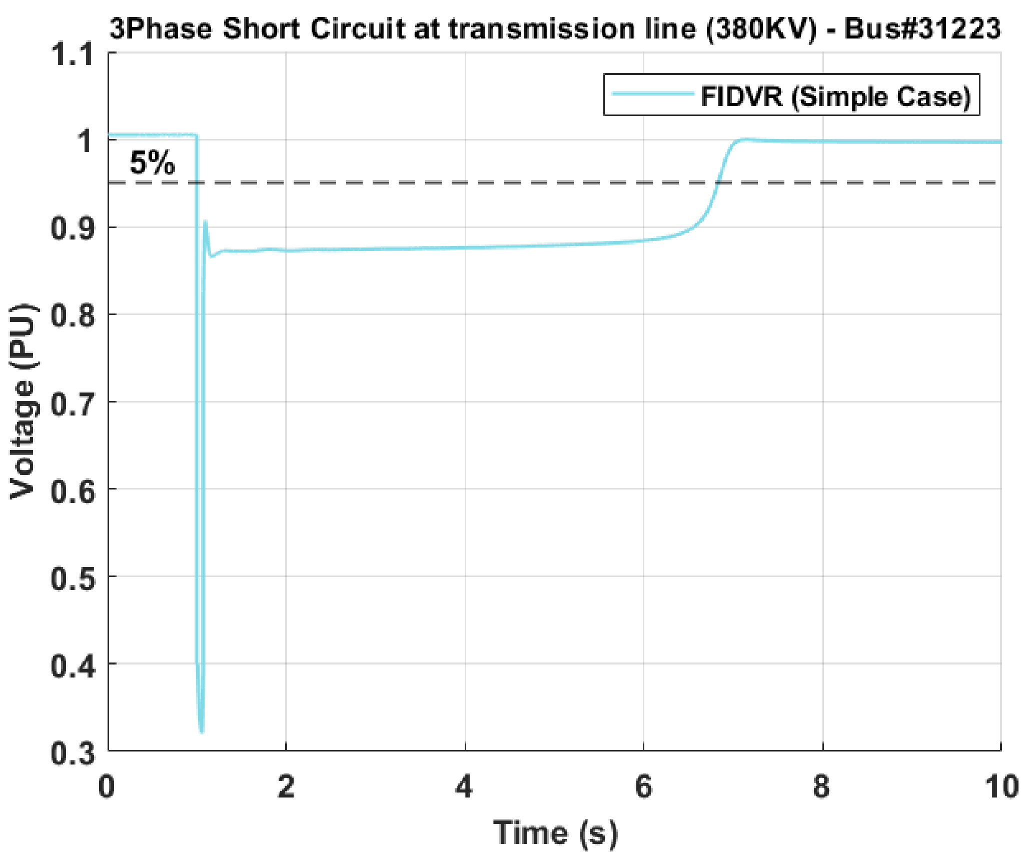

Figure 5.18: FIDVR event without mitigation.

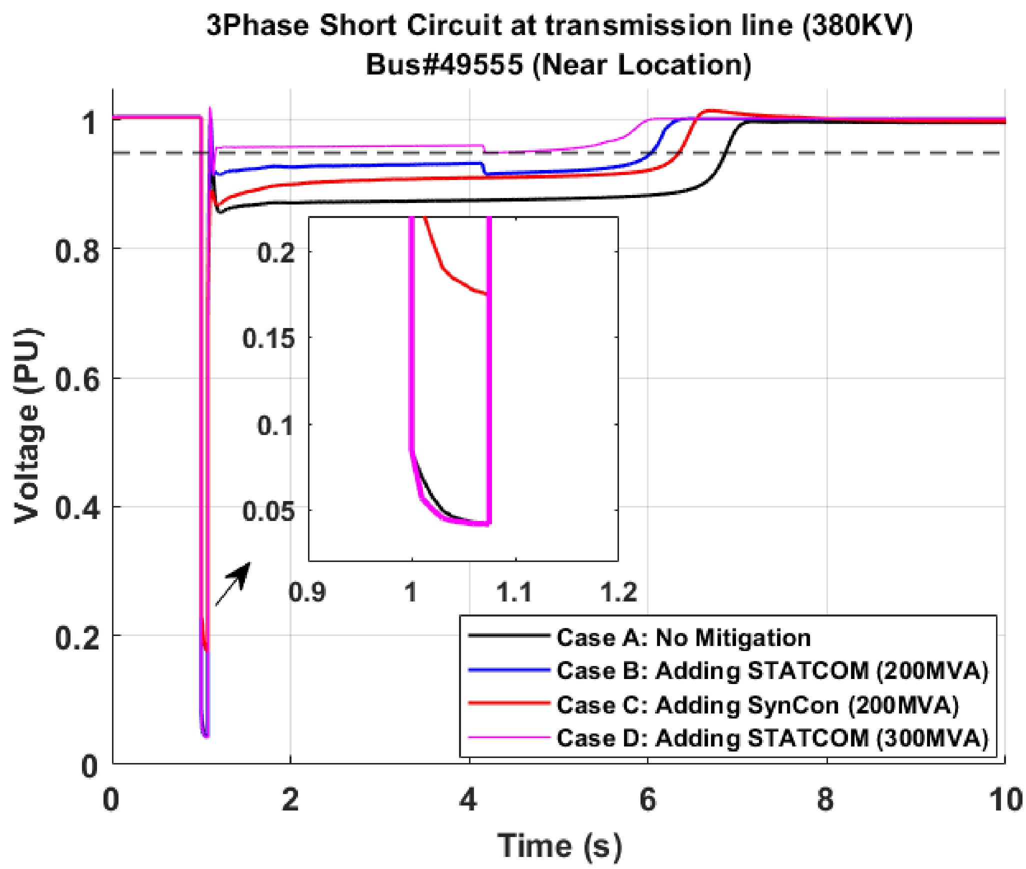

Figure 5.19: Comparison between STATCOM and SynCon in mitigating an FIDVR event (Near fault location).

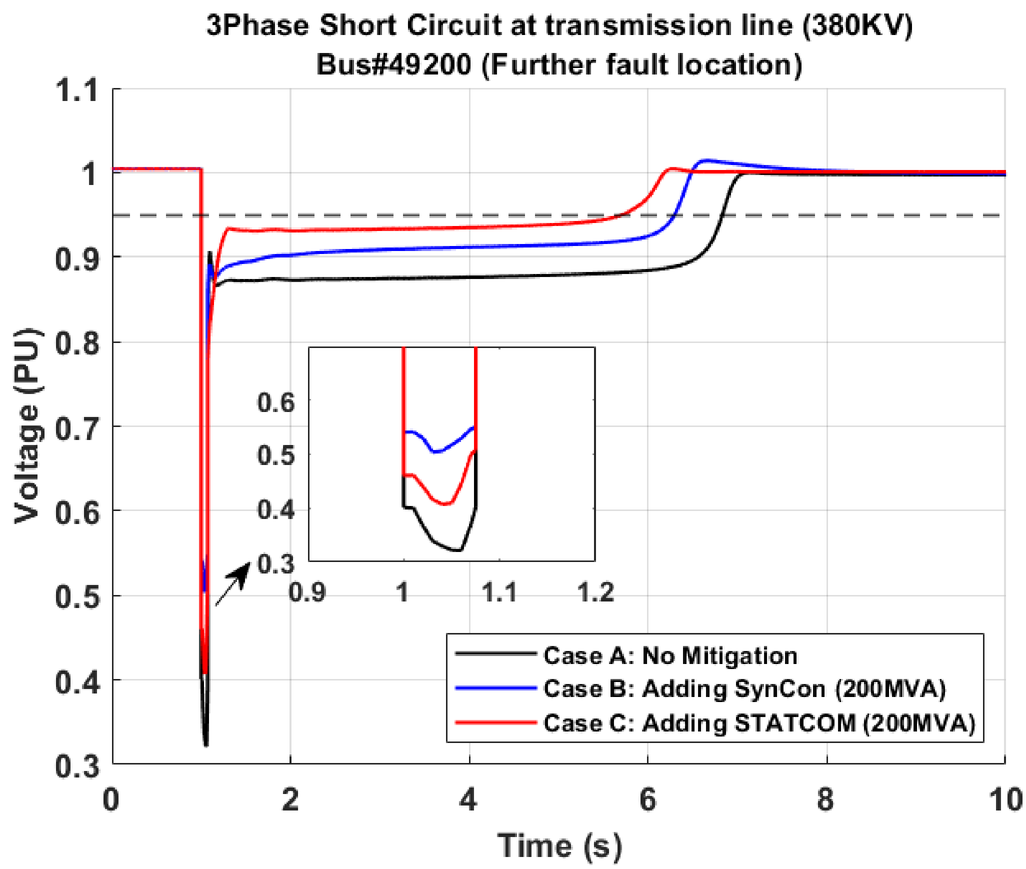

Figure 5.20: Comparison between STATCOM and SynCon in mitigating an FIDVR event (Further fault location).

Figures 5.21 and **5.22** illustrate the recovery times for SynCon and STATCOM, respectively. The SynCon required 5.31 seconds to recover to the safe region (defined as within 5% of the pre-fault voltage) and reached its final steady-state voltage after 7.00 seconds. Conversely, the STATCOM demonstrated faster performance, achieving recovery to the safe region in 4.80 seconds and stabilizing at the final voltage in 5.50 seconds. While the SynCon experienced a smaller initial voltage dip due to its higher fault current contribution, the STATCOM proved more effective in restoring voltage levels quickly, making it preferable for faster recovery.

5.5.4.3 SynCon vs. STATCOM: Mitigating FIDVR as the Electrical Distance Increases

The effectiveness of voltage compensation devices, such as SynCons and STATCOMs, in mitigating FIDVR is heavily influenced by the electrical distance between the fault location and the compensation devices. This electrical distance is calculated by the Thevenin equivalent impedance between two buses in the grid [111, 112, 113]. As this distance increases, the amount of fault current injected by these devices get reduced, leading to a lower impact on voltage response.

Fault current injection is most efficient when the voltage compensation devices are located closer to the fault, as the impedance between the fault and the devices is lower. This lower impedance allows for greater fault current injection, thereby improving the voltage response more effectively. Conversely, as the electrical distance increases, the impedance rises, reducing the ability of these devices to significantly influence the voltage response.

Since faults can occur at any point within the grid, the strategic placement of SynCons and STATCOMs is crucial. Ideally, these devices should be placed where they can inject a substantial amount of fault current, improving their impact on voltage recovery.

To determine the electrical distance, or Thevenin impedance, between nodes i and j, a specific methodology is followed. First, the admittance matrix Y is constructed,

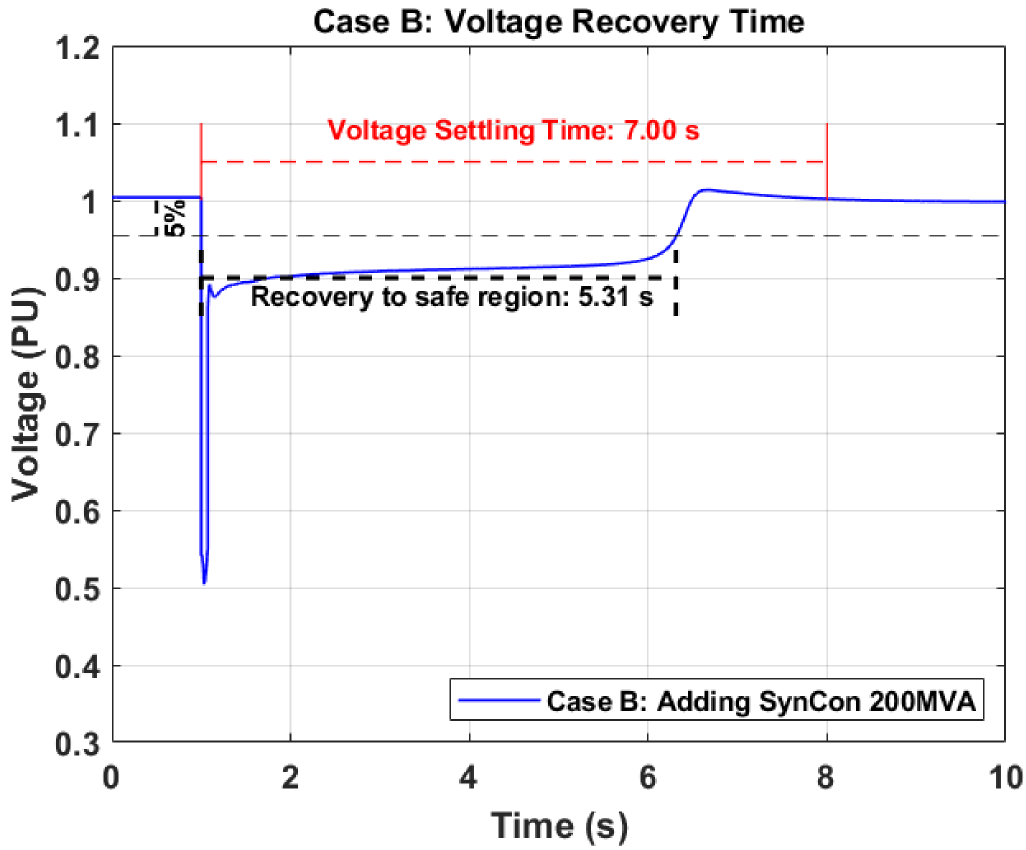

Figure 5.21: SynCon recovery time during FIDVR event.

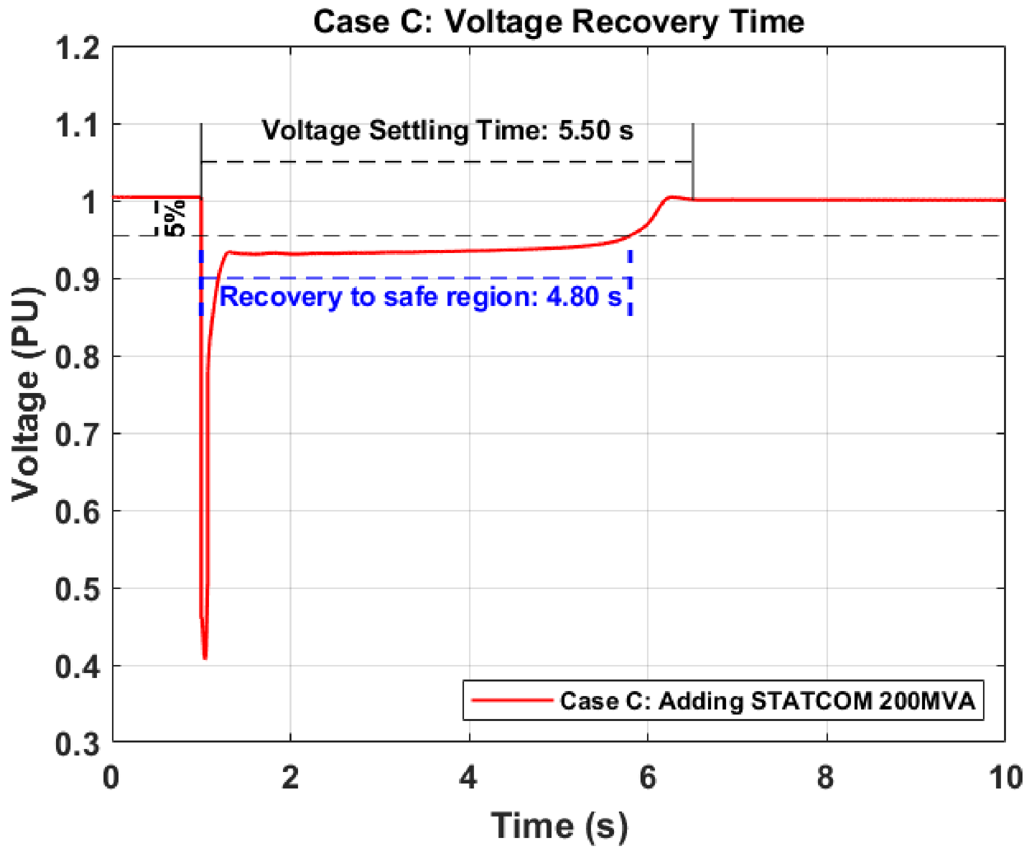

Figure 5.22: STATCOM recovery time during FIDVR event.

then inverted to obtain the impedance matrix Z. The Thevenin impedance Z_{ij}^{thev} is calculated using the formula [113]:

$$Z_{ij}^{\text{thev}} = Z_{ii} + Z_{jj} - 2Z_{ij} \tag{5.10}$$

where Z_{ii} and Z_{jj} are the diagonal elements of the impedance matrix at buses i and j, respectively, and Z_{ij} represents the off-diagonal terms. This calculation provides the necessary impedance values to assess the optimal placement and expected performance of voltage compensation devices in relation to fault locations within the grid.

Figure 5.23 illustrates the current injection behavior of SynCon and STATCOM devices under varying electrical distances. When the electrical distance is minimal, the SynCon can instantly inject a substantial amount of fault current, which is determined by its rated capacity, the difference between its internal and terminal voltages due to the sudden change, and its sub-transient reactance. In contrast, at minimal electrical distances, the STATCOM may block as the terminal voltage drops below its low-voltage threshold, preventing current injection. However, as the electrical distance increases and the terminal voltage stays within its set thresholds, the STATCOM can rapidly provide its full capacity, preventing blocking. Meanwhile, the SynCon's fault current injection decreases as the electrical distance increases, due to the reduced voltage difference between its internal and terminal voltages.

In summary, when the fault is very close to the compensation devices, SynCon can inject a large amount of fault current, whereas STATCOM may be blocked due to low voltage conditions. As the electrical distance from the fault location to the compensation device increases, the fault current contribution from SynCon reduces more significantly compared to STATCOM. This highlights the importance of considering electrical distance when evaluating the effectiveness of these compensation devices in enhancing grid stability and mitigating FIDVR.

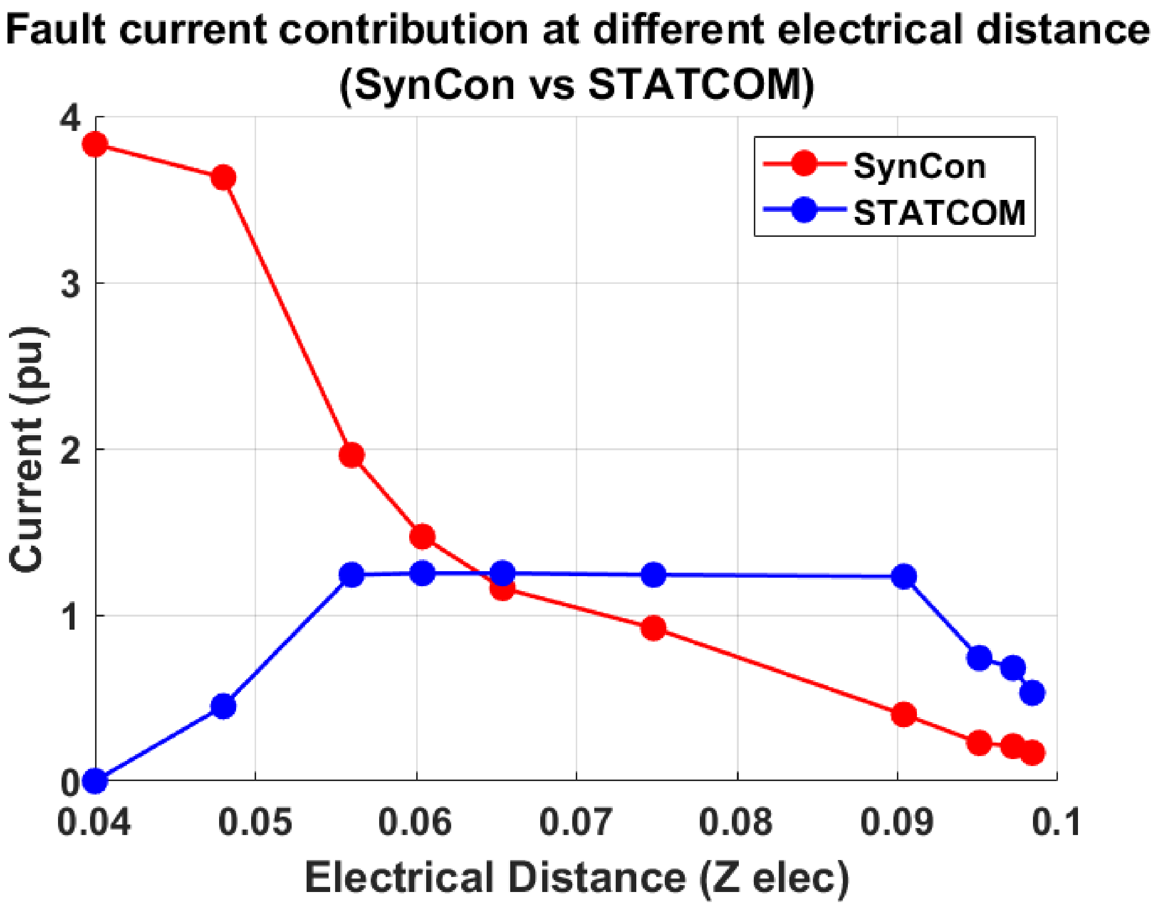

Figure 5.23: Fault current contribution of STATCOM vs. SynCon at different electrical distances.

5.5.5 Case E: The impact of adding more transmission lines on voltage stability with high solar PV penetration

Although solar PV installations are often concentrated near load centers to minimize transmission losses, this study recognized that the geographical location of the entire country is highly suitable for widespread solar PV adoption. As a result, SGs were replaced with solar PV systems at the same locations across the grid. To accommodate the specific demands of solar power, both load and generation capacities were re-scaled to account for the energy needs of energy storage systems (ESSs) and to anticipate a future expansion exceeding 60% of peak load. Notably, in the Southern Operating Area (SOA), 40% of the total load is supplied from the Western Operating Area (WOS) via long 380 kV transmission lines.

In an alternative scenario, the increased stress on these transmission lines due to the rise in peak load was mitigated by adding an additional transmission line. Specifically, a new circuit was installed between the Central Operating Area (COA) and SOA. This additional infrastructure was intended to enhance the resilience of the grid and responsiveness to load fluctuations.

The effectiveness of this strategy was evaluated by observing the system response when the largest generation unit was tripped. The results, as shown in **Figure 5.24**, indicate an improvement in voltage response following the contingency. These findings highlight the potential benefits of strategic transmission line expansion in regions experiencing significant renewable energy penetration and increasing peak load demands.

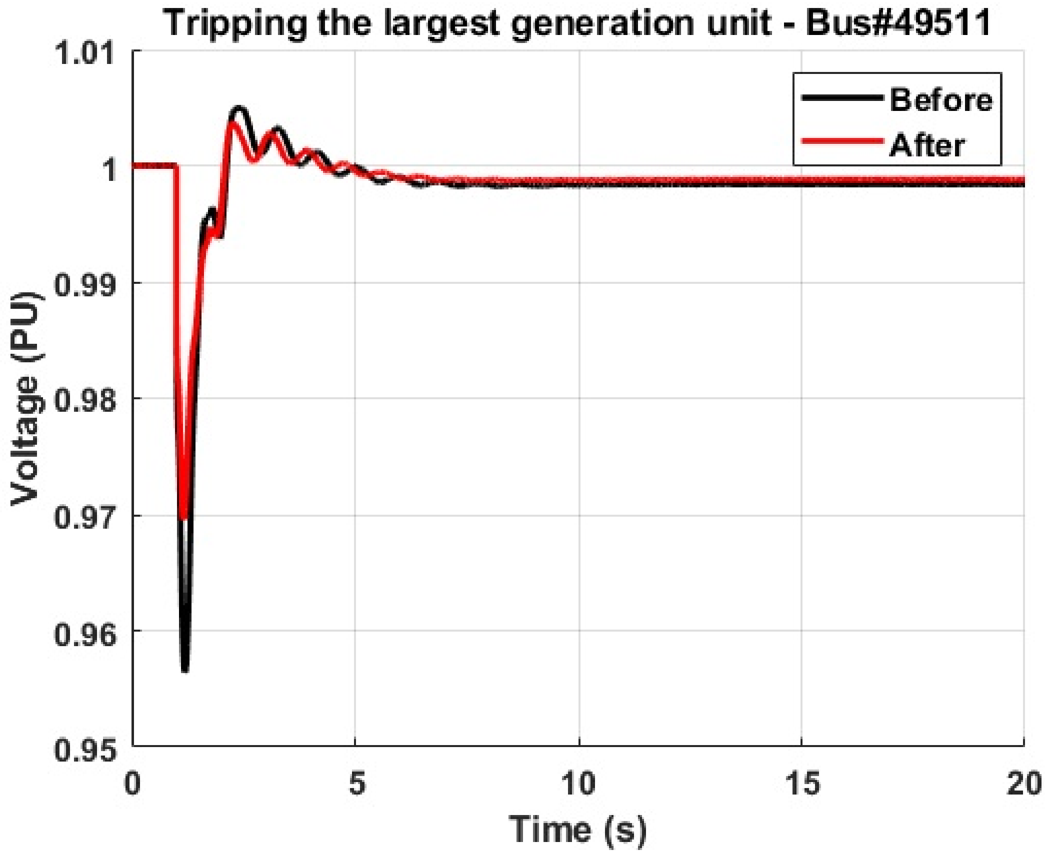

Figure 5.24: Voltage response after adding a transmission line between bus COA and SOA.

5.5.6 Case F: The impact of relocating solar PV near central loads on voltage stability with high solar PV penetration

This part of the study examined the impact of relocating solar PV panels near central loads in the SOA to improve voltage stability. By placing solar PV installations closer to load centers, the distance over which power is transmitted is reduced, lowering transmission losses and improving voltage stability under peak load conditions.

The effectiveness of this strategy was assessed based on its response to the tripping of the largest generation unit. The results showed a slight improvement in voltage response following the relocation of solar PV panels as presented in **Figure 5.25**. These findings suggest that strategic placement of solar PV systems can enhance voltage stability, particularly in regions with high renewable energy penetration and significant peak load demands.

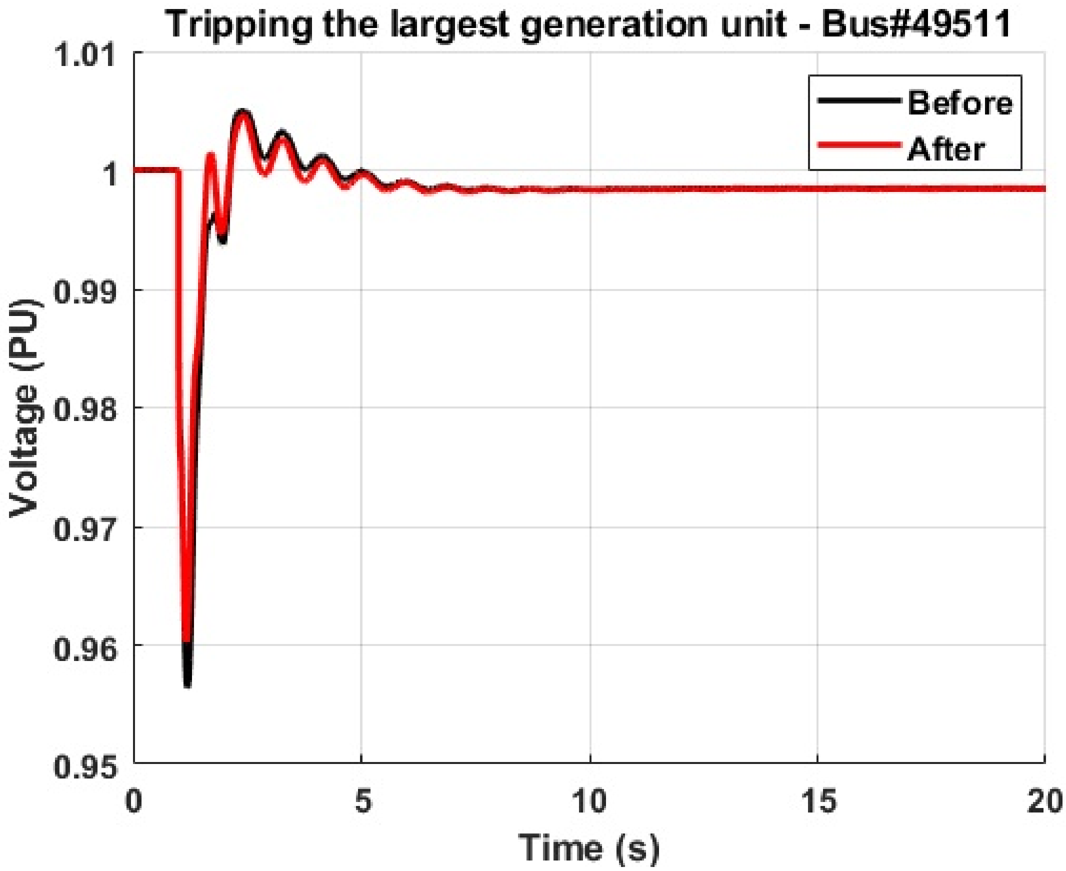

Figure 5.25: Voltage response after relocating solar PV near central loads.

Chapter 6

Enhancing Frequency Stability in the Saudi electric Grid for Solar Power Integration

6.1 Introduction

Frequency stability is a critical aspect of power system operation, particularly with the recent rapid development and increased focus on RESs [10, 11, 12]. It refers to the ability of the grid to maintain a consistent frequency under all operating conditions [61]. Unstable events can lead to blackouts, load tripping, and damage to equipment and infrastructure if stability is not properly managed [16, 55].

Traditionally, frequency stability was inherently supported by SGs, which regulate frequency due to their rotating masses, as detailed in Chapter 2 [10, 114]. However, the growing penetration of IBRs, such as solar PV systems, introduces new challenges. These resources rely on power electronic converters, which lack the physical inertia provided by SMs, making the grid more vulnerable to frequency deviations during disturbances [10, 11].

Under normal conditions, the acceptable range of frequency deviation is typically between 59.97 Hz and 60.03 Hz [94]. Fluctuations within this range are common due to load variations. However, during abnormal conditions such as the loss of a generator, the frequency can deviate significantly, stressing the system and necessitating the implementation of robust solutions.

SynCons are a key solution in maintaining frequency stability, as they provide inertia similar to SGs and can enhance the ability of the system to respond to frequency deviations [38, 64, 66, 74, 87, 88, 115]. Additionally, BESS can further enhance the role of SynCons, helping to regulate frequency rapidly when needed [116, 117, 118, 119, 120]. Given that BESS is primarily proposed in this study to provide energy during night-time, their high cost must be justified by fulfilling additional roles, such as enhancing stability. This chapter investigates frequency stability with high IBR penetration and considers the role of SynCons in providing inertia to regulate frequency and improve grid stability.

6.2 Problem statement

The integration of IBRs such as solar PV systems presents significant challenges to maintaining frequency stability in modern power grids. Traditional SGs inherently provide system inertia through their rotating masses, which naturally resist changes in frequency during disturbances. This inertia plays a critical role in slowing down the RoCoF after a fault, providing the operators time to respond.

In contrast, solar PV systems operate using power electronics that lack the rotating masses necessary to contribute physical inertia. As a result, high levels of solar PV integration can significantly reduce the overall system inertia, leading to faster frequency deviations and an increased risk of frequency instability during grid disturbances. Without sufficient inertia, the grid becomes more vulnerable to rapid frequency fluctuations, raising the likelihood of under-frequency events and potential load-shedding scenarios as shown in **Figure 6.1**.

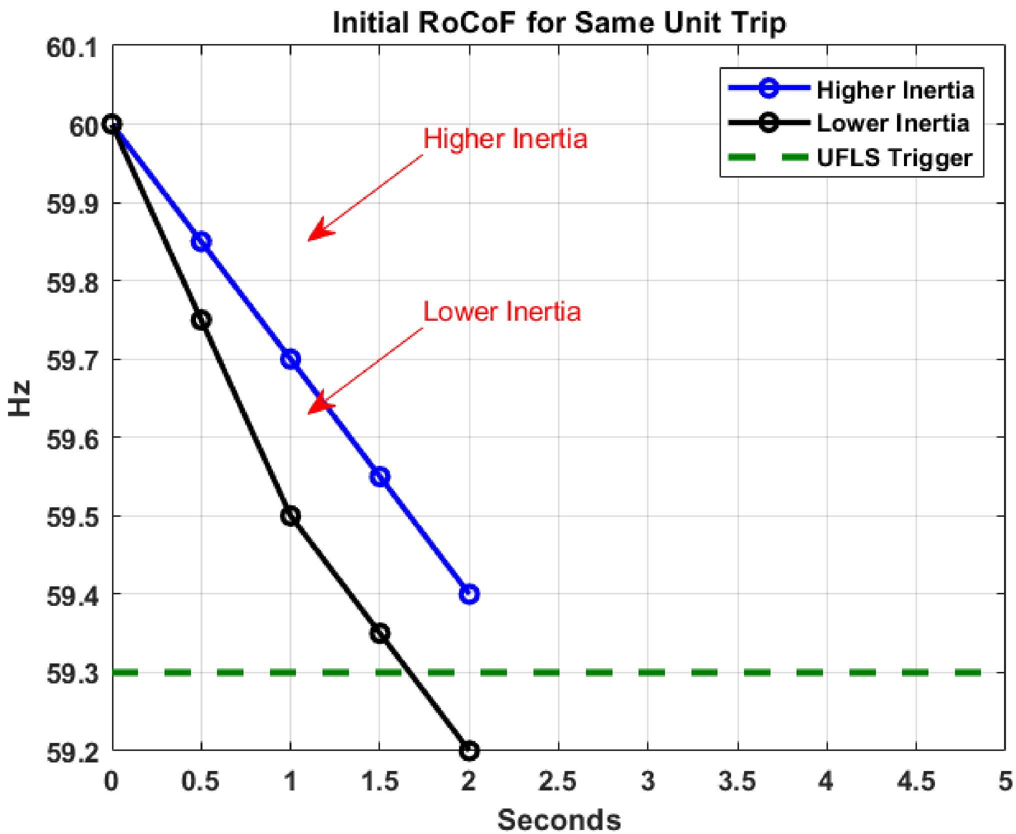

Figure 6.1: Impact of system inertia on the rate of change of frequency (RoCoF) following a unit trip.

6.3 Basic of Frequency Stability

The relationship between power imbalance and frequency deviation is given by [53, 75, 121]:

$$\Delta f = \frac{1}{2H} \int (\Delta P_m - \Delta P_e)\, dt \tag{6.1}$$

where Δf is the frequency deviation, H is the inertia constant, ΔP_m is the change in mechanical power, and ΔP_e is the change in electrical power.

The inertia constant, which measures the stored kinetic energy in the rotating mass of the generator, is defined as:

$$H = \frac{1}{2} \frac{J\omega_s^2}{S_b} \tag{6.2}$$

where J is the moment of inertia, ω_s is the synchronous speed, and S_b is the system base apparent power.

In the context of maintaining frequency stability, SynCons play a crucial role by providing inertia to the system. When a disturbance occurs in the grid, such as a sudden loss of generation or a spike in demand, the balance between generation and load is disrupted, causing the system frequency to deviate from its nominal value [10]. The rotating mass of SynCons resists this frequency change by temporarily releasing or absorbing kinetic energy.

6.3.1 Frequency Stability response behavior

The following metrics assist in understanding the frequency stability and the behavior of the system during disturbances:

- **Rate of Change of Frequency (RoCoF):**
  This metric measures the rate at which the frequency changes following a disturbance. High RoCoF values indicate rapid frequency shifts, which can

destabilize the power system [53, 75, 121]. Monitoring RoCoF provides insight into the immediate impact of a disturbance and the available inertia within the system. It is presented as follow [53, 75, 121]:

$$\text{RoCoF} = \frac{df}{dt} = \frac{1}{2H}(\Delta P_m - \Delta P_e) \tag{6.3}$$

where $\frac{df}{dt}$ is the rate of change of frequency, ΔP_m is the change in mechanical power, and ΔP_e is the change in electrical power. As shown in the RoCoF equation, a higher inertia constant slows the rate of frequency change. This dynamic response provides extra time for other frequency control methods to respond effectively.

- **Frequency Nadir:**
  This is the lowest point to which the frequency dips following a disturbance, occurring before any frequency control actions take effect. It indicates the impact of the disturbance and can be used to evaluate the effectiveness of the available inertia within the system

6.4 Methodology

This section outlines the methodology used to enhance frequency stability after transitioning the Saudi grid to fully solar PV. The study was conducted in PSSE, following the same procedure introduced for voltage stability in Chapter 5.

Frequency stability assessment, testing, and improvement were carried out using the following case scenarios:

- **Case A: Determining the solar PV penetration limit for stable frequency response:**
  In this case, solar PV penetration in the Saudi model was gradually increased

to determine the penetration limit before frequency response became unstable. No mitigation methods were applied in this scenario.

- **Case B: Testing frequency response as synCons increase the SCR:** This case involved testing frequency stability in three scenarios where SynCons were used to increase the SCR by specific values under different contingencies. The goal was to evaluate how varying the SCR impacts frequency stability and to assess the effectiveness of SynCons in maintaining system stability [72].

- **Case C: Impact of adding a transmission line on frequency stability with high solar PV penetration:**
  This scenario investigated how adding a new transmission line to the grid impact on frequency stability. The analysis focused on how the new line improves power flow, reduces constraints, and helps maintain a stable frequency during contingencies.

- **Case D: Impact of relocating solar PV near central loads on frequency stability with high solar PV penetration:**
  This case evaluated the potential benefits of relocating solar PV panels closer to central loads to enhance frequency stability. The study aimed to explore how such relocations might influence system resilience and frequency performance.

6.5 Results and Discussion

6.5.1 Case A: Evaluating the Impact of Solar PV Penetration on Frequency Stability

In this section, the frequency response of the Saudi electric grid is investigated as solar PV gradually replaces SGs. The goal is to assess how increasing solar PV penetration impacts the grid's ability to maintain frequency stability following a disturbance.

Initially, the frequency response was analyzed with a 60% solar PV penetration under the scenario of tripping the largest generator. As shown in **Figure 6.2**, the system's frequency response was slow to recover, struggling to return to its pre-fault values.

Additionally, as solar PV penetration increased to 80%, the frequency response showed more significant challenges. **Figure 6.3** illustrates that the system experienced a worse frequency nadir and greater difficulty returning to a stable condition after the contingency.

When the penetration level reached 100%, the frequency response became highly unstable. The power flow could not converge after applying the contingency. This instability highlights the limitations of operating a grid with 100% solar PV penetration without adequate methods to enhance frequency stability. The lack of physical inertia in solar PV systems has a significant impact on the RoCoF, highlighting the need for effective mitigation strategies. Implementing solutions such as SynCons or BESS could provide the necessary inertia and support to maintain the desired stability.

6.5.2 Case B: Test frequency response when SynCons increase the SCR Gradually

In this part of the study, the integration of SynCons is approached in three scenarios, with each scenario increasing the SCR by a specific value.

6.5.2.1 Frequency Response when SynCons increase the SCR by 1:

In this case, the SynCons were used to increase the SCR by 1. However, the network did not converge due to a lack of sufficient inertia and power imbalance [72].

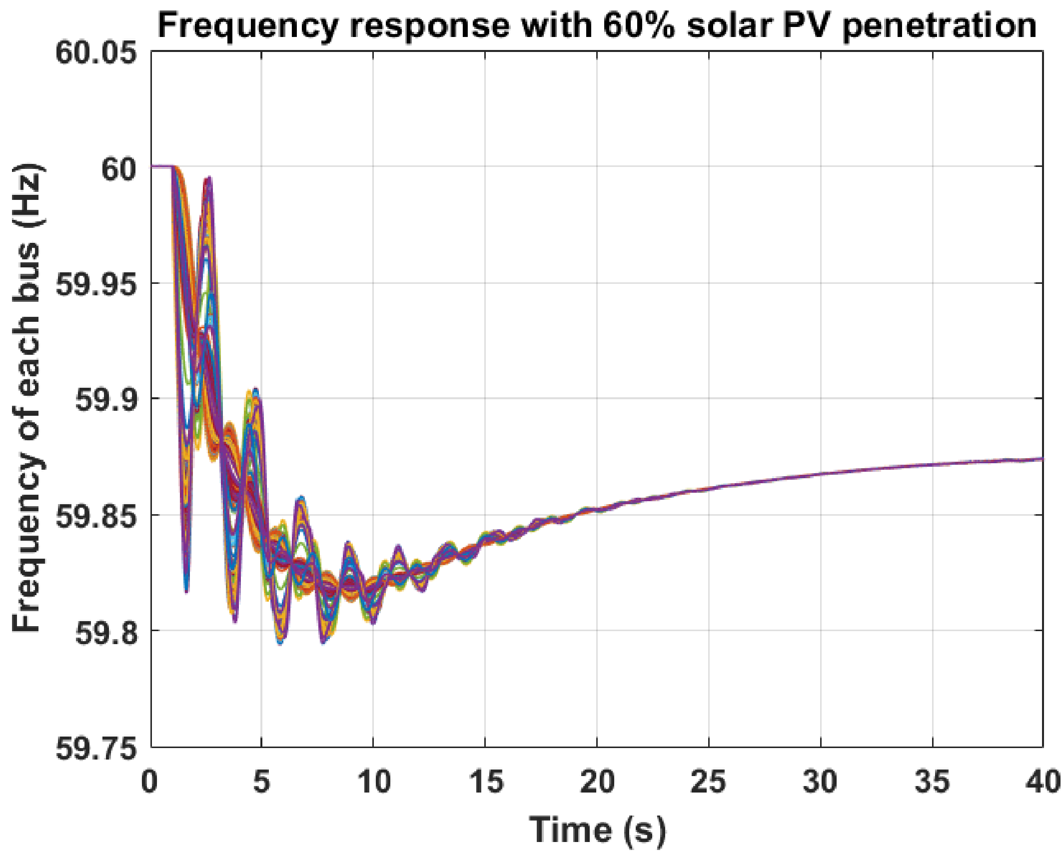

Figure 6.2: Frequency response with 60% solar PV with tripping the largest generator.

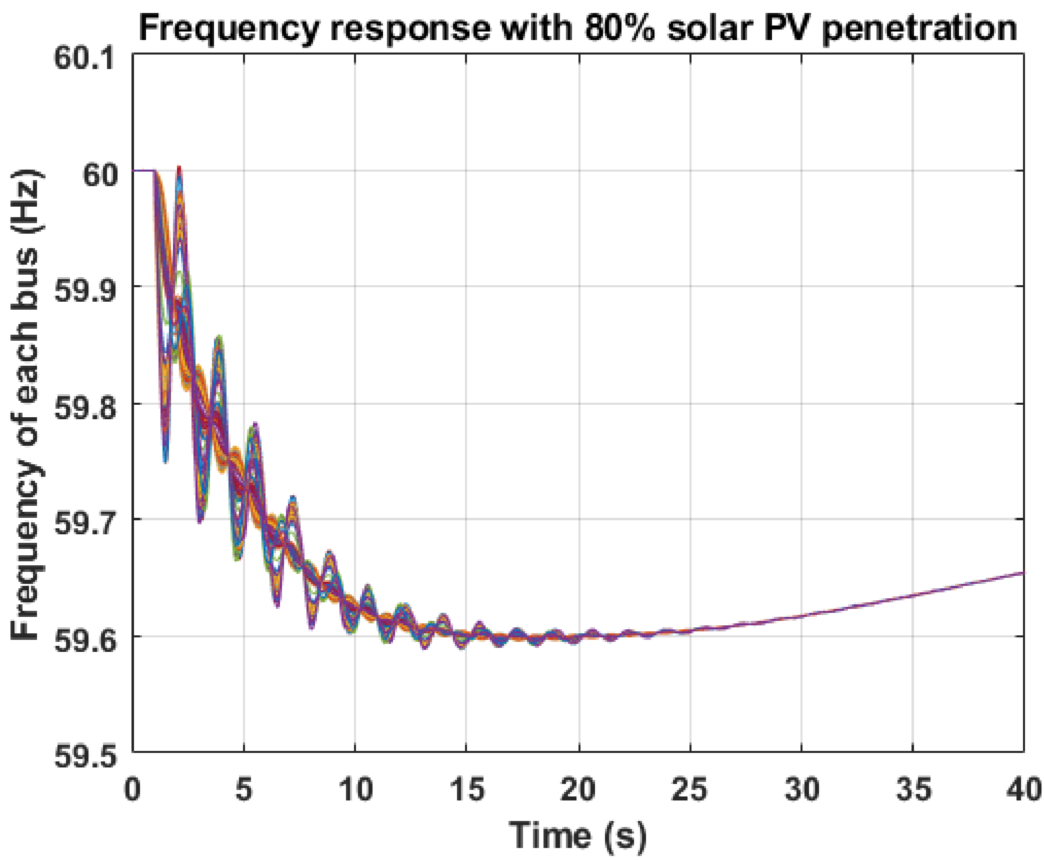

Figure 6.3: Frequency response with 80% solar PV with tripping the largest generator.

6.5.2.2 Frequency Response when SynCons increase the SCR by 2:

With the SCR increased by 2 using SynCons, the system struggled to return to a steady-state condition after a unit trip, as shown in **Figure 6.4**. This indicates that the inertia provided was still insufficient to stabilize the system [72].

6.5.2.3 Frequency Response when SynCons increase the SCR by 3:

When the SCR was increased by 3 with the help of SynCons, the overall performance improved significantly. The frequency response was able to return close to its nominal value after the contingency, settling at 59.99 Hz. This demonstrates that the inertia contribution and the SCMVA provided by the SynCons effectively mitigated the challenges introduced by the integration of solar PV, as illustrated in **Figure 6.5** [72].

As previously noted, BESS plays a critical role in grids powered by renewable energy. Given the high costs associated with BESS, it is crucial to maximize their utility. BESS can further enhance active power compensation following a contingency and improve frequency response, as shown in **Figure 6.6**. Additionally, **Figure 6.7** highlights the respective contributions of SynCons, BESS, and inverters to the frequency response and the RoCoF [71].

6.5.3 Case C: impact of adding a transmission line on frequency stability with high solar PV penetration

This case investigates the effects of adding a new transmission line on frequency response. In theory, adding a transmission line can enhance system stability by improving power flow and mitigating constraints, which in turn helps to maintain a more stable frequency during contingencies. **Figure 6.8** illustrates the frequency response before and after the transmission line was added.

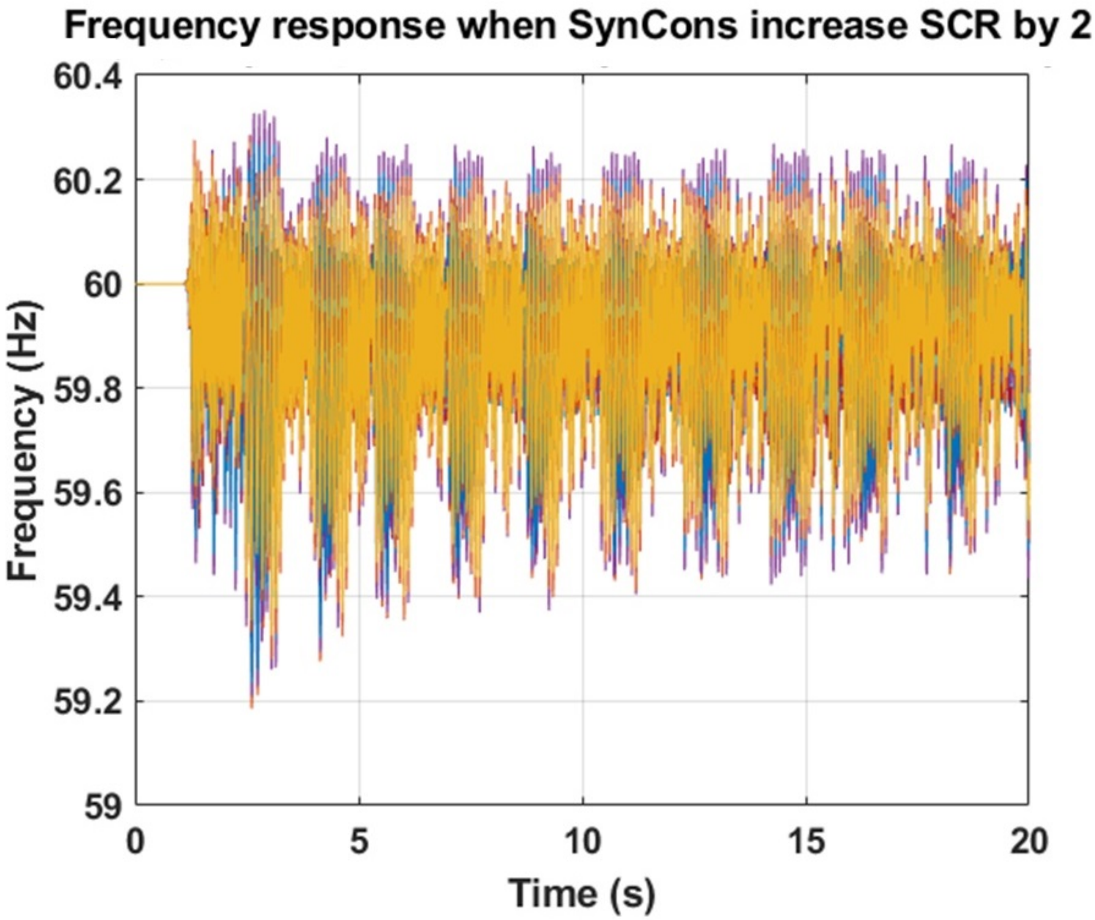

Figure 6.4: Frequency response Frequency response at 100% solar PV when SynCon increase the SCR by 2 during a generator trip event.

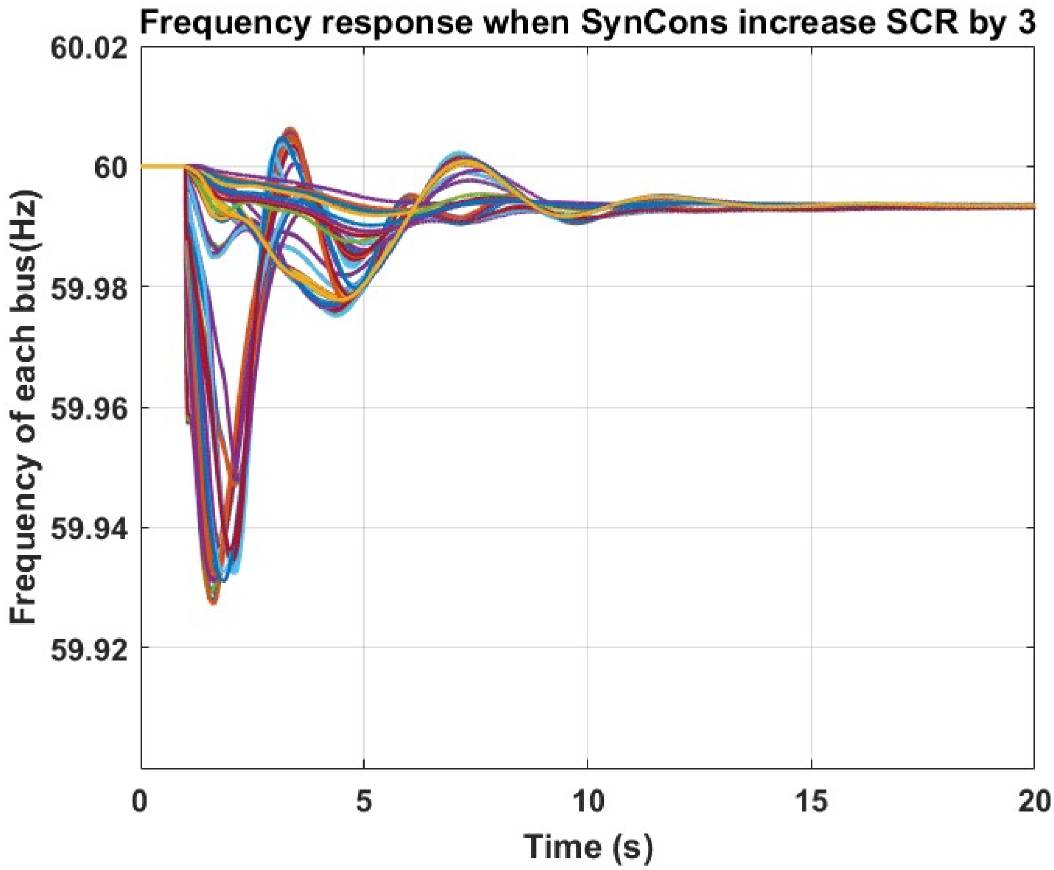

Figure 6.5: Frequency response at 100% solar PV when SynCon increase the SCR by 3 during a generator trip event.

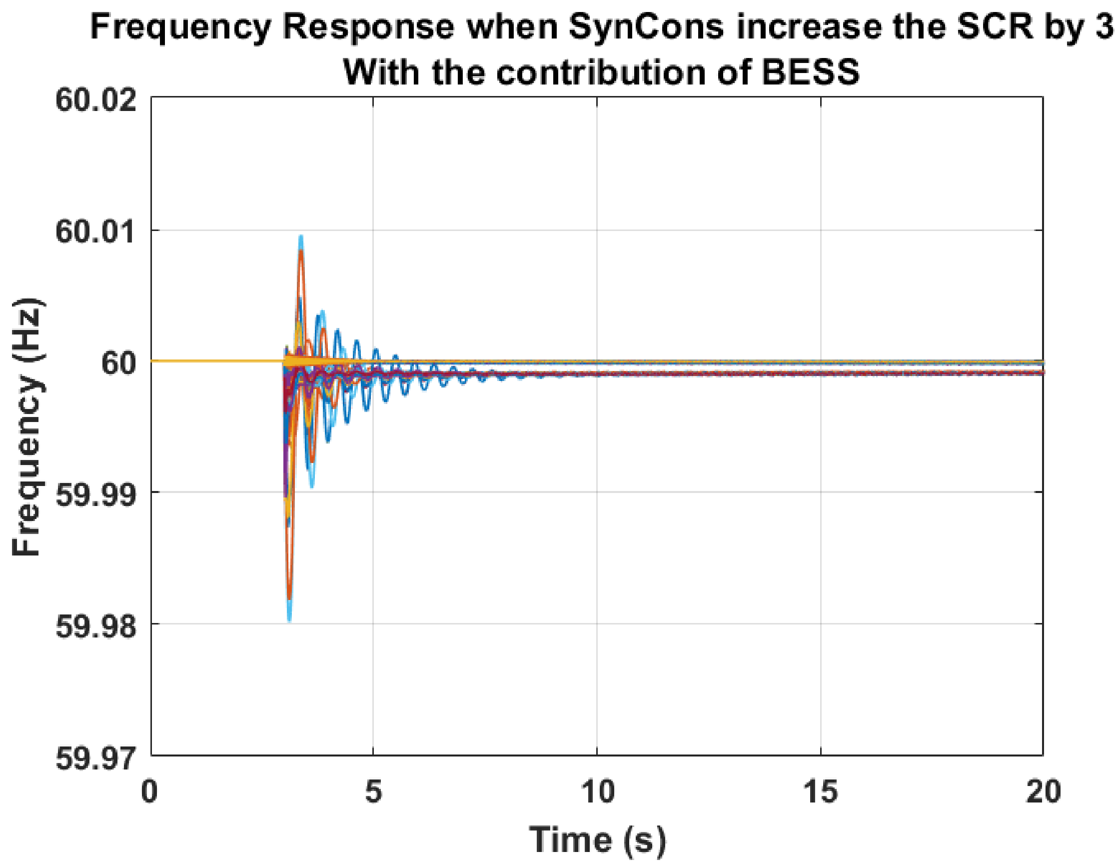

Figure 6.6: Frequency response at 100% solar PV when SynCon increase the SCR by 3 during a generator trip event (with the contribution of BESS).

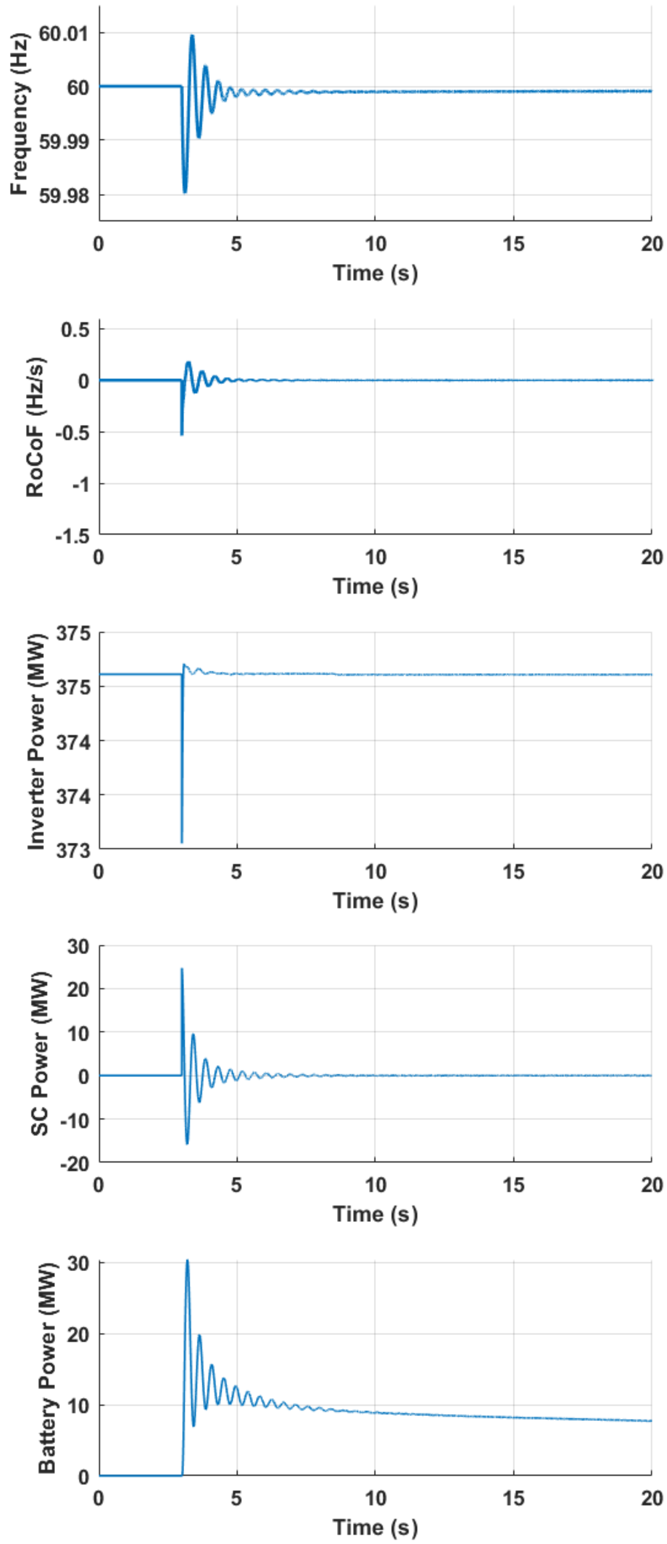

Figure 6.7: System response at 100% solar PV when SynCon increase the SCR by 3 during a generator trip event).

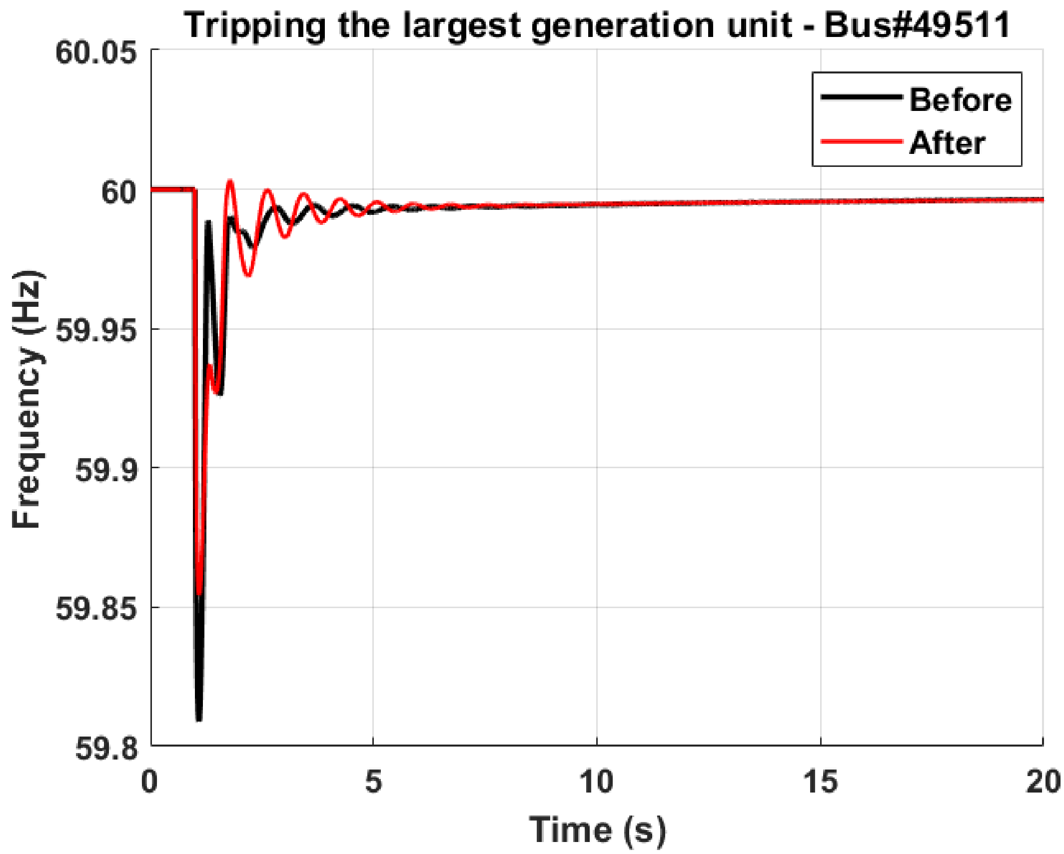

Figure 6.8: The Impact of adding transmission line on frequency Response.

6.5.4 Case D: impact of relocating solar PV near central loads on frequency stability with high solar PV penetration

This case examines the impact of relocating solar PV panels closer to central loads on frequency stability. This approach can reduce transmission losses, thereby contributing to a more resilient frequency response. **Figure 6.9** depicts the frequency response after relocating the solar PV panels near center loads at the SOA.

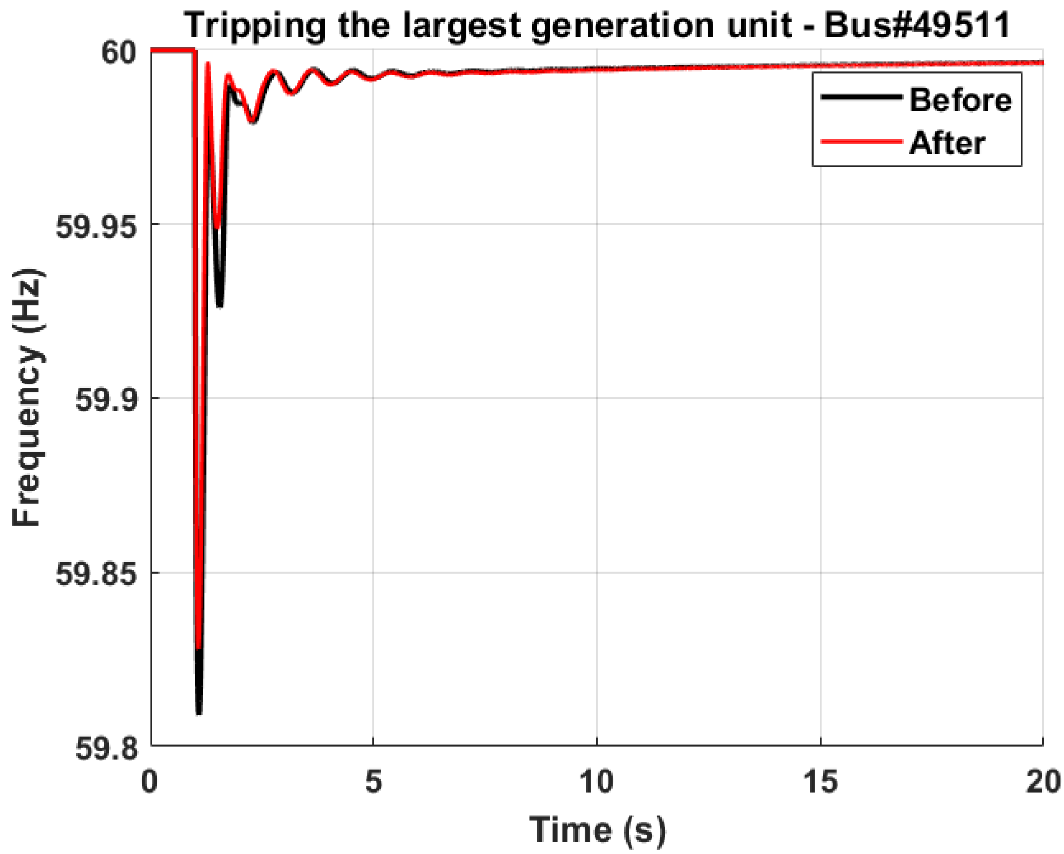

Figure 6.9: The Impact of relocating solar PV near central load on frequency Response.

Chapter 7

Improving the Protection System in the Saudi Electric Grid for Solar Power Integration

7.1 Introduction

The fundamental purpose of power system protection is to continuously monitor and rapidly detect faults. This ensures that any issues are quickly identified and addressed before they can expand into more significant problems [122]. The continuous deployment of solar PV systems in power grids requires a focus on protection technologies to maintain reliable and safe operating conditions [54]. As indicated in Chapter 2, SGs in traditional generation can deliver substantial fault currents that enable the rapid detection and isolation of faults, providing more operational flexibility. However, the shift towards IBRs reduces this high fault level benefit since they typically generate lower fault currents due to their limited over-current capabilities [66]. This creates challenges in adopting conventional protection mechanisms to detect and isolate faults accurately [66, 52, 54, 123, 124].

To address the challenge of low fault current in grids with a high penetration of IBRs, several innovative solutions have been proposed and developed [87, 88, 89, 123, 125]. One effective method is the use of adaptive relay settings that adjust to improve fault detection in grids with high penetration of solar PV generation [126]. Additionally, advanced inverter technologies are being developed to deliver higher fault currents, improving the overall fault current capacity of the grid [41, 125]. Another valuable approach is the integration of mitigation devices such as SynCons that provide substantial fault current support after grid disturbances [87, 88, 89].

Among these solutions, the integration of SynCons stands out as highly useful. By injecting a high amount of fault current, SynCons ensure that protection systems such as circuit breakers and relays function effectively, even in grids with a high penetration of renewable energy sources. Therefore, adapting protection schemes to accommodate the dynamic behavior of IBRs is crucial for ensuring continuous and reliable operation.

This chapter focuses on facilitating the integration of RES and optimizing the protection system in a fully solar PV power grid. It aims to determine the minimum SCR required to ensure reliable operation of traditional protection schemes, using SynCon as the fault current provider. By restoring sufficient fault current levels, this approach makes conventional overcurrent protection systems effective once again, addressing one of the key challenges posed by the shift to IBRs-powered grids.

7.2 Background

Overcurrent relays count on the magnitude of fault current to detect abnormal conditions and activate circuit breakers. However, in scenarios involving IBRs, where fault currents are typically lower, the performance of these relays can be restricted. This may result in reduced sensitivity and selectivity, causing delays in fault detection, improper fault isolation, or even failure to identify faults [122].

In contrast, traditional SGs can deliver substantial fault currents during short-circuit events, often exceeding their rated capacity by several times [52]. Such high fault current levels are typically sufficient for overcurrent relays to detect and clear faults within a few cycles. **Figure 7.1** shows the current output of a standard SG during a 3-phase short circuit event. As depicted, the SG can generate fault currents up to 5.57 PU, ensuring a robust contribution that protective relays can reliably sense.

7.3 Problem Statement

As solar PV penetration increases, the fault current contribution decreases, making fault detection by protective relays increasingly difficult. This gradual shift in short-circuit current has significant implications for the reliability and stability of the power system. **Figure 7.2** illustrates the reduction in fault current as solar PV penetration rises incrementally from 20% to 80%.

At 100% solar PV penetration, inverters are unable to supply substantial fault current, creating significant challenges for overcurrent relays to operate effectively. **Figure 7.3** shows the behavior of a typical inverter during a 3-phase short-circuit event. As shown, the inverter shuts down almost immediately when the fault occurs. This lack of fault current disrupts the fundamental operation of overcurrent relays, making it difficult to detect and isolate faults.

7.4 Methodology

This section describes the methodology used to enhance fault current levels through the integration of SynCons, with the SCR serving as a metric for system strength. The primary objective is to identify the required SCR that ensures fault current levels comparable to those in traditional power grids. As outlined in Chapter 2, fault current is directly proportional to SCR, meaning an increase in SCR will

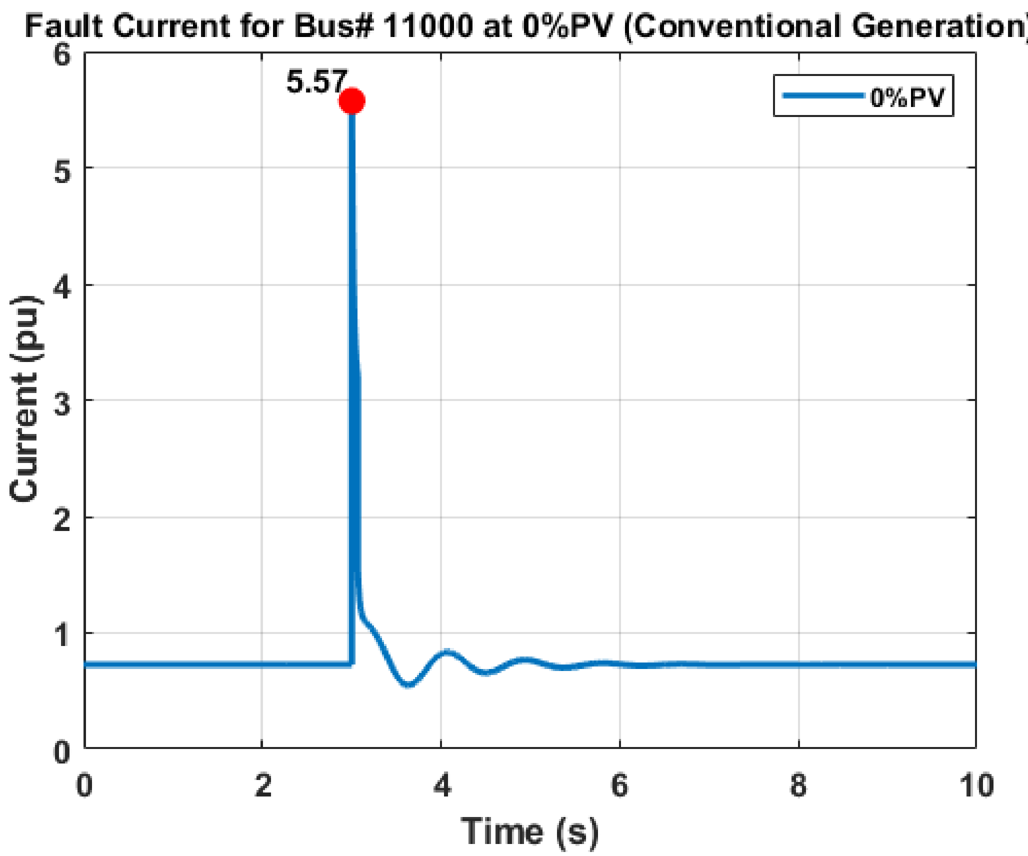

Figure 7.1: Injected current from a typical synchronous generator.

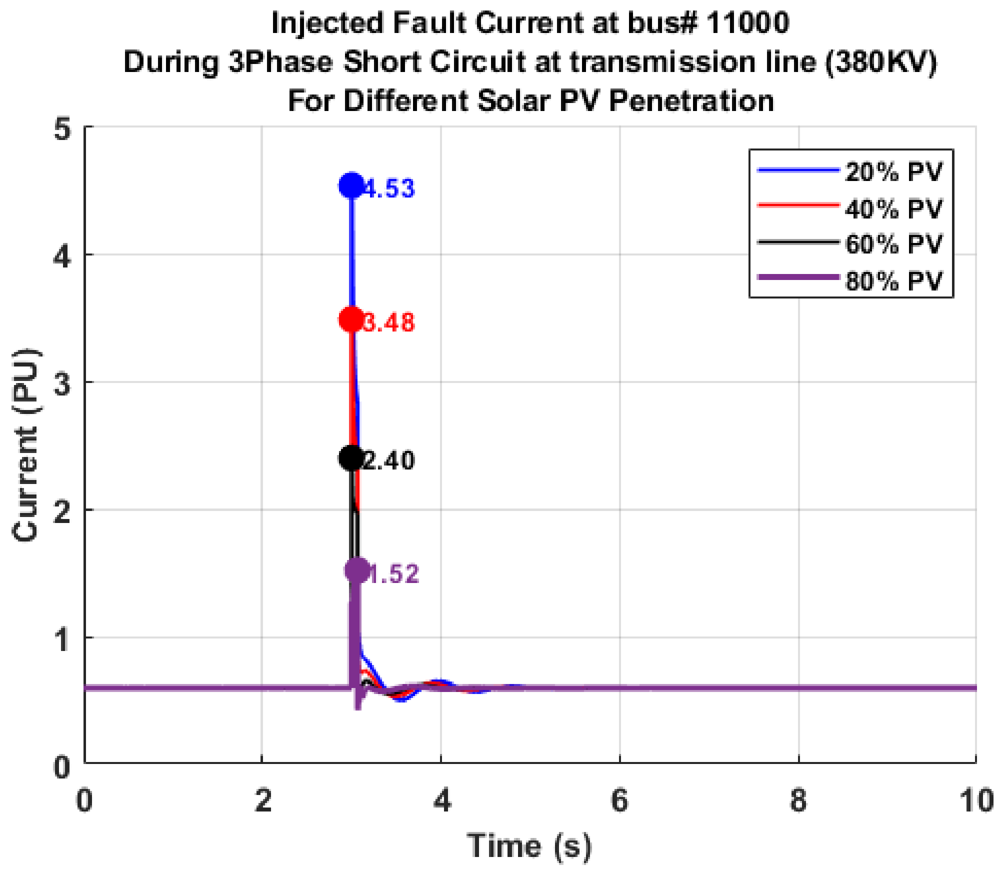

Figure 7.2: Injected fault current with different solar PV penetration.

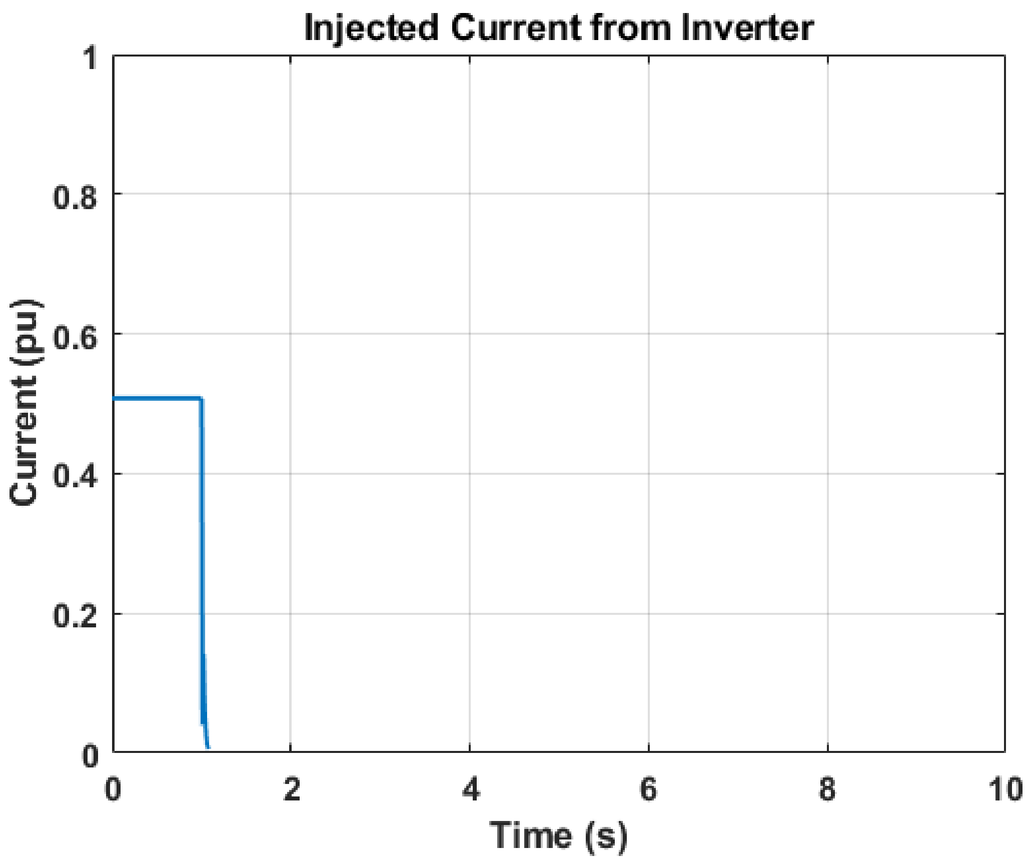

Figure 7.3: Injected current from a typical inverter at 100% solar PV penetration.

enhance fault current levels, making them sufficient to activate overcurrent relays and ensuring reliable operation.

To address the reduction in fault current caused by RES integration, this study uses instantaneous overcurrent relays (IOC). These relays are designed to detect faults efficiently when the fault current exceeds a defined threshold. The time inverse overcurrent relay model (TIOCR1) in PSSE was adjusted to function as an IOC for this analysis.

The TIOCR1 settings were modified to ensure accurate fault detection. The pickup current threshold was set 10% above the nominal load current to prevent unnecessary tripping under normal conditions. The tripping time was set to 0.04 seconds to guarantee rapid fault isolation.

To evaluate the incremental contributions of SynCons, three case studies were conducted as follows:

- Case A: Increases the SCR by 1.
- Case B: Increases the SCR by 2.
- Case C: Increases the SCR by 3.

7.5 Results and Discussion

The simulation results provide valuable insights into how the system behaves as the SCR is incrementally increased through the three case studies. Each case indicates the impact of different levels of SCR on fault current.

- **Case A: Increment in SCR by 1**
  This increment resulted in a fault current of approximately 2 PU, as illustrated in **Figure 7.4**. Although this improvement enhances the fault current, the overall level remains significantly lower compared to that of a conventional SG.

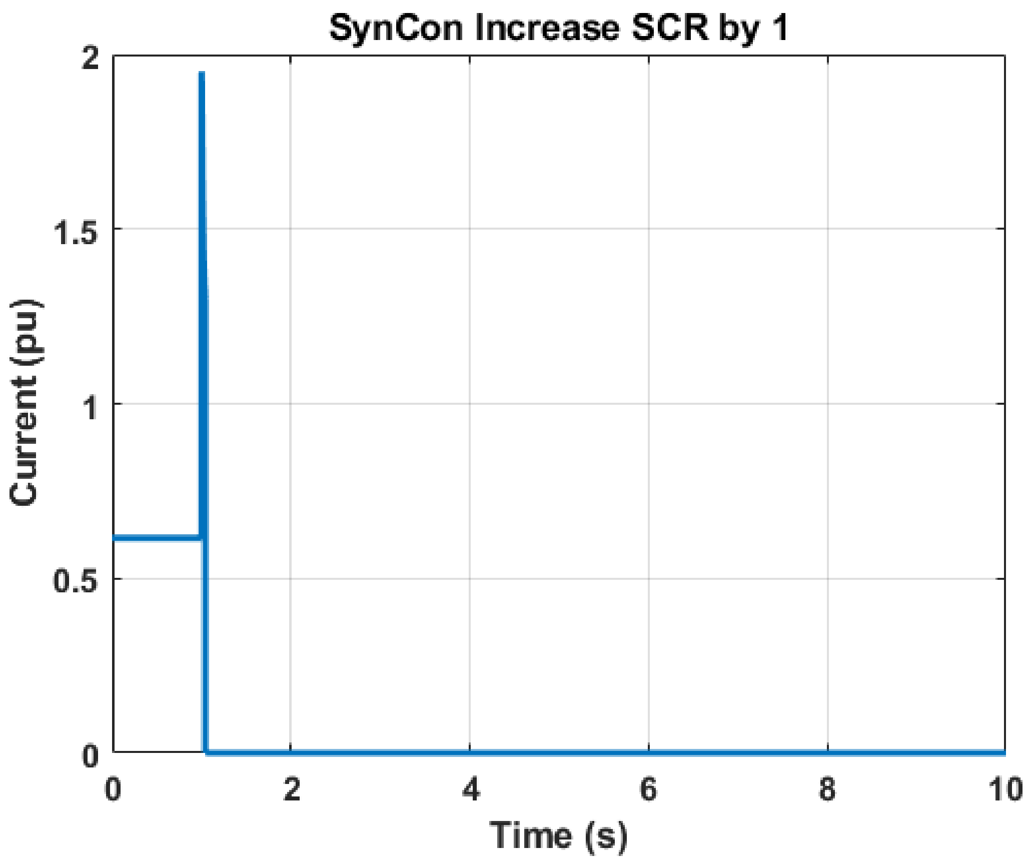

Figure 7.4: Fault current when SynCon increase SCR by 1

- **Case B: Increment in SCR by 2**

  Increasing the SCR by 2 resulted in a fault current of approximately 3.8 PU, as depicted in **Figure 7.5**. This represents a significant improvement over Case A. Nevertheless, the fault current still falls short of the levels typically observed in conventional SG systems.

- **Case C: Increment in SCR by 3**

  Increasing the SCR by 3 resulted in a fault current of approximately 5.75 PU, as depicted in **Figure 7.6**. This value slightly exceeds the fault current typically delivered by an SG operating in a conventional generation system, as previously shown in **Figure 7.1**. These results indicate that an SCR increase of 3 significantly enhances fault current availability, reaching levels comparable to traditional systems. Furthermore, **Figure 7.7** highlights the relay's tripping time, which occurred within 0.04 seconds, indicating fast and reliable fault detection.

While increasing fault current using SynCons has shown clear benefits, several important factors must be considered for developing an effective protection strategy. The primary goal of this study was to determine the minimum SCR necessary to restore fault current to levels sufficient for traditional overcurrent relays to function reliably in fully decarbonized grids. The findings suggest that an SCR increase of 3 provides fault current levels comparable to those in conventional systems, enabling the continued use of traditional protection schemes.

It is crucial to recognize that the effectiveness of any protection strategy depends not only on fault current levels but also on the choice of protection schemes. Overcurrent protection, differential, and distance protection each have different sensitivities and requirements for reliable operation. Moreover, proper coordination between protective devices is essential to ensure selective tripping and avoid unnecessary disruptions. Primary protection devices should operate first, with backup devices prepared to operate if necessary.

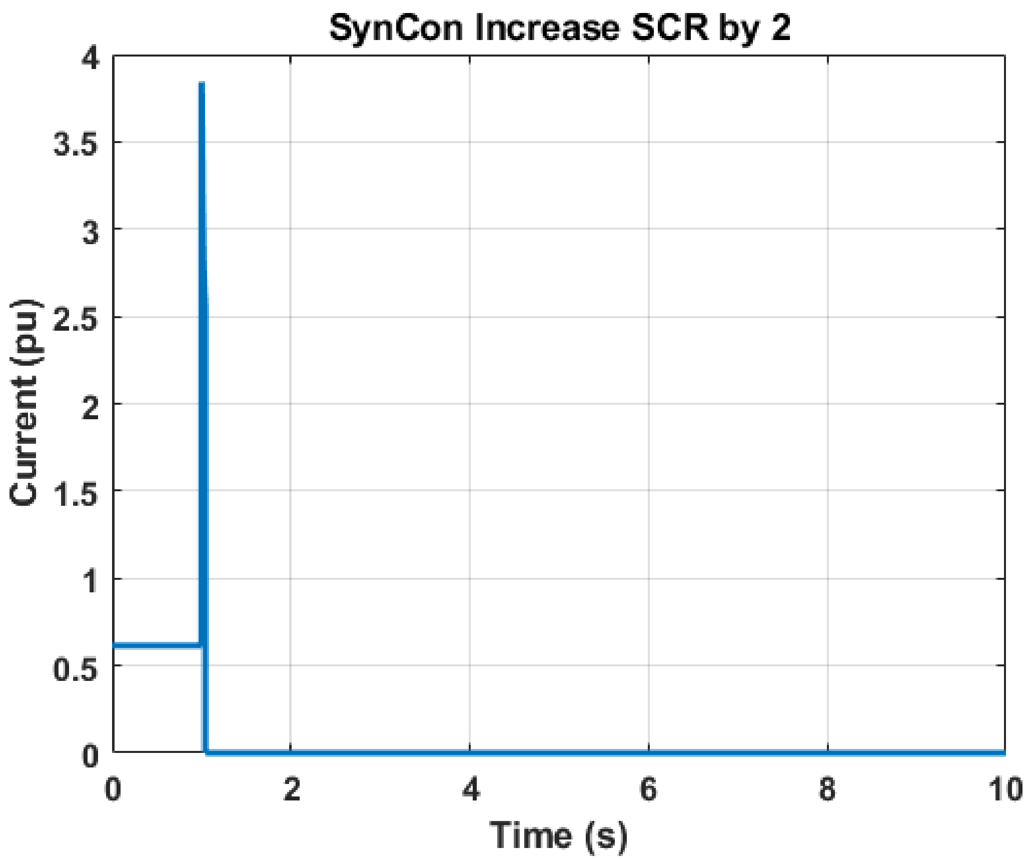

Figure 7.5: Fault current when SynCon increase SCR by 2

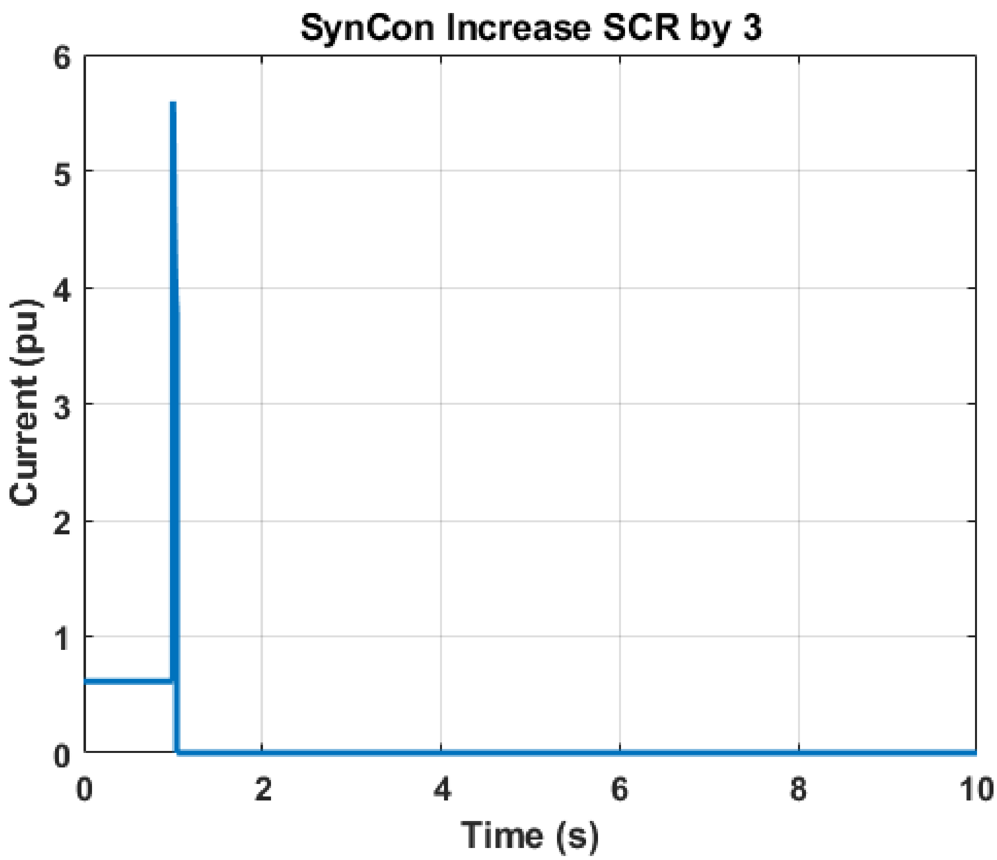

Figure 7.6: Fault current when SynCon increases SCR by 3.

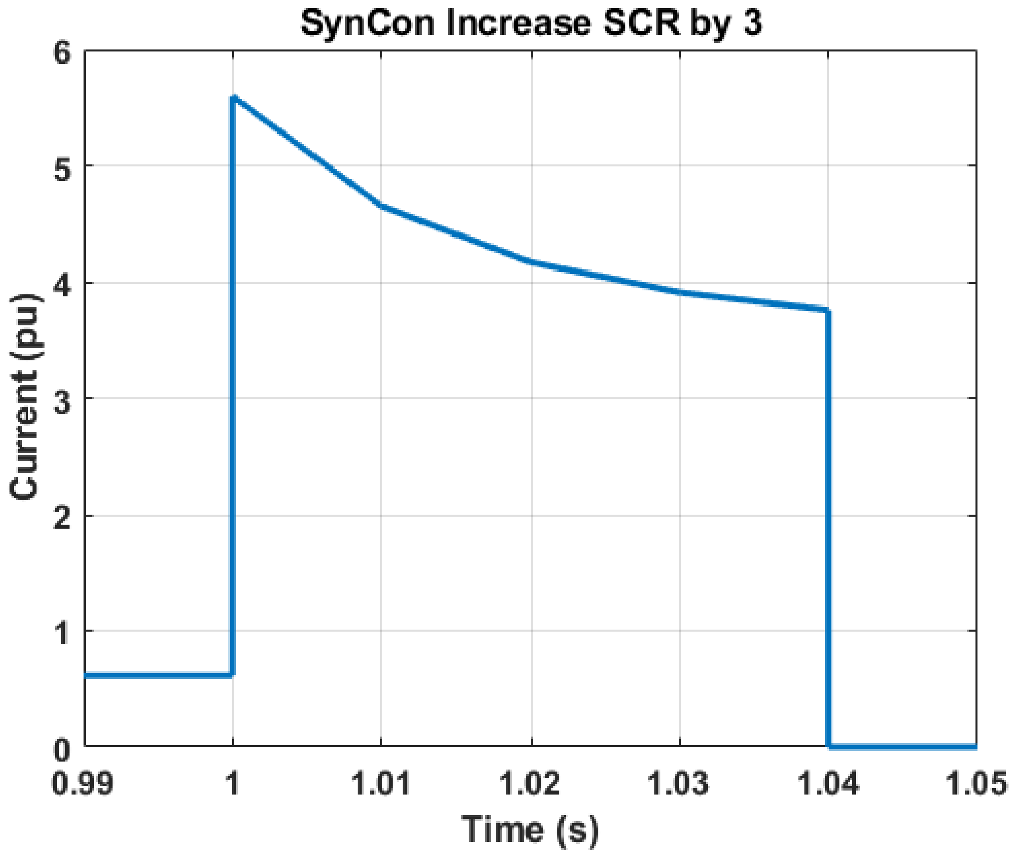

Figure 7.7: Fault current interruption time by over-current relay with SynCon increasing SCR by 3.

Additionally, any modifications to fault current levels and SCR must comply with industry standards and regulatory guidelines, such as those provided by IEEE, IEC, and local grid codes. These standards ensure that improvements to protection schemes align with established best practices and safety requirements.

In conclusion, the integration of SynCons to increase SCR and fault current levels is an effective solution for improving the reliability of overcurrent protection schemes in grids with high solar PV penetration. By restoring fault current to sufficient levels, traditional protection systems remain valid and functional, allowing for the continued use of established protection strategies in fully decarbonized grids. However, further research and a comprehensive approach that accounts for protection scheme selection, device coordination, and compliance to regulatory standards are necessary for a robust and reliable protection strategy.

Chapter 8

Conclusion & Future Work

The primary aim of this dissertation is to enhance the strength and inertia of the Saudi power grid following its full integration with solar PV systems.

The conclusions and summary of this dissertation include the following:

- **Analyzing the impact of solar PV penetration:**

  As solar PV replaces SGs, the SCMVA of the system gradually declines, leading to insufficient levels that negatively affect the overall performance and stability of the Saudi electric grid. Voltage stability is also impacted as the reduction in SCMVA decreases reactive power compensation, raising the risk of voltage instability. Additionally, frequency stability is affected since solar PV lacks the physical inertia that SGs provide, making the system more prone to frequency fluctuations. Hosting capacity depends on the desired SCR that operators aim to maintain, along with the capacity of IBRs at the POI. As the rated active power of inverters increases, system strength decreases further. Indicators such as SCR and WSCR showed significant declines as SGs were retired, emphasizing the urgent need for solutions to maintain grid stability.

- **The role of SynCons in enhancing power system strength under fully solar PV penetration:**

  SynCons significantly enhanced SCMVA by increasing fault current levels, thereby strengthening the grid. System strength indicators, such as SCR and WSCR, reached optimal levels, meeting NERC and EROCT recommendations. SynCons were implemented in three cases, with each case increasing SCR by a specific value. Case C, which raised SCR by 3 and had the largest SynCon capacity, resulted in the highest SCMVA improvements for the Saudi model.

- **Identify weak locations:**
  The analysis showed that the southern and northern regions of the Saudi grid experienced more significant weaknesses compared to other operating regions. Newton-Raphson power flow analysis identified buses in these areas with substantial voltage drops. Further, the PV curve indicated that these regions had more weak and mid-strength buses, showing a greater sensitivity to active power increases. The QV curve highlighted a higher demand for reactive power in these areas to maintain voltage stability, confirming their risk.

- **Voltage stability mitigation:**
  The highest level of solar PV penetration the Saudi grid could handle before voltage stability became insufficient was 60%. SynCons needed to raise SCR by 3 to achieve stable voltage response in a fully solar PV grid. Both static and dynamic loads were used to test voltage stability under various loading scenarios, proving that the case with an SCR increase of 3 maintained excellent voltage response.

- **Comparison between SynCons vs. STATCOM in mitigating FIDVR:**
  The analysis shows that SynCons effectively reduce voltage dips, while STATCOM enables a faster recovery of voltage levels to the safe range, highlighting its quick response capabilities in maintaining grid stability. However, when faults occur close to the compensation devices, SynCons inject a higher fault current, whereas STATCOM may become blocked under low voltage conditions. As the electrical distance from the fault increases, the fault current contribution from SynCons decreases more rapidly than that of STATCOM. This indicates the

importance of electrical distance in assessing the effectiveness of these devices in enhancing grid stability and mitigating FIDVR event.

- **Frequency stability enhancement:**
  The highest level of solar PV penetration before the system struggled to return frequency to a steady-state condition was 60%. The best performance was observed in the scenario where SynCons increased SCR by 3, showing highly satisfactory frequency response. Additionally, the integration of battery storage, which supplies energy during night-time, further supported SynCons in mitigating rapid frequency fluctuations, yielding more better results.

- **Adding transmission lines:**
  Adding new lines increases the overall transmission capacity, allowing for higher maximum power transfer during contingencies. This helps reduce congestion in overloaded areas, enabling more efficient distribution of power across the grid. Additionally, the new lines provide multiple pathways for power flow, improving the ability to manage reactive power, which increase the power system strength. Lastly, this approach decreases transmission losses by shortening the distance electricity must travel and redistributing power flow, ultimately enhancing grid efficiency.

- **Relocate solar PV near center loads:**
  Placing solar PV closer to demand centers reduces the distance that electricity needs to travel, thereby minimizing transmission losses. Shorter transmission distances lead to greater efficiency in energy delivery, enhancing overall grid performance. Additionally, centralizing solar PV near load centers improves voltage stability by providing power directly where it is most needed. This reduces the strain on long-distance transmission lines and helps maintain more stable voltage profiles, especially in regions prone to voltage drops.

- **Improve the protection system:**

  SynCons were found to inject significant fault current during short-circuit conditions, allowing protection devices to operate more effectively and ensuring reliable fault detection and clearance. The case that increased SCR by 3 showed a sufficient increase in fault current, providing protection engineers with more flexibility when designing protection schemes. Additionally, SynCons assisted typical inverters that lack fault ride-through capability by injecting enough fault current for detection by protection relays, ensuring grid reliability in scenarios where solar PV inverters alone may not be sufficient.

Future Work

- Extending the analysis to include additional renewable sources, such as wind energy, would provide a more comprehensive understanding of the challenges facing the Saudi grid.

- A detailed methodology for calculating the inertia of the system will be developed.

- Further studies should propose advanced protection schemes specifically designed for grids with high levels of renewable energy integration.

- Exploring the economic implications of large-scale solar PV and energy storage integration will be valuable for system planners.

- Investigating the impact of solar PV integration on the interconnected grid between Saudi Arabia and neighboring countries could provide valuable insights into cross-border power flows, grid stability, and potential economic benefits from regional power trading.

Bibliography

[1] International Energy Agency (IEA). World energy outlook 2022. `www.iea.org/reports`, 2022. [Online; accessed 20-December-2023]. 1

[2] International Renewable Energy Agency (IRENA). World energy transitions outlook 2022, 2022. 1

[3] IRENA. Middle east renewable energy statistics, 2021. 1

[4] U.S. Department of Commerce. Saudi arabia renewable energy - market intelligence. `https://www.trade.gov/market-intelligence/saudi-arabia-renewable-energy`. [Online; accessed 28-December-2023]. 1

[5] Amjad Ali. Transforming saudi arabia's energy landscape towards a sustainable future: Progress of solar photovoltaic energy deployment. *Sustainability*, 15(10):8420, 2023. 1

[6] L. Yu, H. Sun, S. Xu, B. Zhao, and J. Zhang. A critical system strength evaluation of a power system with high penetration of renewable energy generations. *CSEE Journal of Power and Energy Systems*, 8(3):710–720, 2022. 1

[7] Government of Saudi Arabia. Saudi arabia vision 2030 news. `http://vision2030.gov.sa/en`. Accessed: 2023. 1

[8] Y. H. A. Amran, Y. H. M. Amran, R. Alyousef, and H. Alabduljabbar. Renewable and sustainable energy production in saudi arabia according to saudi

vision 2030; current status and future prospects. *Journal of Cleaner Production*, 247:119602, 2020. 1

[9] K. Jha and A. G. Shaik. A comprehensive review of power quality mitigation in the scenario of solar pv integration into utility grid. *e-Prime - Advances in Electrical Engineering, Electronics and Energy*, 3:Art. no. 100103, 2023. 2, 54

[10] P. Denholm, T. Mai, R. W. Kenyon, B. Kroposki, and M. O'Malley. Inertia and the power grid: A guide without the spin. Technical Report NREL/TP-6A20-73856, National Renewable Energy Laboratory, University of Colorado Boulder, 2020. 2, 19, 20, 54, 109, 112

[11] B. Badrzadeh, Z. Emin, S. Goyal, et al. Towards system strength. *CIGRE Science and Engineering*, 20, Feb 2021. 2, 13, 19, 20, 21, 54, 109

[12] P. Denholm, D. J. Arent, S. F. Baldwin, et al. The challenges of achieving a 100% renewable electricity system in the united states. *Joule*, 5(6):1331–1352, 2021. 2, 54, 109

[13] M. Shafiullah, S. D. Ahmed, and F. A. Al-Sulaiman. Grid integration challenges and solution strategies for solar pv systems: A review. *IEEE Access*, 10:52233–52257, 2022. 2, 3, 13, 20

[14] H. A. Alkhazim, S. I. Bajunaid, W. A. Alsulami, and M. S. Alghamdi. Impact of inverter based resources on power system protective relaying, fault calculation and protection setting: A systematic literature review. In *2022 Saudi Arabia Smart Grid (SASG)*, pages 1–11, Riyadh, Saudi Arabia, 2022. 2, 3, 13, 21

[15] M. I. Saleem, S. Saha, U. Izhar, and L. m. Ang. Integration challenges of inverter based renewable energy sources in weak grids. In *2022 IEEE Industry Applications Society Annual Meeting (IAS)*, pages 1–18, Detroit, MI, USA, 2022. 2, 3

[16] H. Gu, R. Yan, and T. Saha. Review of system strength and inertia requirements for the national electricity market of australia. *CSEE Journal of Power and Energy Systems*, 5(3):295–305, Sept 2019. 2, 13, 19, 109

[17] J. Till, S. You, Y. Liu, and P. Du. Impact of high pv penetration on voltage stability. In *2020 IEEE/PES Transmission and Distribution Conference and Exposition*, pages 1–5, Chicago, IL, USA, 2020. 2

[18] D. Wu, G. Li, M. Javadi, A. M. Malyscheff, M. Hong, and J. N. Jiang. Assessing impact of renewable energy integration on system strength using site-dependent short circuit ratio. *IEEE Transactions on Sustainable Energy*, 9(3):1072–1080, July 2018. 2, 54

[19] Nahid-Al-Masood, R. Yan, T. K. Saha, and N. Modi. Frequency response and its enhancement using synchronous condensers in presence of high wind penetration. In *2015 IEEE Power and Energy Society General Meeting*, pages 1–5, Denver, CO, USA, 2015. 2, 3

[20] M. O. Qays, I. Ahmad, D. Habibi, A. Aziz, and T. Mahmoud. System strength shortfall challenges for renewable energy-based power systems: A review. *Renewable and Sustainable Energy Reviews*, 183:113447, 2023. 2, 3, 54

[21] M. Maharjan, A. Ekic, M. Beedle, J. Tan, and D. Wu. Evaluating grid strength under uncertain renewable generation. *International Journal of Electrical Power and Energy Systems*, 146:108737, 2023. 2

[22] M. G. Dozein, P. Mancarella, T. K. Saha, and R. Yan. System strength and weak grids: Fundamentals, challenges, and mitigation strategies. In *2018 Australasian Universities Power Engineering Conference (AUPEC)*, pages 1–7, Auckland, New Zealand, 2018. 2

[23] NERC. Short-circuit modeling and system strength. White paper, North American Electric Reliability Corporation, Feb 2018. 3, 92

[24] NERC. Integrating inverter-based resources into low short circuit strength systems. Reliability guideline, North American Electric Reliability Corporation, Dec 2017. 3

[25] L. Yu, H. Sun, S. Xu, B. Zhao, and J. Zhang. A critical system strength evaluation of a power system with high penetration of renewable energy generations. *CSEE Journal of Power and Energy Systems*, 8(3):710–720, May 2022. 3, 14

[26] Y. Zhang, S. H. F. Huang, J. Schmall, J. Conto, J. Billo, and E. Rehman. Evaluating system strength for large-scale wind plant integration. In *2014 IEEE PES General Meeting — Conference and Exposition*, pages 1–5, National Harbor, MD, USA, 2014. 3

[27] M. N. H. Shazon, Nahid-Al-Masood, H. M. Ahmed, S. R. Deeba, and E. Hossain. Exploring the utilization of energy storage systems for frequency response adequacy of a low inertia power grid. *IEEE Access*, 9:129933–129950, 2021. 3

[28] M.R. Amin, M. Negnevitsky, E. Franklin, K.S. Alam, and S.B. Naderi. Application of battery energy storage systems for primary frequency control in power systems with high renewable energy penetration. *Energies*, 14:1379, 2021. 3

[29] O. B. Adewuyi, R. Shigenobu, K. Ooya, T. Senjyu, and A. M. Howlader. Static voltage stability improvement with battery energy storage considering optimal control of active and reactive power injection. *Electric Power Systems Research*, 172:303–312, 2019. 3

[30] M. R. Jannesar, S. Sadr, and M. Savaghebi. Dynamic stability enhancement in low-inertia power systems using battery energy storage. In *2022 12th Smart Grid Conference (SGC)*, pages 1–5, Kerman, Iran, Islamic Republic of, 2022. 3

[31] P. M. Chavan and G. R. Walke. Using statcom interfacing of renewable energy source to grid and power quality improvement. In *2015 International Conference on Energy Systems and Applications*, pages 329–332, Pune, India, 2015. 3

[32] Abdelaziz Salah Saidi. Impact of grid-tied photovoltaic systems on voltage stability of tunisian distribution networks using dynamic reactive power control. *Ain Shams Engineering Journal*, 13:101537, 2022. 3

[33] R. Sadiq, Z. Wang, C. Y. Chung, C. Zhou, and C. Wang. A review of statcom control for stability enhancement of power systems with wind/pv penetration. `https://doi.org/10.1002/2050-7038.13079`, 2021. First published 28 August 2021. 3

[34] U. Princy, S. Jaseena, S. Sreedharan, and S. Sreejith. Voltage stability analysis of power system network integrated with renewable source and svc. In *2017 Innovations in Power and Advanced Computing Technologies (i-PACT)*, pages 1–6, Vellore, India, 2017. 3

[35] Ha Thi Nguyen, Guangya Yang, A. H. Nielsen, and P. H. Jensen. Frequency stability improvement of low inertia systems using synchronous condensers. In *2016 IEEE International Conference on Smart Grid Communications (SmartGridComm)*, pages 650–655, Sydney, NSW, Australia, 2016. 3

[36] H. T. Nguyen, D. V. Pombo, and H. W. Bindner. Frequency stability assessment for the future power system of são vicente island. In *2021 IEEE PES Innovative Smart Grid Technologies Europe (ISGT Europe)*, pages 01–05, Espoo, Finland, 2021. 3

[37] P. T. Manditereza. Rocof enhancement using synchronous condensers in systems integrated with renewable energy sources. In *2020 IEEE PES/IAS PowerAfrica*, pages 1–5, Nairobi, Kenya, 2020. 3

[38] A. S. Surya, M. Partahi Marbun, M. Marwah, K. G. H. Mangunkusumo, B. B. S. D. A. Harsono, and H. Bernando Tambunan. Study of synchronous condenser impact in jawa-madura-bali system to provide ancillary services. In *2020 12th International Conference on Information Technology and Electrical Engineering (ICITEE)*, pages 234–238, Yogyakarta, Indonesia, 2020. 3, 110

[39] N.-A. Masood, S. U. Mahmud, M. N. Ansary, and S. R. Deeba. Improvement of system strength under high wind penetration: A techno-economic assessment using synchronous condenser and svc. *Department of Electrical and Electronic Engineering, Bangladesh University of Engineering and Technology, Dhaka, 1205, Bangladesh, and Apsis Solutions Limited, Dhaka, 1213, Bangladesh, and Department of Electrical and Computer Engineering, North South University, Dhaka, 1229, Bangladesh*, 246(123426), 5 2022. 3

[40] Y. Li, Y. Gu, and T. C. Green. Revisiting grid-forming and grid-following inverters: A duality theory. *IEEE Transactions on Power Systems*, 37(6):4541–4554, Nov 2022. 3

[41] D. B. Rathnayake et al. Grid forming inverter modeling, control, and applications. *IEEE Access*, 9:114781–114807, 2021. 3, 127

[42] D. Elliott. *The Government Takes an Interest in the 1970s*. Energy, Climate and the Environment. Palgrave Macmillan, Cham, 2019. 8

[43] International Renewable Energy Agency. Solar energy. `https://www.irena.org/Energy-Transition/Technology/Solar-energy`. [Online; accessed 28-December-2023]. 8

[44] A. J. Lari, A. Egwebe, F. Touati, A. S. Gonzales, and A. A. Khandakar. Reliable photovoltaics output power prediction in qatar. In *2021 14th International Conference on Developments in eSystems Engineering (DeSE)*, pages 546–551, Sharjah, United Arab Emirates, 2021. 8

[45] Saudi Electricity Company. Saudi electricity company, annual report. Technical report, Saudi Electricity Company, 2022. https://www.se.com.sa/en/Investors/Reports-and-Presentations/Annual-Reports. 9

[46] Water and Electricity Regulatory Authority (WERA). Annual statistic handbook for electricity, fifteenth edition, 2022. https://wera.gov.sa/en/Pages/default.aspx. 9

[47] Ministry of Energy of Saudi Arabia. Power and electricity. https://www.moenergy.gov.sa/, 2022. 9

[48] A. M. Massoud, S. Ahmed, S. J. Finney, and B. W. Williams. Inverter-based versus synchronous-based distributed generation; fault current limitation and protection issues. In *2010 IEEE Energy Conversion Congress and Exposition*, pages 58–63, Atlanta, GA, USA, 2010. 13

[49] North American Electric Reliability Corporation (NERC). Short-circuit modeling and system strength. White paper, North American Electric Reliability Corporation, Feb 2018. 13, 15

[50] K.V. Vidyanandan and Balkrishn Kamath. Grid integration of renewables: challenges and solutions. *Indian Journal of Power and River Valley Development*, 71(5-6):22–30, 2021. 13, 14

[51] D. Kim, H. Cho, B. Park, and B. Lee. Evaluating influence of inverter-based resources on system strength considering inverter interaction level. *Sustainability*, 12(8):Art. no. 3469, 2020. 14

[52] J. Keller and B. Kroposki. Understanding fault characteristics of inverter-based distributed energy resources. Tech. Rep. NREL/TP-550-46698, National Renewable Energy Laboratory (NREL), Jan 2010. 15, 17, 19, 20, 21, 126, 128

[53] P. Kundur. Power system stability and control, 1st edition. *Book published by McGraw-Hill*, 1994. New York. 15, 19, 20, 55, 57, 61, 66, 69, 71, 112, 113

[54] M. Nilsson. Short-circuit analysis of the onsite electric power system at ringhals unit 4. M.sc. thesis, Chalmers Univ. Technol., 2010. Dept. Energy Environ., Div. Electric Power Eng., Gothenburg, Sweden. 16, 17, 18, 21, 126

[55] B. Kroposki et al. Achieving a 100% renewable grid: Operating electric power systems with extremely high levels of variable renewable energy. *IEEE Power and Energy Magazine*, 15(2):61–73, 2017. 17, 20, 21, 51, 109

[56] D. Sweeting. Applying iec 60909, short-circuit current calculations. In *2011 Record of Conference Papers Industry Applications Society 58th Annual IEEE Petroleum and Chemical Industry Conference (PCIC)*, pages 1–6, Toronto, ON, Canada, 2011. 18

[57] Siemens Industry, Inc., Siemens Power Technologies International. *Program Application Guide Volume 1, PSS®E 34.8.1*, Dec 2020. 18

[58] B. de Metz-Noblat, F. Dumas, and C. Poulain. Calculation of short-circuit currents. Cahier Technique 158, Schneider Electric, Sep 2005. 18

[59] Sajjad Uddin Mahmud. Optimal sizing of synchronous condensers to improve system strength under high wind power penetration in a power grid. Master's thesis, Bangladesh University of Engineering and Technology, Dhaka-1000, Bangladesh, 8 2020. 18

[60] S. Alzahrani, R. Shah, and N. Mithulananthan. Examination of effective var with respect to dynamic voltage stability in renewable rich power grids. *IEEE Access*, 9:75494–75508, 2021. 19, 20

[61] P. Kundur et al. Definition and classification of power system stability ieee/cigre joint task force on stability terms and definitions. *IEEE Transactions on Power Systems*, 19(3):1387–1401, Aug 2004. 19, 20, 66, 109

[62] J. Joshi, A. K. Swami, Vibhu Jately, and B. Azzopardi. A comprehensive review of control strategies to overcome challenges during lvrt in pv systems. *IEEE Access*, 2021. 20

[63] North American Electric Reliability Corporation. Reliability guideline: Reactive power planning. `http://www.nerc.com`, Dec 2016. 20

[64] Pieter Tielens and Dirk Van Hertem. The relevance of inertia in power systems. *Renewable and Sustainable Energy Reviews*, 55:999–1009, 2016. 20, 110

[65] J. L. Blackburn and T. J. Domin. Protective relaying: Principles and applications, 4th edition. *Book published by CRC Press*, 2014. Boca Raton, FL. 20

[66] Paul Denholm and Ben Kroposki. Understanding power systems protection in the clean energy future. Technical Report NREL/TP-6A40-82269, National Renewable Energy Laboratory (NREL), May 2022. 20, 21, 110, 126

[67] J. Keller, B. Kroposki, R. Bravo, and S. Robles. Fault current contribution from single-phase pv inverters. In *2011 37th IEEE Photovoltaic Specialists Conference*, pages 001822–001826, 2011. 20

[68] S. Manson and E. McCullough. Practical microgrid protection solutions: Promises and challenges. *IEEE Power and Energy Magazine*, 19(3):58–69, May-Jun 2021. 20

[69] A. Bidram M. J. Reno, S. Brahma and M. E. Ropp. Influence of inverter-based resources on microgrid protection: Part 1: Microgrids in radial distribution systems. *IEEE Power and Energy Magazine*, 19(3):36–46, 2021. 21

[70] Abigail E. Till. *Impact of Renewables on Grid Strength, Transient Stability, and Grid Operation Characterization*. Phd diss., University of Tennessee, 2023. 35

[71] W. M. Albukhari, Y. Liu, A. Till, and K. M. Alshuaibi. Mitigating voltage instability in the saudi grid for a decarbonized, fully solar power system. In *2024 IEEE Power and Energy Society Innovative Smart Grid Technologies Conference (ISGT)*, pages 1–5, Washington, DC, USA, 2024 2024. 48, 81, 87, 118

[72] W. M. Albukhari, Y. Liu, A. Till, and K. M. Alshuaibi. Frequency stability enhancement in a fully solar power grid: A case study on the saudi model. In *2024 IEEE Power and Energy Society Innovative Smart Grid Technologies Conference (ISGT)*, pages 1–5, Washington, DC, USA, 2024 2024. 48, 114, 115, 118

[73] U.S. Energy Information Administration. Annual energy outlook 2022. `https://www.eia.gov/aeo`, 2022. Accessed: [insert date of access here]. 54

[74] J. P. Skliutas, R. D'Aquila, J. M. Fogarty, R. Konopinski, P. Marken, C. Schartner, and G. Zhi. Planning the future grid with synchronous condensers. 2013 Grid of the Future Symposium, US National Committee, `http://www.cigre.org`, 2013. General Electric Company, United States and Canada. 54, 57, 58, 110

[75] Ettore Bompard, Andrea Mazza, and Lucian Toma. *Classical grid control: Frequency and voltage stability*, chapter Classical grid control: Frequency and voltage stability, pages 31–65. Knovel, 2021. 54, 55, 112, 113

[76] KC Agrawal. *Industrial Power Engineering Handbook*. Newnes, Oct 2001. 55, 58

[77] T. K. Nagsarkar and M. S. Sukhija. *Power System Analysis*. Oxford University Press, 2 edition, 2014. 55, 57

[78] Puyu Wang, Qingwen Mou, Xing Liu, Wei Gu, and Xuan Chen. Start-up control of a synchronous condenser integrated hvdc system with power electronics based static frequency converter. *IEEE Access*, 7:146914–146921, 2019. 55, 57

[79] Mulukutla S. Sarma. *Introduction to Electrical Engineering*. Oxford Series in Electrical and Computer Engineering. Oxford University Press, 2001. 55, 57

[80] S. Salivahanan, R. Rengaraj, and G.R. Venkatakrishnan. *Basic Electrical and Instrumentation Engineering*. McGraw Hill Education (India) Private Limited, 2018. 55

[81] Rakosh Das Begamudre. *Extra High Voltage AC Transmission Engineering*. New Age International, 2006. 55

[82] Christian Payerl. Introduction to abb synchronous condenser offering: A solution to improve grid strength. ABB Marketing Material, Access year 2024. Contact: christian.payerl@se.abb.com, Tel.: +46 21 320475, Mob.: +46 70 2601024. 57, 58

[83] Han Shao, Padmanathan Narayanasamy, Kafil M. Razeeb, Robert P. Lynch, and Fernando M. F. Rhen. Electrical Storage. In *Energy Storage Options and Their Environmental Impact*. The Royal Society of Chemistry, 10 2018. 57

[84] Dragan Jovcic. *High Voltage Direct Current Transmission: Converters, Systems and DC Grids*. John Wiley and Sons Ltd, Aug 2019. 57

[85] E. Marrazi, G. Yang, and P. Weinreich-Jensen. Allocation of synchronous condensers for restoration of system short-circuit power. *Journal of Modern Power Systems and Clean Energy*, 6:17–26, 2018. 57

[86] Rick Wallace Kenyon, Anderson Hoke, Jin Tan, Benjamin Kroposki, and Bri-Mathias Hodge. Grid-following inverters and synchronous condensers: A grid-forming pair? In *2020 Clemson University Power Systems Conference*, Clemson, South Carolina, Mar 2020. University of Colorado, Boulder; National Renewable Energy Laboratory. 57

[87] A. Stiger, R.A. Rivas, and M. Halonen. Synchronous condensers contribution to inertia and short circuit current in cooperation with statcom. In *2019 IEEE PES GTD Grand International Conference and Exposition Asia (GTD Asia)*, pages 955–959, 2019. 57, 110, 127

[88] Sarbajit Basu, Vishwajit Roy, and Michael Giesselmann. Application of synchronous condensers for enhanced resilience of a renewable energy dominated electric grid. In *2020 IEEE Global Humanitarian Technology Conference (GHTC)*, pages 1–8, 2020. 58, 110, 127

[89] Ronald C. Matthews, Shamina Hossain-McKenzie, and Matthew J. Reno. Fault current correction strategies for effective fault location in inverter-based systems. In *2019 IEEE 46th Photovoltaic Specialists Conference (PVSC)*, pages 3124–3131, 2019. 58, 127

[90] Jundi Jia, Guangya Yang, Arne Hejde Nielsen, and Vahan Gevorgian. Investigation on the combined effect of vsc-based sources and synchronous condensers under grid unbalanced faults. *IEEE Transactions on Power Delivery*, 34(5):1898–1908, 2019. 58

[91] Siemens Industry, Inc., Siemens Power Technologies International. *Model Library, PSS®E 34.8.1*, Dec 2020. 58, 76, 77, 79, 92

[92] Nasser Hosseinzadeh, Asma Aziz, Apel Mahmud, Ameen Gargoom, and Mahbub Rabbani. Voltage stability of power systems with renewable-energy inverter-based generators: A review. *Electronics*, 10(2):115, 2021. 66

[93] Rabiaa Gadal, Aziz Oukennou, Faissal El Mariami, Abdelziz Belfqih, and Naima Agouzoul. Voltage stability assessment and control using indices and facts: A comparative review. *Journal of Electrical and Computer Engineering*, pages 1–18, 2023. 66

[94] Guorui Zhang. Epri power systems dynamics tutorial. Technical Report 1016042, Electric Power Research Institute (EPRI), Palo Alto, CA, July 2009. Final Report. 66, 110

[95] Thierry Van Cutsem and Costas Vournas. *Voltage Stability of Electric Power Systems*. Springer Science+Business Media Dordrecht, Dordrecht, 1998. 69, 71

[96] J. Duncan Glover, Mulukutla S. Sarma, and Thomas J. Overbye. *Power System Analysis and Design*. Cengage Learning, Stamford, CT, USA, 5th, si edition edition, 2011. 69

[97] Zetty Adibah Kamaruzzaman and Azah Mohamed. Impact of grid-connected photovoltaic generator using p-v curve and improved voltage stability index. In *2014 IEEE International Conference on Power and Energy (PECon)*, pages 196–200, 2014. 71

[98] B.H. Chowdhury and C.W. Taylor. Voltage stability analysis: V-q power flow simulation versus dynamic simulation. *IEEE Transactions on Power Systems*, 15(4):1354–1359, 2000. 71, 74

[99] Hsiao-Dong Chiang, Ian Dobson, Robert J. Thomas, James S. Thorp, and Lazhar Fekih-Ahmed. On voltage collapse in electric power systems. *IEEE Transactions on Power Systems*, 5(2):601–611, May 1990. 74

[100] Y. Song, D. J. Hill, and T. Liu. Static voltage stability analysis of distribution systems based on network-load admittance ratio. *IEEE Transactions on Power Systems*, 34(3):2243–2253, 2019. 74

[101] Yun-Hwan Lee, Bo-Hyun Park, Seung-Chan Oh, Byong-Jun Lee, Jeong-Hoon Shin, and Tae-Kyun Kim. Implementation of under voltage load shedding for fault induced delayed voltage recovery phenomenon alleviation. *Journal of Electrical Engineering and Technology*, 9(2):406–414, 2014. 74, 76, 78

[102] Sarma (NDR) Nuthalapati, editor. *Use of Voltage Stability Assessment and Transient Stability Assessment Tools in Grid Operations*. Power Electronics and Power Systems. Springer, Cham, Switzerland, 2021. 74, 76

[103] A. Borghetti, R. Caldon, A. Mari, and C. A. Nucci. On dynamic load models for voltage stability studies. *IEEE Transactions on Power Systems*, 12(1):293–303, February 1997. Istituto di Elettrotecnica Industriale, University of Bologna, Italy; Dipartimento di Ingegneria Elettrica, University of Padova, Italy. 76

[104] Anmar Arif, Zhaoyu Wang, Jianhui Wang, Barry Mather, Hugo Bashualdo, and Dongbo Zhao. Load modeling—a review. *IEEE Transactions on Smart Grid*, 9(6):5986–5999, 2018. 76

[105] NERC. Dynamic load modeling technical reference document. Technical report, North American Electric Reliability Corporation (NERC), December 2016. NERC — Dynamic Load Modeling Technical Reference Document — September 2016. 87

[106] Richard J. Bravo. Distribution fidvr events analysis. In *2015 Seventh Annual IEEE Green Technologies Conference*, pages 1–8, 2015. 92

[107] Sandeep Sharma, Saket Gupta, Mohd Zuhaib, Vijay Bhuria, Hasmat Malik, Abdulaziz Almutairi, Asyraf Afthanorhan, and Mohammad Asef Hossaini. A comprehensive review on statcom: Paradigm of modeling, control, stability, optimal location, integration, application, and installation. *IEEE Access*, 12:2701–2729, 2024. 92

[108] Ieee guide for specification of transmission static synchronous compensator (statcom) systems. *IEEE Std 1052-2018*, pages 1–115, 2019. 92

[109] Zhihao Jiang. *Impacts of High Renewable Power Grids on System Planning and Monitoring*. PhD thesis, University of Tennessee, 2023. 92

[110] Siemens Industry, Inc., Siemens Power Technologies International. *Program Application Guide Volume 2, PSS®E 34.8.1*, Dec 2020. 96

[111] Muhammad Nauman Rafiq, Dhruv Sharma, Di Wu, John N. Jiang, and Chongqing Kang. Average electrical distance-based bus clustering method for network equivalence. In *2017 19th International Conference on Intelligent System Application to Power Systems (ISAP)*, pages 1–6, 2017. 100

[112] E. Bernabeu, Y. Chen, and J. Baranowski. Pjm's pseudo-tie screening criteria based on electrical distance. In *2019 IEEE Power and Energy Society General Meeting (PESGM)*, pages 1–4, 2019. 100

[113] PJM Interconnection. Dynamic transfers: Electrical distance test. Applied Innovation, Available: `www.pjm.com`, 2019. Last updated January 2, 2019. 100, 103

[114] Weichao Li and Shouyuan Wu. Analysis of synchronous generator inertia response and primary frequency regulation. In *2021 8th International Forum on Electrical Engineering and Automation (IFEEA)*, pages 107–110, 2021. 109

[115] M. Reza. *Stability Analysis of Transmission Systems with High Penetration of Distributed Generation*. PhD thesis, Delft University of Technology, 2006. 110

[116] Neil McIlwaine, Aoife M. Foley, Dlzar Al Kez, Robert Best, Xi Lu, and Chongyu Zhang. A market assessment of distributed battery energy storage to facilitate higher renewable penetration in an isolated power system. *IEEE Access*, 10:2382–2398, 2022. 110

[117] Tianqiao Zhao, Alessandra Parisio, and Jovica V. Milanović. Distributed control of battery energy storage systems for improved frequency regulation. *IEEE Transactions on Power Systems*, 35(5):3729–3738, 2020. 110

[118] AKM Kamrul Hasan, Mohammed H. Haque, and Syed Mahfuzul Aziz. Enhancing frequency response characteristics of low inertia power systems using battery energy storage. *IEEE Access*, 12:116861–116874, 2024. 110

[119] Mahdi Rouholamini, Caisheng Wang, Hashem Nehrir, Xiaosong Hu, Zechun Hu, Hirohisa Aki, Bo Zhao, Zhixin Miao, and Kai Strunz. A review of modeling, management, and applications of grid-connected li-ion battery storage systems. *IEEE Transactions on Smart Grid*, 13(6):4505–4524, 2022. 110

[120] Xuan Wu, Jenny Zhao, and Antonio J. Conejo. Optimal battery sizing for frequency regulation and energy arbitrage. *IEEE Transactions on Power Delivery*, 37(3):2016–2023, 2022. 110

[121] ENTSO-E. Inertia and rate of change of frequency (rocof). Technical report, ENTSO-E, Rue de Spa 8, 1000 Brussels, Belgium, Dec 2020. 112, 113

[122] J. Lewis Blackburn and Thomas J. Domin. *Protective Relaying: Principles and Applications*. Taylor and Francis Group, LLC, third edition, 2006. 126, 127

[123] Aboutaleb Haddadi, Evangelos Farantatos, Ilhan Kocar, and Ulas Karaagac. Impact of inverter based resources on system protection. *Energies*, 14(4), 2021. 126, 127

[124] J.C. Quispe and E. Orduña. Transmission line protection challenges influenced by inverter-based resources: a review. *Protection and Control of Modern Power Systems*, 7:28, 2022. Received 10 February 2022, Accepted 01 July 2022, Published 18 July 2022. 126

[125] Maximiliano Ferrari, Leon M. Tolbert, and Emilio C. Piesciorovsky. Grid forming inverter with increased short-circuit contribution to address inverter-based microgrid protection challenges. *IEEE Open Journal of the Industrial Electronics Society*, 5:481–500, 2024. 127

[126] Xiang Zhao, Zhenxing Wang, Chuangxin Luo, Rui Xiong, Quanyuan Jiang, Qi Zhu, and Ruihua Zou. Adaptive overcurrent protection scheme coordination in presence of distributed generation using radial basis neural network. *Protection and Control of Modern Power Systems*, 8:1–11, 2023. 127

Appendix

Appendix A

Short Circuit MVA Analysis with Different Solar PV Penetration

A.1 Short Circuit MVA Reduction Across Buses

Table A.1: SCMVA reduction across buses (Part 1)

Bus	20% PV ΔSCMVA (MVA)	40% PV ΔSCMVA (MVA)	60% PV ΔSCMVA (MVA)	80% PV ΔSCMVA (MVA)	100% PV ΔSCMVA (MVA)
11000	-0.51	-584.88	-586.02	-590.23	-711.46
11001	-0.51	-17.03	-18.41	-23.54	-711.46
11002	-0.51	-17.03	-18.41	-23.54	-711.46
11004	-0.51	-584.88	-586.02	-590.23	-711.46
11005	-0.83	-583.71	-585.50	-593.36	-703.02
11007	-0.68	-3.16	-4.73	-591.22	-682.26
11008	-0.83	-2.28	-4.11	-593.36	-703.02
11010	-0.68	-1.84	-3.33	-591.22	-682.26
11301	-2.96	-8.05	-14.51	-537.59	-1340.60
11302	-2.96	-8.05	-14.51	-537.59	-1340.60

Continued on next page

Table A.2: SCMVA reduction across buses (Part 2)

Bus	20% PV ΔSCMVA (MVA)	40% PV ΔSCMVA (MVA)	60% PV ΔSCMVA (MVA)	80% PV ΔSCMVA (MVA)	100% PV ΔSCMVA (MVA)
11303	-2.96	-8.05	-14.51	-36.02	-1340.60
11304	-2.96	-510.18	-516.54	-537.59	-1340.60
11305	-1007.05	-1011.92	-1018.07	-1038.28	-1340.60
11306	-2.96	-8.05	-516.54	-537.59	-1340.60
11307	-3.15	-1012.16	-1018.70	-1040.18	-1358.26
11308	-2.96	-8.05	-516.54	-1038.28	-1340.60
11309	-2.96	-510.18	-516.54	-1038.28	-1340.60
11324	-3.15	-8.57	-1018.70	-1040.18	-1358.26
11325	-3.15	-8.57	-1018.70	-1040.18	-1358.26
11326	-1006.97	-1012.16	-1018.70	-1040.18	-1358.26
11330	-520.10	-1042.83	-1048.35	-1085.39	-1388.78
11331	-518.06	-545.52	-550.72	-1073.96	-1335.89
11332	-518.06	-1038.32	-1042.93	-1073.96	-1335.89
11333	-413.91	-417.88	-828.12	-858.98	-1130.20
11334	-413.91	-417.88	-434.85	-858.98	-1130.20
11336	-421.44	-444.16	-462.93	-913.23	-1158.31
11337	-22.60	-836.81	-853.59	-913.23	-1158.31
11338	-21.34	-44.07	-453.49	-513.13	-758.20
11341	-9.14	-1034.20	-1044.51	-1102.37	-1735.31
11342	-9.14	-531.45	-542.18	-602.98	-1735.31
11343	-513.35	-1034.20	-1044.51	-1102.37	-1735.31
11344	-9.14	-531.45	-542.18	-1102.37	-1735.31
11345	-513.35	-531.45	-542.18	-1102.37	-1735.31
11346	-1.82	-20.20	-41.05	-685.90	-1586.93
11348	-1.82	-615.33	-1221.82	-1266.25	-1586.93
11349	-1.82	-615.33	-634.87	-1266.25	-1586.93
11354	-616.66	-622.04	-625.25	-1274.07	-1544.32
11355	-616.66	-622.04	-625.25	-1274.07	-1544.32

Continued on next page

Table A.3: SCMVA reduction across buses (Part 3)

Bus	20% PV ΔSCMVA (MVA)	40% PV ΔSCMVA (MVA)	60% PV ΔSCMVA (MVA)	80% PV ΔSCMVA (MVA)	100% PV ΔSCMVA (MVA)
11362	-11.23	-19.72	-1036.17	-1053.70	-1426.26
11363	-10.17	-76.65	-94.89	-616.42	-1543.35
11364	-10.17	-1019.65	-1034.11	-1074.17	-1543.35
11374	-638.71	-639.77	-640.77	-650.51	-767.11
11375	-8.61	-9.80	-10.92	-21.99	-767.11
11376	-8.61	-9.80	-10.92	-650.51	-767.11
11377	-638.71	-639.77	-640.77	-650.51	-767.11
11387	-10.78	-13.13	-14.49	-922.95	-1070.87
11389	-22.89	-27.86	-30.72	-63.58	-1209.59
11390	-0.02	-263.94	-285.62	-318.62	-326.64
11391	-0.02	-21.68	-285.62	-318.62	-326.64
11392	-0.02	-21.68	-54.35	-318.62	-326.64
11401	-34.39	-50.79	-64.52	-1044.88	-1224.60
11402	-960.10	-973.16	-983.95	-1045.99	-1227.74
11403	-995.13	-999.31	-1001.70	-1028.77	-1296.01
13100	-21.70	-616.53	-630.76	-654.81	-785.63
13101	-9.15	-9.96	-616.45	-635.60	-800.59
13102	-9.15	-9.96	-51.64	-75.99	-800.59
13103	-24.44	-25.31	-631.45	-651.61	-800.59
13104	-594.61	-595.31	-631.45	-651.61	-800.59
13105	-9.81	-10.68	-36.98	-636.72	-785.63
13106	-618.53	-631.40	-645.64	-669.71	-800.59
13107	-618.53	-631.40	-645.64	-669.71	-800.59
13108	-20.24	-34.47	-629.92	-669.71	-800.59
13109	-20.24	-34.47	-68.72	-669.71	-800.59
13110	-0.52	-595.13	-605.62	-654.81	-785.63
13111	-0.49	-10.93	-606.07	-669.71	-800.59
13112	-0.49	-10.93	-38.64	-669.71	-800.59

Continued on next page

Table A.4: SCMVA reduction across buses (Part 4)

Bus	20% PV ΔSCMVA (MVA)	40% PV ΔSCMVA (MVA)	60% PV ΔSCMVA (MVA)	80% PV ΔSCMVA (MVA)	100% PV ΔSCMVA (MVA)
13113	-0.49	-9.96	-10.99	-57.76	-800.59
13114	-0.49	-9.96	-10.99	-621.29	-800.59
13115	-0.52	-10.68	-11.79	-621.68	-785.63
13116	-0.49	-10.93	-22.38	-669.71	-800.59
13117	-0.49	-10.93	-22.38	-669.71	-800.59
13118	-0.49	-595.31	-596.21	-621.29	-800.59
13119	-0.49	-25.31	-26.42	-57.76	-800.59
13120	-0.46	-1.12	-596.07	-599.50	-688.17
13121	-0.46	-1.12	-10.81	-14.95	-688.17
13122	-0.46	-1.12	-1.98	-608.90	-688.17
13123	-0.46	-1.12	-1.98	-608.90	-688.17
13124	-0.46	-9.80	-10.81	-14.95	-688.17
13125	-0.46	-595.23	-596.07	-599.50	-688.17
13126	-0.46	-1.12	-1.98	-5.49	-688.17
13127	-0.46	-1.12	-1.98	-5.49	-688.17
13128	-594.57	-603.88	-604.87	-608.90	-688.17
13129	-9.02	-603.88	-604.87	-608.90	-688.17
13130	-603.11	-603.88	-604.87	-608.90	-688.17
13131	-603.11	-603.88	-604.87	-608.90	-688.17
13191	-10.27	-20.94	-27.50	-1128.79	-1537.85
13192	-10.27	-1092.05	-1098.07	-1128.79	-1537.85
13193	-1082.18	-1092.05	-1098.07	-1128.79	-1537.85
13194	-1082.18	-1092.05	-1098.07	-1128.79	-1537.85
13195	-9.70	-607.82	-613.04	-630.87	-880.28
13196	-595.92	-607.60	-612.73	-630.23	-875.80
13197	-9.70	-607.82	-613.04	-630.87	-880.28
13198	-595.92	-607.60	-612.73	-630.23	-875.80
13199	-2.04	-6.06	-613.04	-630.87	-880.28

Continued on next page

Table A.5: SCMVA reduction across buses (Part 5)

Bus	20% PV ΔSCMVA (MVA)	40% PV ΔSCMVA (MVA)	60% PV ΔSCMVA (MVA)	80% PV ΔSCMVA (MVA)	100% PV ΔSCMVA (MVA)
13200	-2.01	-5.95	-612.73	-630.23	-875.80
13201	-2.04	-6.06	-11.00	-621.15	-880.28
13202	-2.01	-5.95	-10.80	-37.31	-875.80
13203	-9.70	-607.82	-613.04	-630.87	-880.28
13204	-595.92	-607.60	-612.73	-630.23	-875.80
13205	-2.04	-599.87	-604.69	-630.87	-880.28
13206	-2.01	-13.85	-19.12	-630.23	-875.80
13207	-2.04	-599.87	-604.69	-630.87	-880.28
13208	-2.01	-13.85	-19.12	-630.23	-875.80
13209	-595.95	-599.87	-604.69	-621.15	-880.28
13210	-9.56	-13.85	-19.12	-37.31	-875.80
13211	-2.04	-6.06	-11.00	-37.98	-880.28
13212	-2.01	-5.95	-10.80	-620.65	-875.80
13213	-2.23	-600.34	-605.57	-623.39	-872.81
13215	-600.46	-605.00	-614.97	-623.99	-870.28
13216	-5.99	-10.39	-20.09	-622.60	-859.34
13217	-600.45	-605.00	-613.32	-623.98	-870.24
13218	-5.99	-10.39	-612.43	-622.60	-859.34
13219	-11.02	-18.26	-618.61	-641.26	-876.84
13220	-596.10	-602.43	-618.20	-640.44	-872.47
13221	-11.02	-611.57	-618.61	-641.26	-876.84
13222	-596.10	-611.29	-618.20	-640.44	-872.47
13223	-2.47	-602.59	-609.10	-641.26	-876.84
13224	-2.43	-17.96	-25.17	-640.44	-872.47
13225	-2.47	-18.26	-25.60	-641.26	-876.84
13226	-2.43	-602.43	-608.82	-640.44	-872.47
13227	-2.47	-18.26	-25.60	-49.52	-876.84
13228	-2.43	-602.43	-608.82	-629.42	-872.47

Continued on next page

Table A.6: SCMVA reduction across buses (Part 6)

Bus	20% PV ΔSCMVA (MVA)	40% PV ΔSCMVA (MVA)	60% PV ΔSCMVA (MVA)	80% PV ΔSCMVA (MVA)	100% PV ΔSCMVA (MVA)
13229	-2.47	-602.59	-618.61	-641.26	-876.84
13230	-2.43	-17.96	-618.20	-640.44	-872.47
13231	-602.16	-607.39	-610.34	-625.34	-878.94
13232	-8.20	-13.56	-16.60	-625.34	-878.94
13233	-600.45	-605.00	-613.32	-623.98	-870.24
13234	-5.99	-10.39	-612.43	-622.60	-859.34
13235	-7.55	-10.91	-613.32	-623.98	-870.24
13236	-7.20	-604.51	-612.43	-622.60	-859.34
13237	-600.45	-605.00	-614.96	-625.97	-870.24
13238	-5.99	-10.39	-20.09	-30.94	-859.34
13239	-7.55	-10.91	-21.09	-623.98	-870.24
13240	-7.20	-604.51	-614.01	-622.60	-859.34
13241	-6.11	-10.78	-21.10	-32.67	-1177.30
13242	-907.53	-911.90	-921.49	-932.09	-1166.42
13244	-7.02	-11.47	-920.72	-930.89	-1167.64
13245	-11.70	-17.38	-20.60	-36.93	-878.94
13246	-11.70	-17.38	-20.60	-629.82	-878.94
13247	-8.20	-604.02	-606.82	-625.34	-878.94
13248	-602.16	-604.02	-606.82	-625.34	-878.94
13249	-2.47	-18.26	-25.60	-641.26	-876.84
13250	-2.43	-602.43	-608.82	-640.44	-872.47
13251	-11.02	-611.57	-618.61	-641.26	-876.84
13252	-596.10	-611.29	-618.20	-640.44	-872.47
13253	-2.47	-9.14	-15.90	-641.26	-876.84
13254	-2.43	-8.97	-15.60	-640.44	-872.47
13255	-11.02	-18.26	-25.60	-641.26	-876.84
13256	-596.10	-602.43	-608.82	-640.44	-872.47
13261	-1200.55	-1214.80	-1229.41	-1272.71	-1835.03

Continued on next page

Table A.7: SCMVA reduction across buses (Part 7)

Bus	20% PV ΔSCMVA (MVA)	40% PV ΔSCMVA (MVA)	60% PV ΔSCMVA (MVA)	80% PV ΔSCMVA (MVA)	100% PV ΔSCMVA (MVA)
13262	-8.22	-23.21	-38.72	-85.48	-1835.03
13263	-1200.55	-1214.80	-1229.41	-1272.71	-1835.03
13264	-8.22	-1214.80	-1229.41	-1272.71	-1835.03
13265	-8.22	-23.21	-38.72	-1272.71	-1835.03
13266	-8.22	-1214.80	-1229.41	-1272.71	-1835.03
13267	-8.22	-1214.80	-1229.41	-1272.71	-1835.03
13268	-29.64	-83.33	-2641.12	-2781.57	-4127.17
13269	-29.64	-83.33	-138.35	-301.07	-4127.17
13270	-29.54	-83.21	-138.32	-302.42	-4098.57
13271	-10.08	-28.50	-47.58	-1356.90	-2044.75
13272	-10.08	-28.50	-47.58	-1356.90	-2044.75
13273	-10.08	-1280.98	-1300.12	-1356.90	-2044.75
13274	-10.08	-1280.98	-1300.12	-1356.90	-2044.75
13275	-1248.43	-1265.94	-1300.12	-1356.90	-2044.75
13276	-24.31	-44.05	-1300.12	-1356.90	-2044.75
13277	-10.08	-28.50	-1283.91	-1356.90	-2044.75
13278	-10.08	-28.50	-64.46	-1356.90	-2044.75
13279	-29.54	-83.21	-138.32	-2754.85	-4098.57
13280	-8.50	-31.27	-54.12	-127.14	-1563.48
13290	-35.73	-52.91	-62.62	-126.55	-1765.80
13291	-23.06	-37.53	-69.19	-104.13	-1652.42
13292	-23.06	-37.53	-69.19	-104.13	-1652.42
13294	-10.20	-1294.70	-1313.26	-1369.07	-2664.86
13295	-2.06	-249.03	-255.62	-275.89	-1828.43
13296	-1276.66	-1294.70	-1313.26	-1369.07	-2664.86
13297	-242.69	-249.03	-255.62	-275.89	-1828.43
180351	-0.77	-2.19	-1387.44	-1396.86	-1508.79
180391	-0.87	-2.46	-8.23	-707.63	-833.93

Continued on next page

Table A.8: SCMVA reduction across buses (Part 8)

Bus	20% PV ΔSCMVA (MVA)	40% PV ΔSCMVA (MVA)	60% PV ΔSCMVA (MVA)	80% PV ΔSCMVA (MVA)	100% PV ΔSCMVA (MVA)
20216	-73.53	-326.86	-4170.34	-4556.38	-8144.09
20217	-73.53	-326.86	-4170.34	-4556.38	-8144.09
20218	-73.53	-326.86	-957.23	-1455.68	-8144.09
20219	-73.53	-3658.41	-4170.34	-4556.38	-8144.09
20941	-1.79	-4.14	-579.40	-590.29	-894.25
20976	-17.70	-47.02	-67.20	-159.32	-1635.80
21255	-124.67	-324.98	-793.08	-4959.20	-7871.84
21257	-124.67	-324.98	-4296.66	-4959.20	-7871.84
21271	-6.43	-22.94	-625.21	-648.85	-1160.71
21272	-6.43	-608.03	-625.21	-648.85	-1160.71
21273	-6.43	-14.51	-23.06	-648.85	-1160.71
21274	-6.43	-14.51	-23.06	-648.85	-1160.71
21275	-600.17	-608.03	-616.29	-638.39	-1160.71
21276	-14.25	-22.94	-32.14	-56.95	-1160.71
21277	-6.43	-608.03	-625.21	-648.85	-1160.71
21278	-6.43	-22.94	-625.21	-648.85	-1160.71
21279	-6.43	-608.03	-616.29	-648.85	-1160.71
21280	-6.43	-22.94	-32.14	-648.85	-1160.71
21281	-6.43	-14.51	-32.14	-56.95	-1160.71
21282	-6.43	-14.51	-616.29	-638.39	-1160.71
21283	-6.43	-14.51	-23.06	-56.95	-1160.71
21284	-6.43	-14.51	-23.06	-638.39	-1160.71
21285	-6.43	-22.94	-32.14	-648.85	-1160.71
21286	-6.43	-608.03	-616.29	-648.85	-1160.71
21287	-6.43	-608.03	-616.29	-638.39	-1160.71
21288	-6.43	-22.94	-32.14	-56.95	-1160.71
21289	-600.17	-608.03	-616.29	-648.85	-1160.71
21291	-14.25	-22.94	-32.14	-648.85	-1160.71

Continued on next page

Table A.9: SCMVA reduction across buses (Part 9)

Bus	20% PV ΔSCMVA (MVA)	40% PV ΔSCMVA (MVA)	60% PV ΔSCMVA (MVA)	80% PV ΔSCMVA (MVA)	100% PV ΔSCMVA (MVA)
21292	-6.43	-14.51	-625.21	-648.85	-1160.71
21293	-6.43	-14.51	-625.21	-648.85	-1160.71
21294	-205.43	-4414.19	-4619.01	-5102.14	-8449.86
21295	-6.43	-14.51	-23.06	-56.95	-1160.71
21296	-6.43	-14.51	-23.06	-638.39	-1160.71
21297	-4205.11	-4414.19	-4619.01	-5102.14	-8449.86
21515	-61.97	-2636.55	-2750.51	-2995.79	-5329.18
21516	-61.97	-2636.55	-2750.51	-2995.79	-5329.18
21517	-61.97	-172.09	-301.92	-2995.79	-5329.18
21518	-61.97	-172.09	-301.92	-592.46	-5329.18
21520	-134.26	-209.60	-294.28	-544.19	-5310.04
21521	-2600.39	-2667.05	-2740.86	-2952.05	-5310.04
21522	-2600.39	-2667.05	-2740.86	-2952.05	-5310.04
21523	-134.26	-209.60	-294.28	-544.19	-5310.04
21524	-134.26	-209.60	-294.28	-544.19	-5310.04
21525	-2600.39	-2667.05	-2740.86	-2952.05	-5310.04
21526	-134.26	-209.60	-294.28	-2952.05	-5310.04
21527	-2600.39	-2667.05	-2740.86	-2952.05	-5310.04
21528	-134.26	-2667.05	-2740.86	-2952.05	-5310.04
21531	-1745.66	-1796.00	-1907.27	-2124.00	-3669.58
21532	-33.57	-88.55	-212.86	-2124.00	-3669.58
21533	-33.57	-1796.00	-1907.27	-2124.00	-3669.58
21534	-1745.66	-1796.00	-1907.27	-2124.00	-3669.58
21535	-31.49	-1791.82	-1896.59	-2101.48	-3595.07
21536	-31.49	-83.13	-1896.59	-2101.48	-3595.07
21537	-7.95	-1378.16	-1406.58	-1465.83	-2139.58
21538	-7.95	-21.15	-1406.58	-1465.83	-2139.58
21539	-7.95	-21.15	-1406.58	-1465.83	-2139.58

Continued on next page

Table A.10: SCMVA reduction across buses (Part 10)

Bus	20% PV ΔSCMVA (MVA)	40% PV ΔSCMVA (MVA)	60% PV ΔSCMVA (MVA)	80% PV ΔSCMVA (MVA)	100% PV ΔSCMVA (MVA)
21561	-6.16	-14.68	-1204.21	-1232.52	-1813.34
21562	-6.16	-14.68	-27.15	-1232.52	-1813.34
21567	-2682.21	-2727.58	-2796.10	-3000.03	-5009.57
21568	-2682.21	-2727.58	-2796.10	-3000.03	-5009.57
21569	-97.67	-149.66	-229.40	-3000.03	-5009.57
21581	-1495.94	-1544.47	-1602.24	-1729.23	-3316.19
21582	-1495.94	-1544.47	-1602.24	-1729.23	-3316.19
21584	-7.15	-19.88	-35.59	-1822.79	-2505.17
21585	-7.15	-19.88	-1789.25	-1822.79	-2505.17
21586	-885.14	-1774.59	-1789.25	-1822.79	-2505.17
21587	-885.14	-1774.59	-1789.25	-1822.79	-2505.17
21588	-885.14	-897.66	-1789.25	-1822.79	-2505.17
21589	-7.15	-19.88	-913.05	-948.85	-2505.17
21590	-7.15	-897.66	-913.05	-948.85	-2505.17
21591	-7.15	-19.88	-35.59	-72.39	-2505.17
21981	-1.92	-17.98	-23.48	-1258.50	-1720.61
21982	-1.92	-17.98	-23.48	-108.08	-1720.61
21983	-1.92	-17.98	-23.48	-1258.50	-1720.61
21984	-1.92	-17.98	-23.48	-1258.50	-1720.61
21985	-1.92	-1184.26	-1188.95	-1258.50	-1720.61
22980	-4205.11	-4414.19	-4619.01	-5102.14	-8449.86
22990	-205.43	-452.90	-702.77	-1323.32	-8449.86
29715	-46.59	-1171.47	-1175.95	-1355.78	-1635.34
29716	-46.59	-179.91	-186.24	-1355.78	-1635.34
29717	-2.18	-1114.16	-1158.26	-1399.72	-1679.25
29720	-8.20	-664.11	-666.41	-788.23	-954.00
29721	-624.28	-725.33	-730.90	-938.88	-1265.81
29723	-2.83	-109.86	-734.74	-1253.21	-1322.11

Continued on next page

Table A.11: SCMVA reduction across buses (Part 11)

Bus	20% PV ΔSCMVA (MVA)	40% PV ΔSCMVA (MVA)	60% PV ΔSCMVA (MVA)	80% PV ΔSCMVA (MVA)	100% PV ΔSCMVA (MVA)
29724	-1.01	-645.37	-668.24	-550.74	-974.49
29725	-2.83	-80.56	-148.72	-1253.21	-1322.11
29726	-1.15	-45.98	-77.46	-846.92	-1039.65
29821	-1.86	-5.02	-7.21	-17.69	-862.18
29823	-1.86	-655.54	-657.60	-667.34	-862.18
30181	-16.84	-53.23	-1759.67	-1939.50	-3575.75
30182	-16.84	-53.23	-215.49	-1939.50	-3575.75
30183	-16.84	-53.23	-215.49	-424.27	-3575.75
30184	-16.84	-53.23	-215.49	-424.27	-3575.75
30188	-3275.62	-3331.02	-3696.24	-4236.59	-6929.30
30189	-131.14	-195.49	-629.53	-4236.59	-6929.30
30198	-131.14	-195.49	-3696.24	-4236.59	-6929.30
30199	-131.14	-195.49	-3696.24	-4236.59	-6929.30
30220	-0.11	-0.39	-0.74	-1.69	-361.59
30384	-0.06	-18.91	-19.96	-105.72	-134.52
30385	-0.07	-177.92	-178.88	-183.05	-211.48
30411	-0.51	-923.24	-928.20	-949.31	-1074.14
30737	-240.43	-271.25	-353.36	-768.85	-5805.93
30738	-240.43	-271.25	-353.36	-3352.56	-5805.93
30739	-2916.24	-2942.35	-3011.50	-3352.56	-5805.93
30741	-2916.24	-2942.35	-3011.50	-3352.56	-5805.93
31521	-2.40	-5.45	-16.21	-29.22	-636.61
31522	-442.84	-445.79	-456.12	-468.49	-636.61
31523	-2.40	-5.45	-16.21	-468.49	-636.61
31524	-442.84	-445.79	-456.12	-468.49	-636.61
31531	-7.70	-18.49	-1102.91	-1140.97	-1571.30
31532	-1058.42	-1068.49	-1102.91	-1140.97	-1571.30
31533	-7.70	-18.49	-1102.91	-1140.97	-1571.30

Continued on next page

Table A.12: SCMVA reduction across buses (Part 12)

Bus	20% PV ΔSCMVA (MVA)	40% PV ΔSCMVA (MVA)	60% PV ΔSCMVA (MVA)	80% PV ΔSCMVA (MVA)	100% PV ΔSCMVA (MVA)
31534	-7.70	-18.49	-1102.91	-1140.97	-1571.30
31541	-6.15	-864.46	-892.90	-924.79	-1294.75
31542	-6.15	-15.34	-45.86	-924.79	-1294.75
31543	-6.15	-864.46	-892.90	-924.79	-1294.75
31544	-6.15	-15.34	-892.90	-924.79	-1294.75
31711	-1.52	-953.72	-963.09	-978.91	-1209.01
31712	-1.52	-5.73	-15.70	-32.76	-1209.01
31715	-0.89	-1201.59	-1204.12	-1211.14	-1358.41
31716	-0.89	-4.23	-7.01	-14.75	-1358.41
31721	-2.01	-5.96	-1400.56	-1421.53	-1707.45
31722	-2.01	-5.96	-1400.56	-1421.53	-1707.45
31725	-1.93	-733.45	-743.80	-754.86	-931.36
31726	-1.93	-10.76	-743.80	-754.86	-931.36
31731	-2.29	-7.29	-1581.85	-1610.16	-2033.78
31732	-2.29	-7.29	-37.94	-70.88	-2033.78
31751	-9.63	-13.65	-21.63	-1608.72	-2001.19
31752	-1560.05	-1563.68	-1570.86	-1608.72	-2001.19
31753	-9.63	-13.65	-21.63	-1608.72	-2001.19
31771	-4.74	-8.12	-1580.50	-1604.03	-1989.34
31772	-4.74	-8.12	-1580.50	-1604.03	-1989.34
31780	-1.83	-24.60	-40.60	-793.26	-1043.76
31781	-1.83	-753.34	-767.74	-793.26	-1043.76
31782	-1.15	-1400.96	-1409.90	-1425.90	-1593.47
31783	-1.15	-15.46	-1409.90	-1425.90	-1593.47
31784	-1.15	-1400.96	-1409.90	-1425.90	-1593.47
33231	-1210.48	-1217.19	-1230.28	-1265.53	-1704.12
33232	-1210.48	-1217.19	-1230.28	-1265.53	-1704.12
33233	-12.91	-20.01	-33.96	-72.14	-1704.12

Continued on next page

Table A.13: SCMVA reduction across buses (Part 13)

Bus	20% PV ΔSCMVA (MVA)	40% PV ΔSCMVA (MVA)	60% PV ΔSCMVA (MVA)	80% PV ΔSCMVA (MVA)	100% PV ΔSCMVA (MVA)
33241	-12.91	-20.01	-33.96	-1265.53	-1704.12
33242	-12.91	-20.01	-33.96	-72.14	-1704.12
33243	-1210.48	-1217.19	-1230.28	-1265.53	-1704.12
33244	-8.52	-13.22	-22.47	-1530.95	-1845.39
33251	-12.91	-20.01	-33.96	-72.14	-1704.12
33252	-12.91	-1217.19	-1230.28	-1265.53	-1704.12
33253	-1210.48	-1217.19	-1230.28	-1265.53	-1704.12
33254	-8.52	-13.22	-22.47	-48.00	-1845.39
33261	-12.91	-20.01	-33.96	-1265.53	-1704.12
33262	-12.91	-20.01	-1230.28	-1265.53	-1704.12
33263	-12.91	-1217.19	-1230.28	-1265.53	-1704.12
33264	-12.91	-20.01	-33.96	-1265.53	-1704.12
33265	-1210.48	-1217.19	-1230.28	-1265.53	-1704.12
33266	-1210.48	-1217.19	-1230.28	-1265.53	-1704.12
33267	-8.52	-13.22	-1507.39	-1530.95	-1845.39
33271	-30.35	-38.49	-48.25	-70.77	-1438.54
33272	-1025.77	-1032.52	-1040.58	-1059.01	-1438.54
33273	-30.35	-38.49	-48.25	-70.77	-1438.54
33278	-3.16	-31.07	-1063.23	-1084.83	-1478.31
33279	-3.16	-1036.02	-1063.23	-1084.83	-1478.31
33280	-7.96	-77.36	-154.81	-215.77	-1930.09
33281	-7.96	-77.36	-154.81	-215.77	-1930.09
33284	-8.53	-13.22	-1507.41	-1530.96	-1845.20
33401	-1492.73	-1522.30	-1568.11	-1699.78	-2649.59
33402	-5.67	-27.34	-1254.87	-1355.56	-2131.74
33403	-6.61	-25.13	-77.77	-1357.54	-2082.15
33404	-6.61	-25.13	-1248.24	-1357.54	-2082.15
33405	-11.30	-42.84	-91.29	-1699.78	-2649.59

Continued on next page

Table A.14: SCMVA reduction across buses (Part 14)

Bus	20% PV ΔSCMVA (MVA)	40% PV ΔSCMVA (MVA)	60% PV ΔSCMVA (MVA)	80% PV ΔSCMVA (MVA)	100% PV ΔSCMVA (MVA)
33406	-8.55	-32.46	-1262.73	-1355.56	-2131.74
33407	-6.61	-1230.80	-1265.51	-1357.54	-2082.15
33408	-6.61	-1230.80	-1265.51	-1357.54	-2082.15
33409	-11.30	-37.13	-91.29	-1699.78	-2649.59
33410	-8.55	-1221.01	-1262.73	-1355.56	-2131.74
33411	-6.61	-25.13	-77.77	-1357.54	-2082.15
33412	-6.61	-25.13	-1248.24	-1357.54	-2082.15
33413	-17.31	-65.60	-155.21	-2873.41	-4094.08
33414	-11.20	-42.44	-100.40	-219.27	-2306.29
33415	-6.61	-1215.45	-1248.24	-1335.58	-2082.15
33416	-6.61	-40.94	-77.77	-177.92	-2082.15
33430	-7.42	-28.69	-1439.27	-1514.60	-2313.96
33431	-7.41	-1414.56	-1439.50	-1514.83	-2314.19
33432	-7.41	-28.69	-55.37	-1514.83	-2314.19
33433	-7.42	-28.69	-55.37	-137.62	-2313.96
33434	-7.41	-28.69	-55.37	-1514.83	-2314.19
33435	-7.41	-28.69	-55.37	-137.62	-2314.19
33436	-7.42	-28.69	-55.37	-1514.60	-2313.96
33437	-7.41	-28.69	-1439.50	-1514.83	-2314.19
33438	-7.41	-1414.56	-1439.50	-1514.83	-2314.19
33439	-7.42	-1414.33	-1439.27	-1514.60	-2313.96
33440	-7.41	-28.69	-55.37	-137.62	-2314.19
33441	-7.41	-28.69	-55.37	-137.62	-2314.19
33442	-7.42	-1414.33	-1439.27	-1514.60	-2313.96
33443	-7.41	-28.69	-55.37	-1514.83	-2314.19
33444	-7.41	-28.69	-1439.50	-1514.83	-2314.19
33445	-7.42	-28.69	-55.37	-1514.60	-2313.96
33446	-1394.49	-1414.56	-1439.50	-1514.83	-2314.19

Continued on next page

Table A.15: SCMVA reduction across buses (Part 15)

Bus	20% PV ΔSCMVA (MVA)	40% PV ΔSCMVA (MVA)	60% PV ΔSCMVA (MVA)	80% PV ΔSCMVA (MVA)	100% PV ΔSCMVA (MVA)
33447	-7.41	-28.69	-55.37	-137.62	-2314.19
33471	-25.91	-95.12	-136.53	-1600.32	-2307.73
33472	-25.91	-1470.64	-1507.53	-1600.32	-2307.73
33473	-25.91	-95.12	-136.53	-1600.32	-2307.73
33474	-25.91	-95.12	-136.53	-243.53	-2307.73
33475	-1407.74	-1470.64	-1507.53	-1600.32	-2307.73
33476	-1407.74	-1470.64	-1507.53	-1600.32	-2307.73
33477	-25.91	-1470.64	-1507.53	-1600.32	-2307.73
33478	-25.91	-1470.64	-1507.53	-1600.32	-2307.73
33479	-25.91	-1470.64	-1507.53	-1600.32	-2307.73
33480	-25.91	-95.12	-1507.53	-1600.32	-2307.73
33483	-18.05	-1318.71	-1345.05	-1412.07	-1960.98
33484	-1274.17	-1318.71	-1345.05	-1412.07	-1960.98
39481	-9.36	-885.66	-895.38	-925.58	-1375.96
39482	-9.36	-20.58	-31.34	-65.16	-1375.96
39483	-9.36	-20.58	-31.34	-925.58	-1375.96
39484	-875.46	-885.66	-895.38	-925.58	-1375.96
41007	-876.66	-886.19	-917.87	-974.27	-1401.88
41008	-29.91	-41.60	-81.20	-154.42	-1401.88
41020	-21.77	-30.27	-59.01	-518.66	-886.75
41021	-21.77	-30.27	-59.01	-518.66	-886.75
44045	-2.46	-21.91	-38.44	-61.58	-969.90
44046	-473.64	-479.41	-514.67	-524.55	-816.32
44047	-2.46	-21.91	-38.44	-633.21	-969.90
44048	-36.85	-45.14	-572.79	-584.60	-914.49
44049	-30.12	-36.93	-79.41	-91.60	-855.60
44050	-2.96	-26.34	-46.13	-73.71	-1024.41
44051	-4.41	-39.25	-68.63	-109.49	-1501.43

Continued on next page

Table A.16: SCMVA reduction across buses (Part 16)

Bus	20% PV ΔSCMVA (MVA)	40% PV ΔSCMVA (MVA)	60% PV ΔSCMVA (MVA)	80% PV ΔSCMVA (MVA)	100% PV ΔSCMVA (MVA)
44052	-4.47	-977.41	-1001.08	-1033.15	-1505.56
44053	-638.43	-646.12	-692.70	-705.60	-1056.30
46008	-0.50	-629.90	-662.67	-744.43	-937.22
46009	-0.50	-66.82	-662.67	-744.43	-937.22
48011	-0.63	-37.92	-89.68	-800.85	-1098.31
48012	-0.63	-37.92	-747.65	-800.85	-1098.31
48013	-0.61	-704.82	-743.05	-794.52	-1073.97
48014	-0.61	-27.12	-76.52	-146.56	-1075.89
49511	-85.04	-2435.32	-2873.68	-3020.03	-4467.30
49512	-85.04	-274.16	-2873.68	-3020.03	-4467.30
49513	-85.04	-274.16	-2873.68	-3020.03	-4467.30
49557	-3519.40	-4021.89	-5148.03	-5463.51	-7765.92
49558	-346.21	-4021.13	-5145.86	-5461.03	-7762.12
49559	-344.77	-988.20	-5140.44	-5454.81	-7752.62
51955	-14.51	-235.69	-317.56	-430.23	-2852.32
51956	-7.65	-127.11	-172.78	-237.00	-2232.90
51957	-7.65	-1289.52	-1323.52	-1370.47	-2232.90
57027	-13.28	-24.79	-588.19	-648.02	-1137.09
57028	-13.51	-25.22	-132.82	-730.37	-1219.24
57029	-14.07	-26.27	-137.96	-216.20	-1235.42
57034	-4.92	-9.23	-627.53	-652.22	-923.32
57035	-16.47	-25.04	-926.08	-949.95	-1310.80
57036	-16.47	-25.04	-83.42	-115.14	-1310.80
57037	-593.68	-599.65	-639.31	-660.12	-988.97
59612	-0.15	-2.62	-3.61	-596.16	-665.13
61607	-500.28	-506.40	-514.59	-539.01	-733.86
61608	-8.37	-15.33	-24.73	-539.01	-733.86
61610	-8.37	-15.33	-24.73	-539.01	-733.86

Continued on next page

Table A.17: SCMVA reduction across buses (Part 16)

Bus	20% PV ΔSCMVA (MVA)	40% PV ΔSCMVA (MVA)	60% PV ΔSCMVA (MVA)	80% PV ΔSCMVA (MVA)	100% PV ΔSCMVA (MVA)
62011	-3.41	-8.39	-912.71	-925.79	-1181.92
62012	-3.41	-8.39	-65.72	-83.15	-1181.92
62609	-2.33	-5.74	-605.79	-615.48	-816.83
62610	-2.33	-5.74	-45.20	-57.23	-816.83
64613	-4.40	-364.47	-387.28	-421.90	-1718.73
64614	-4.40	-1096.07	-1112.94	-1138.37	-1718.73
64618	-4.40	-1096.07	-1112.94	-1138.37	-1718.73
64619	-4.40	-1096.07	-1112.94	-1138.37	-1718.73

Vita

Waleed M Albukhari got his Bachelor's degree in Electrical Engineering from Riyadh Technical College in 2013. He received his Master's degree from the Department of Electrical Engineering at the University of Tennessee at Chattanooga in 2016. In 2021, he started his Ph.D. study at the University of Tennessee Knoxville. His research of interest includes power system strength and renewable energy integration.